Variability, drivers, and utility of genetic diversity-area relationships in terrestrial vertebrates

Chloé Schmidt[1,2,3,4*], Sean Hoban[5], Deborah M. Leigh[6,7,8,9], Walter Jetz[3,4†], Colin J. Garroway[10†]

[1] Department of Biology, Dalhousie University; Halifax, NS, Canada

[2] German Centre for Integrative Biodiversity Research (iDiv) Halle-Jena-Leipzig; Leipzig, Germany

[3] Department of Ecology and Evolutionary Biology, Yale University, New Haven, CT, USA

[4] Center for Biodiversity and Global Change, Yale University, New Haven, CT, USA

[5] The Center for Tree Science, The Morton Arboretum; Lisle, IL, USA

[6] Swiss Federal Research Institute for Forest, Snow, and Landscape Research WSL; Birmensdorf, Switzerland

[7] LOEWE Centre for Translational Biodiversity Genomics, Senckenberganlage 25, 60325 Frankfurt, Germany

[8] Senckenberg Research Institute, Senckenberganlage 25, 60325 Frankfurt, Germany

[9] Institute of Ecology, Evolution, and Diversity, Faculty of Biosciences, Goethe University Frankfurt, Max-von-Laue-Str. 9, 60438 Frankfurt, Germany

[10] Department of Biological Sciences, University of Manitoba; Winnipeg, MB, Canada

[†] Co-senior authors

[*]Correspondence: chloe.schmidt@dal.ca

Abstract

Maintaining genetic diversity within and among populations is critical for conservation and a prominent goal of the Kunming-Montreal Global Biodiversity Framework. However, direct estimates of genetic diversity are unavailable for most species, and time and resources are insufficient to fill these substantial data gaps and meet conservation target timelines. Robust, proxy-based predictions of genetic diversity loss would therefore be valuable for conserving genetic diversity for the many species lacking DNA-based data. We evaluated one such approach, the Genetic Diversity Area Relationship (GDAR), which describes the relationship between genetic diversity and the geographic area occupied by a species. We estimated differences in genetic diversity relative to the size of sample area using 55 previously published datasets from 51 species and found that GDARs were highly variable across species and strongly dependent on population structure. The mean change in allele count relative to area sampled across all species did not predict genetic diversity differences for individual species well. Traits correlated with population structure explained little variation in the GDAR. Our findings suggest that using a single GDAR is not appropriate to predict genetic diversity loss for individual species following area loss. Further work is needed to identify accurate methods to estimate species-specific levels of genetic diversity decline with area without genetic data. Although the GDAR remains valuable to highlight likely global patterns and scales of genetic diversity loss across many species, our results suggest it is currently too inaccurate for species-specific use.

Keywords: species-area relationship, F_{ST}, population differentiation, conservation, macrogenetics, vertebrates, biodiversity, zMAR, genetic indicators

Introduction

Genetic diversity is a fundamental component of biodiversity that is critical for the long-term resilience of populations and species[1,2]. Parties to the Convention on Biological Diversity formally committed to conserving genetic diversity and to measuring the progress toward this goal in 2022 with the signing of Kunming-Montreal Global Biodiversity Framework[3] ("KM GBF" Goal A, Target 4[4]). However, monitoring genetic diversity change is difficult and has been neglected due to cost, expertise barriers in data production, and difficulties in sample collection. Consequently, we do not have sufficient genetic data for the assessment and monitoring of most species[5], and the substantial resources needed for direct genetic assessments of species at the global scale are not on the horizon[6]. With the necessarily ambitious KM GBF target of halting the loss of genetic diversity and restoring conditions to support adaptive capacity by 2030, approximations or indicators of genetic diversity are urgently needed to support genetic diversity monitoring and conservation.

Diversity-area relationships from species to alleles

Genetic diversity change could potentially be approximated by extending the concept of species-area relationships (SAR) to genetic diversity[7,8]. The SAR is a simple, widely-used relationship in conservation that describes how species richness decreases from larger toward progressively smaller areas[9–11]. For conservation purposes, the SAR has been used to approximate changes in species richness across regions differing in amounts of habitat over space and time. Applying the SAR at a genetic level could similarly be a shorthand for gauging genetic diversity loss as habitat and range size shrink[7,8].

The traditional simple power law formulation of the SAR is: log (S) = log(c) + z* log (A), where *S* is the number of species in a region with area *A*, *c* is a constant, and the exponent *z* characterizes the linear rate of increase in species number with area. Different approaches for characterizing SARs exist[12]; a traditional one is that of a nested design (Fig. 1), where consecutively larger surrounding areas are assessed to estimate the rate at which the number of species sampled increases.

The generalizability of SARs across different ecological settings has been well studied, and the shape of the SAR relationship, and thus its conservation utility, is variable and context-specific (e.g., endemics area relationships[13], countryside SAR[14]). The simplicity of the SAR and its direct link to population size (approximated by area) and, thus, genetic drift, offers an intriguing potential pathway for considering area effects on genetic diversity. Similar genetic diversity-area relationships (GDARs) that hold across species would facilitate estimating and forecasting genetic change for species whose ranges have shrunk and genetic data is unavailable or difficult to collect. The expected mean losses of genetic variants as species ranges shrink may be predictable in a way similar to the power-law SAR[7,8].

If an accurate, reliable GDAR existed and held for spatial and temporal differences in area, predicting genetic diversity loss in a given species would require only knowledge of the area of a species range that has been lost, and the corresponding change in numbers of alleles (*z* values in the SAR formula). This could allow managers to identify species and locations that have lost, or might soon lose, significant amounts of genetic diversity due to habitat loss. The simplicity of GDARs would make them powerful tools for managers and policymakers[15]. Overall, a GDAR that held across species would vastly expand the scope of species and places where estimates of

genetic diversity loss could be considered in conservation practice, circumventing some of the limitations surrounding genetic data collection.

Interest in applying the SAR concept to genetic diversity conservation is growing, including proposals to explore whether average *z* values could suitably predict genetic diversity loss across species[8], or whether *z* values could be estimated separately for species with high versus low population structure[7]. An exploration of power law relationships between genetic diversity and area across 20 species, spanning plants, insects, birds, and mammals, suggested that a mean *z* value of 0.3 (values ranged between 0.015—0.824) may be sufficient to capture general patterns of change across species[5].

However, the promise of the GDAR as a predictor of genetic diversity change relative to area has not been fully evaluated. Specifically, forecasting is defined by the slope of the GDAR (*z*), however we do not yet know the extent to which *z* values can be generalized or predicted across species. Genetic diversity declines up to 10% by 2030 may lead to harmful increases in inbreeding and loss of fitness in wild populations[16]. With small margins of error for genetic diversity loss, robust forecasting is key.

Spatial structure in diversity-area relationships

Genetic diversity is not distributed evenly across species ranges[17]. The null expectation is that populations are structured by isolation by distance due to the tendency of individuals to mate with others close by[18]. Population genetic structure is sometimes related to, and therefore may be well-predicted by, ecological attributes of species[19,20] and landscapes[21,22]. For example, we might generally predict that flying, wide-ranging generalist species, such as some bats, would tend to

have a more uniform spatial distribution of alleles (and less genetically structured populations) because individuals are highly mobile and have higher dispersal capacities, increasing gene flow among populations[23]. Alleles would be lost at a relatively constant rate with area (Fig. 1c). We would in turn predict that species with low dispersal capacities and patchy habitat distributions, such as salamanders, would tend to have more clustered distributions of alleles and well-defined genetic population structure due to lower rates of gene flow among populations[23]. Such species could rapidly lose genetic diversity as larger areas that encompass multiple distinct populations are lost (Fig 1c). The change in the number of alleles across spatial scales (z) should therefore depend directly upon the degree to which populations are spatially structured, which in turn is influenced by the landscape, species traits, biogeography, and demographic histories[7,23,24].

Drivers of the GDAR z should thus be associated with measures of population genetic structure. In SARs, the direct link between z and the spatial turnover of species (or portion of species shared between a larger and a nested smaller area—i.e., beta diversity) is well-known[25,26]. For specific sampling design cases and geographic range distributions, the connection is mathematically defined[27,28], and accounting for these beta diversity estimates fully determines z values and vice versa. Given biogeography's historical development and the more direct conservation applications, z values and SAR have seen greater popularity as a research focus than beta diversity. This differs from population genetics, where beta diversity describes spatial genetic structure[18]. The fixation index, F_{ST}, is a standard measure of allele frequency variation that is attributable to population genetic structure that has very well-understood theoretical underpinnings[29,30]. In its simplest form[29], F_{ST} can be estimated as $(H_T - H_S)/H_T$, where H_T is the heterozygosity of the total population without considering subpopulation structure, H_S is the

131 average heterozygosity of subpopulations, and the difference between the total and average
132 heterozygosity of subpopulations is standardized by total population-level heterozygosity.

133 As with the SAR, it is likely that the exponent *z* in the GDAR is a measure of beta diversity at
134 the genetic level, and is thus strongly correlated with F_{ST}. Given our strong theoretical
135 understanding of F_{ST}, assessing its empirical connection to GDAR *z* values has the potential to
136 link newly emerging perspectives related to GDARs with population genetics to advance
137 conservation. By repurposing publicly available microsatellite genetic datasets from wild
138 populations, we expand the number of terrestrial vertebrates with empirically derived GDARs to
139 51 species and assess the empirical variability in GDAR *z* values. Finally, we test putative
140 drivers of *z* and F_{ST} to explore whether ecological predictors would support a straightforward use
141 of GDARs by conservation practitioners. If GDAR *z* values were either reasonably similar
142 among species or if their variation were well-captured and predictable, an opportunity would
143 exist for employing the GDAR relationship to predict genetic diversity change for individual
144 threatened species, rather than just at a global or regional level, helping conservation
145 prioritization.

146

147 **Results and Discussion**

148 ***Variation in genetic diversity area relationships***

149 The GDAR can be estimated identically to the SAR by considering alleles as species. We
150 artificially sampled each genetic dataset using a nested GDAR design (sampling concentric areas
151 of increasing size) and estimated *z* values as the slope of the log-log relationship between the
152 number of alleles sampled and the size of the area from which they were sampled (Fig. 1; see

153 Methods). We first highlight two examples, the little brown bat (*Myotis lucifugus*) and the Mount
154 Lyell salamander (*Hydromantes platycephalus*), that illustrate how GDAR shapes can vary
155 substantially with movement ability (Fig 1C). Due to its flight ability, we predicted that the little
156 brown bat should exhibit less population structure than a comparatively less vagile salamander
157 species due to higher possibility of gene flow. These contrasting population structures should
158 shape the GDAR, with the more structured Mount Lyell salamander losing alleles more quickly
159 as area is lost than the genetically well-mixed little brown bats. Indeed, estimates of *z* for these
160 two species are very different (Fig 1c).

161 This considerable variation in the shape and strength of GDARs extends across the 51 terrestrial
162 vertebrate species we assessed (Fig. 2, Tables S1, S2). Generally, the number of alleles was
163 positively correlated with the size of the geographical area sampled, which explained a
164 substantial proportion of variation in allele count (mean R^2 = 63% across datasets, Fig. S2). *Z*
165 values ranged from 0.05 to 0.27 (mean 0.12), with amphibians and reptiles exhibiting the largest
166 range of values.

167 Allele count is highly sample size dependent, so we also assessed two alternative, commonly
168 used metrics of genetic diversity that are less sensitive to sample size differences[31]: allelic
169 richness, standardized using rarefaction and thus comparable counts of alleles across different
170 sample sizes, and gene diversity[32], the average probability that two randomly sampled alleles are
171 different in a nonrandom mating population. For both metrics, nearly all datasets showed
172 significant area dependence, but with generally much shallower and statistically weaker
173 relationships than those of allele count (mean R^2 allelic richness = 32%, gene diversity: 24%;
174 Fig. 2, Table S1, Fig. S2). This confirms the important role of sample size in driving GDAR

patterns based on counts of alleles. Mean *z* values did not strongly vary across terrestrial vertebrate classes for any genetic metric (Table S2).

The slope of the GDAR approximates population structure

We estimated F_{ST} for each genetic dataset to quantify population genetic structure and assessed its role in explaining GDARs. In a hierarchical regression model combining data across all species, we found population structure interacted substantially with area to explain the rate of genetic diversity change with reduced area sampled (Fig. 3, Table S3). Specifically, species with more population structure (higher F_{ST}) lost alleles more rapidly when sampling smaller and smaller geographic areas. For allelic richness and gene diversity, the effect of sample area was negligible when population structure was statistically held at zero, and it was an order of magnitude smaller than in a model with area alone (Fig. 3, Table S3). For allele count, the metric most affected by sample size, the effect of area was similar in both models, but the interaction effect was stronger (Fig. 3, Table S3). These results demonstrate that population structure sets the shape of GDARs and, ultimately, the initial change in genetic diversity following area loss. Across species, *z* was consistently strongly correlated with F_{ST} for allele count, allelic richness, and gene diversity (Pearson $r_{\text{allele count}} = 0.69$ [0.53 - 0.80, 95% CI], $r_{\text{allelic richness}} = 0.94$ [0.90 - 0.96]; $r_{\text{gene diversity}} = 0.98$ [0.96 - 0.99]; Fig. 3).

The predictive potential of GDARs for conservation

We next assessed the extent to which *z* values could predict the area-dependence of genetic diversity across species. Average *z* values based upon all species did not yield robust predictions

of diversity differences in individual species with a slight tendency to overpredict (Fig 4). While *z* values derived from the data necessarily predicted average differences well, they poorly predicted differences in specific regions within the study area (Fig. 4b). Together, these results suggest that while GDARs may be promising tools for predicting the area-dependence of genetic diversity in aggregate across large numbers of species, they may not be suitable for predicting genetic diversity change for any given single species. Similarly, *z* values for species are likely not informative for predicting genetic diversity change for specific regions within the species range without prior knowledge of spatial genetic diversity patterns.

Ecological predictors of population structure and GDAR

Given the existence of species-level correlates of population structure, it may be possible to roughly infer *z* values for GDARs from species traits. We thus tested the extent to which we could predict F_{ST} and *z* from readily available trait data for 33 mammal species. We used three traits related to the spatial distribution of individuals that likely affect population structure: body size, home range size, and geographic range size. We included the total sampling area of each study as an additional predictor. Together, these variables explained approximately half of the variation in species' global F_{ST} (52%) and less than half of the variation in *z* values (38 – 42% across genetic metrics; Table S4). Partitioning the data into training and test sets, the average relative prediction error was nearly 60% for F_{ST} predictions (mean coefficient of variation [CV] = 0.56), and similar for z_{GD} (0.66) and z_{AR} (0.59). Error was lower for allele count-derived z_{AC} predictions (CV = 0.27). Finally, we tested the capacity of this model to predict F_{ST} in 36 species from an independently collected literature-based dataset containing microsatellite F_{ST} values, MacroPopGen[33,34], and found predictive capacity was poor (CV = 1.05).

These results suggest that without genetic data, approximating *z* based on traits or other data is not straightforward. Given the low predictive capacity of our models when assessed on the data the models were fit with, it is unsurprising that the models also poorly predicted new data from the literature-compiled MacroPopGen data set. Another reason for low predictability across both datasets is that most species samples were not range-wide, as in previous work[8]. Haphazardly sampling regional structure may yield more idiosyncratic results than whole-species population structure, adding statistical noise when making predictions across species. This suggests that high-quality training data are needed to predict F_{ST} or *z* values. However, these are not currently available for most species[5], which could significantly impact the applied use of this method. Broader explorations of the relationship between global F_{ST} and *z* across species and ecological and evolutionary contexts are needed to further assess the practical predictability of *z* in GDARs.

Limitations and opportunities of using GDARs for conservation

Our results affirm the existence of GDARs[7,8] and expand our empirical understanding of GDAR variation and the connection between GDARs and population genetics. However, even for the relatively well-studied species in our analysis, the predictive ability of a broadly parameterized GDAR, or single *z* value, is limited and its practical use for single-species conservation at this time is doubtful.

Our work identifies other limitations and opportunities around further standardization and data collection to support progress toward a more effective use of genetic data for conservation. A standout issue is the very limited availability of genetic data. We used microsatellite data, which remains widely used for wildlife studies—particularly for species lacking reference genomes.

242 However, all of the *z* values we estimated were below 0.3, the average *z* reported in Exposito-
243 Alonso et al.[8], and below 0.25, the intermediate F_{ST} value proposed by Mimura et al.[7]. This is
244 likely due to differences in data types (SNPs versus microsatellites), dataset preparation (e.g.,
245 minor allele filtering in SNP datasets), data structure (individual vs. population-level sampling),
246 sampling extents (local to range-wide), and chosen diversity metrics. It is thus important to
247 consider that factors such as data type, sampling strategy, and diversity metrics affect estimated *z*
248 values and, thus, the magnitude of the estimated loss.

249 Finally, we note two more probable limitations of GDARs. First, genetic diversity loss depends
250 not only on the total area lost but on what *specific* areas are lost. In species with highly structured
251 populations, there are often hot and coldspots of genetic diversity throughout a range, and the
252 area occupied by hot and coldspots will vary[17]. Range contractions in low diversity areas (e.g. at
253 range edges, or sink populations) will have smaller effects on the genetic diversity of a species
254 than losing a diversity hotspot (e.g. glacial refugia, or source populations). This uncertainty can
255 be seen in the range of predicted genetic diversity change using study-specific *z* values (Fig. 4),
256 and the variability in the degree of fit of GDAR relationships, where in some species small areas
257 can contain high genetic diversity (Fig. S2). Estimating the dependence of genetic diversity on
258 area would be enhanced by species-specific knowledge of regions that are particularly
259 genetically diverse, or regions that are well-connected or sustain large populations. This issue
260 mirrors that widely recognized in the use of SARs, in that single *z* values are unable to capture
261 important spatial structure in geographic range sizes and the spatial turnover of species[12].

262 Second, range contractions can cause immediate loss of genetic diversity due to the loss of
263 individuals, however, the magnitude and spatial arrangement of area loss have long-term effects
264 that are not captured by GDARs. Patchy area loss and fragmentation can decrease gene flow

across species ranges. Smaller population sizes and reduced gene flow will, in turn, increase the strength of genetic drift and introduce additional population structure. Increased drift will accelerate the loss of genetic diversity for generations to come, and increases in population structure will cause *z* to increase over time[35–38]. While GDARs may eventually be able to predict the immediate effects of reduced population size, they do not account for increasing rates of loss over time[39].

Conclusions

Our understanding of GDARs is in its infancy, and further development could resolve some of the issues we identify and improve our ability to use general rules to predict genetic diversity loss. However, the relationship between population structure and the shape of GDARs means that additional ecological and evolutionary information is likely necessary to estimate *z* values for a given species or subset of species. Using a standard *z* value across species without knowledge of spatial population structure will most often poorly estimate genetic diversity loss for focal species. Predicted losses may not be comparable across different data types and genetic diversity metrics. Further assessment and validation, including procedures for making informed decisions about the value of scaling exponents in GDARs, may improve their usability. We encourage more work to achieve a greater understanding of the factors that shape GDARs across species before they are incorporated into the conservation genetic toolbox. Access to genetic data, robust proxies of genetic diversity, and knowledge about population structure and diversity hotspots within species remain essential for effectively protecting genetic diversity.

Methods

Genetic diversity area relationships

We used 55 publicly available microsatellite datasets that were previously compiled by Schmidt et al. (for detailed methods on their compilation, see [17,40,41]). Briefly, we queried DataONE (a platform to access multiple data repositories) and the Dryad Digital Repository between 2017 – 2021 using binomial species names and 'microsat*' as keywords. We retained data from wild populations in their native range, and set a minimum sample size of 5 individuals per sample location identified in the original publications. The datasets comprised 51 species with a median 579 individuals per dataset, ranging from 127 – 2232 individuals (Table S1). We set an *a priori* cutoff of at least 10 sample locations per dataset for this study (median: 22 locations; range: 12-100). We did not set thresholds for the minimum area sampled because we were primarily interested in estimating *z* and F_{ST} from each dataset and testing relationships between them, which does not require sample sites to be representative of the species as a whole. We quantified population structure across the entire species sample using global F_{ST}. We estimated global F_{ST} for each dataset in R[42] with the basic.stats() function in the hierfstat package[43], which estimates F_{ST} as $(H_t - H_s)/H_t$, where H_t = total heterozygosity and H_s = mean heterozygosity of subpopulations.

To construct a GDAR for each dataset, we took a nested approach to artificially sample each study area. We sampled a square area centered on each genetic sample location with half-side lengths that were 10, 25, 50, 75, 90, and 99% of the study extent.

For each area sample, we recorded 1) the total number of alleles summed across loci; 2) rarefied allelic richness (hereafter *allelic richness*; rarefied to the smallest sample size of a sample

location for a given dataset); and 3) gene diversity[32] (evenness). These metrics differ in their sensitivity to the presence of rare alleles and thus to the number of individuals sampled. Allele count weights all alleles equally and is most strongly affected by sample size. It is also the most representative of the extinction of a "mutation" or allele, which has been argued to be a key focus of genetic conservation[44]. Gene diversity is most affected by the frequencies of common alleles, while rarefied allelic richness is intermediately affected by rare alleles. Allele count is analogous to the number of single nucleotide polymorphisms, or allelic variants, used in[8]. We estimated *z* of the power-law GDAR (genetic diversity = cA^z) for each genetic metric by taking the slope estimated for the relationship between log area and log genetic diversity. For datasets where this slope was not significant (linear regression, $p < 0.05$), we recorded slope (*z*) values as NA. This resulted in the removal of 4 datasets for allelic richness (zAR), and 6 datasets for gene diversity (zGD) for downstream analyses.

To quantify the dependence between the effects of area and population structure on genetic diversity, we ran a multiple regression with log area, global F_{ST}, and their interaction as predictors of each diversity metric (allele counts, allelic richness, and gene diversity) for a total of 3 models. We included all datasets in a single model with study as a random intercept. Models were fit in the lme4 package[45] in R. We then compared the effect sizes of area to models with only area as a predictor.

We next assessed the extent to which average *z* values could predict the percentage of genetic diversity lost for each of the 55 datasets individually—in other words, we tested whether use of a single *z* value could be useful for predicting loss in a given species, which would represent its use in applied conservation. To do this, we calculated genetic diversity change for each dataset based on (1) the GDAR using *z* values estimated for that dataset, and (2) using the mean *z* values

for each genetic metric. We compared observed and predicted values of genetic diversity loss using the mean *z* value and using the data-specific *z* value for the largest area loss (99%) for each of the nested sample areas per dataset. Because the ratio of area loss was the same across all sites and datasets, predicted genetic diversity loss differed only across datasets when study-specific *z* values were used (Fig. 4). We then averaged the percent loss across area samples to obtain the mean observed loss of genetic diversity for each dataset.

Trait-based predictions of z

We then explored the predictability of global F_{ST} and *z* values from readily accessible species-level trait data. We tested 3 traits that are related to population structure: body mass (g), individual home range area (km^2), and geographic range size (km^2). We restricted our analysis to mammals because they had the most data, and we could make consistent predictions about the relationships between traits and population structure. Generally, larger species tend to disperse further, have larger individual home ranges, and larger geographic ranges[46,47]. Additionally, species with larger home ranges generally have less spatially structured populations, while structure due to isolation by distance is likely higher in species with larger distributional ranges.

We compiled adult body mass data from the PanTHERIA database[48] via the R package traitdata[49]. We used home range sizes available from the HomeRange dataset[50,51], using individual, adult home ranges estimated from wild animals. Finally, we obtained data on geographic range sizes from species distribution maps available from the IUCN[52]. We filled in missing data values from the literature where possible. For species with missing home range data, we used the mean value of the genus if available. Because our focus was on model

predictive capacity, we disregarded collinearity among predictor variables. We also included the sample extent of each dataset (i.e., the area of the bounding box covering all sample sites) as an additional predictor. All three traits were available for 33 of the species in our data set. We related these predictors to global F_{ST} and *z* values using multiple linear regressions. For models with global F_{ST} as a response variable, which varies between 0 and 1, we fit beta regressions with a logit link function in the betareg package[53]. We used normally distributed errors for models with *z* values as response variables because *z* is not by definition bound by 0 and 1.

We then tested model predictive accuracy by partitioning our dataset into training and test datasets (80 and 20% of the data, respectively). We created 1000 partitions and recorded the coefficient of variation (root mean squared error divided by the mean observed *z* or F_{ST}) to measure the relative error rates of each model.

As an additional test, we assessed whether our model maintained similar predictive capacity for mammal F_{ST} values derived from an independent dataset, the MacroPopGen database[33,34]. MacroPopGen reports pairwise or global F_{ST} values for terrestrial vertebrates and freshwater fish across the Americas compiled from literature reports, and is based on studies that used microsatellite data. After filtering for mammal species, we applied additional filters for sample locations with more than 5 individuals and species with 10 or more sample locations for consistency with our compiled dataset. We note F_{ST} estimates from data with fewer individuals sampled or more local sampling are less likely to be associated with species-level traits. When global F_{ST} was not reported, we calculated mean pairwise F_{ST} values for populations within a study, which is correlated with global F_{ST}. In total, 53 F_{ST} estimates from MacroPopGen and trait data were available for 36 species (Table S5). We assessed predictability using the same approach described above.

Acknowledgements: We thank Amy Vandergast, Jonathan Chase, and the University of Manitoba Evolutionary Genetics class (BIOL4510) for insightful discussions and suggestions. This work was conducted as a part of the "Standardizing, Aggregating, Analyzing and Disseminating Global Wildlife Genetic and Genomic Data for Improved Management and Advancement of Community Best Practices Working Group" supported by the John Wesley Powell Center for Analysis and Synthesis, funded by the USGS. C.S. acknowledges the support of iDiv funded by the German Research Foundation (DFG–FZT 118, 202548816). C.G. was supported by a Natural Sciences and Engineering Research Council of Canada Discovery Grant.

References

1. Lande, R. & Shannon, S. The role of genetic variation in adaptation and population persistence in a changing environment. *Evolution* **50**, 434–437 (1996).

2. DeWoody, J. A., Harder, A. M., Mathur, S. & Willoughby, J. R. The long-standing significance of genetic diversity in conservation. *Molecular Ecology* **30**, 4147–4154 (2021).

3. Hoban, S. *et al.* Genetic diversity goals and targets have improved, but remain insufficient for clear implementation of the post-2020 global biodiversity framework. *Conservation Genetics* **24**, 181–191 (2023).

4. CBD. *Decision Adopted by the COP to the CBD 15/4. Kunming-Montreal Global Biodiversity Framework (2022a).* https://www.cbd.int/doc/decisions/cop-15/cop-15-dec-04-en.pdf (2022).

5. Paz-Vinas, I. *et al.* Uneven genetic data limits biodiversity assessments in protected areas globally. *Frontiers in Ecology and the Environment.* Preprint at https://doi.org/10.32942/X2ZC84 (*Accepted*).

6. Hogg, C. J. Translating genomic advances into biodiversity conservation. *Nat Rev Genet* **25**, 362–373 (2024).

7. Mimura, M. *et al.* Understanding and monitoring the consequences of human impacts on intraspecific variation. *Evolutionary Applications* **10**, 121–139 (2017).

8. Exposito-Alonso, M. *et al.* Genetic diversity loss in the Anthropocene. *Science* **377**, 1431–1435 (2022).

9. Connor, E. F. & McCoy, E. D. The Statistics and Biology of the Species-Area Relationship. *The American Naturalist* **113**, 791–833 (1979).

10. Lomolino, M. V. Ecology's Most General, Yet Protean Pattern: The Species-Area Relationship. *Journal of Biogeography* **27**, 17–26 (2000).

11. Storch, D., Keil, P. & Jetz, W. Universal species–area and endemics–area relationships at continental scales. *Nature* **488**, 78–81 (2012).

12. Keil, P., Storch, D. & Jetz, W. On the decline of biodiversity due to area loss. *Nature Communications* **6**, 8837 (2015).

13. Harte, J. & Kinzig, A. P. On the Implications of Species-Area Relationships for Endemism, Spatial Turnover, and Food Web Patterns. *Oikos* **80**, 417–427 (1997).

14. Pereira, H. M., Ziv, G. & Miranda, M. Countryside Species–Area Relationship as a Valid Alternative to the Matrix-Calibrated Species–Area Model. *Conservation Biology* **28**, 874–876 (2014).

15. Hoban, S. *et al.* Monitoring status and trends in genetic diversity for the Convention on Biological Diversity: An ongoing assessment of genetic indicators in nine countries. *Conservation Letters* **16**, e12953 (2023).

16. Frankham, R. Evaluation of proposed genetic goals and targets for the Convention on Biological Diversity. *Conservation Genetics* **1**, 1–6 (2022).

17. Schmidt, C., Mäkinen, J., Lessard, J.-P. & Garroway, C. J. Natural selection is less efficient at species range edges. EcoEvoRxiv Preprint at https://doi.org/10.32942/X2NK6N (2023).

18. Wright, S. The genetical structure of populations. *Annals of Eugenics* **15**, 323–354 (1951).

19. Medina, I., Cooke, G. M. & Ord, T. J. Walk, swim or fly? Locomotor mode predicts genetic differentiation in vertebrates. *Ecology Letters* **21**, 638–645 (2018).

20. Gamba, D. & Muchhala, N. Global patterns of population genetic differentiation in seed plants. *Molecular Ecology* 1–31 (2020) doi:10.1111/mmi.14505.

21. Schmidt, C., Dray, S. & Garroway, C. J. Genetic and species-level biodiversity patterns are linked by demography and ecological opportunity. *Evolution* **76**, 86–100 (2022).

22. Handel, S. N. Pollination ecology, plant population structure, and gene flow. in *Pollination Biology* 163–211 (Academic Press, Orlando, Florida, 1983).

23. Hillman, S. S., Drewes, R. C., Hedrick, M. S. & Hancock, T. V. Physiological vagility and its relationship to dispersal and neutral genetic heterogeneity in vertebrates. *Journal of Experimental Biology* **217**, 3356–3364 (2014).

24. Alsos, I. G. *et al.* Genetic consequences of climate change for northern plants. *Proceedings of the Royal Society B: Biological Sciences* **279**, 2042–2051 (2012).

25. Báldi, A. Habitat heterogeneity overrides the species–area relationship. *Journal of Biogeography* **35**, 675–681 (2008).

26. Triantis, K. A., Mylonas, M., Lika, K. & Vardinoyannis, K. A model for the species–area–habitat relationship. *Journal of Biogeography* **30**, 19–27 (2003).

27. Crist, T. O. & Veech, J. A. Additive partitioning of rarefaction curves and species–area relationships: unifying α-, β- and γ-diversity with sample size and habitat area. *Ecology Letters* **9**, 923–932 (2006).

28. Tjørve, E. & Tjørve, K. M. C. The species-area relationship, self-similarity, and the true meaning of the z-value. *Ecology* **89**, 3528–3533 (2008).

29. Wright, S. Isolation by distance. *Genetics* **28**, 114–138 (1943).

30. Weir, B. S. & Hill, W. G. Estimating F-statistics. *Annual Review of Genetics* **36**, 721–750 (2002).

31. Charlesworth, B. & Charlesworth, D. *Elements of Evolutionary Genetics*. (Roberts & Company Publishers, Greenwood Village, Colorado, USA, 2010).

32. Nei, M. Analysis of gene diversity in subdivided populations. *Proceedings of the National Academy of Sciences of the United States of America* **70**, 3321–3323 (1973).

33. Lawrence, E. R. *et al.* MacroPopGen Database: Geo-referenced population-specific microsatellite data across the American continents. *figshare* (2018).

34. Lawrence, E. R. *et al.* Geo-referenced population-specific microsatellite data across American continents, the MacroPopGen Database. *Scientific Data* **6**, 14 (2019).

35. Pflüger, F. J., Signer, J. & Balkenhol, N. Habitat loss causes non-linear genetic erosion in specialist species. *Global Ecology and Conservation* **17**, e00507 (2019).

36. Gargiulo, R., Budde, K. B. & Heuertz, M. Mind the lag: understanding genetic extinction debt for conservation. *Trends in Ecology & Evolution* (2024) doi:10.1016/j.tree.2024.10.008.

37. Pinto, A. V., Hansson, B., Patramanis, I., Morales, H. E. & van Oosterhout, C. The impact of habitat loss and population fragmentation on genomic erosion. *Conservation Genetics* **25**, 49–57 (2024).

38. Mualim, K. S. *et al.* Genetic diversity loss in the Anthropocene will continue long after habitat destruction ends. bioRXiv Preprint at https://doi.org/10.1101/2024.10.21.619096 (2024).

39. Exposito-Alonso, M. Understanding local plant extinctions before it is too late: bridging evolutionary genomics with global ecology. *New Phytologist* **237**, 2005–2011 (2023).

40. Schmidt, C., Domaratzki, M., Kinnunen, R. P., Bowman, J. & Garroway, C. J. Continent-wide effects of urbanization on bird and mammal genetic diversity. *Proceedings of the Royal Society B: Biological Sciences* **287**, 20192497 (2020).

41. Schmidt, C. & Garroway, C. J. Systemic racism alters wildlife genetic diversity. *Proceedings of the National Academy of Sciences* **119**, 0–3 (2022).

42. R Core Team. R: A Language and Environment for Statistical Computing. (2021).

43. Goudet, J. & Jombart, T. hierfstat: Estimation and Tests of Hierarchical F-Statistics. (2015).

44. Allendorf, F. W., Hössjer, O. & Ryman, N. What does effective population size tell us about loss of allelic variation? *Evolutionary Applications* **17**, e13733 (2024).

45. Bates, D., Mächler, M., Bolker, B. & Walker, S. Fitting linear mixed-effects models using lme4. *Journal of Statistical Software* **67**, (2015).

46. Bowman, J., Jaeger, J. A. G. & Fahrig, L. Dispersal distance of mammals is proportional to home range size. *Ecology* **83**, 2049–2055 (2002).

47. Jetz, W., Carbone, C., Fulford, J. & Brown, J. H. The Scaling of Animal Space Use. *Science* **306**, 266–268 (2004).

48. Jones, K. E. *et al.* PanTHERIA: a species-level database of life history, ecology, and geography of extant and recently extinct mammals. *Ecology* **90**, 2648–2648 (2009).

49. RS-eco. *Traitdata: Easy Access to Various Ecological Trait Data*. https://github.com/RS-eco/traitdata (2022).

50. Broekman, M. J. E. *et al.* HomeRange: A global database of mammalian home ranges. *Global Ecology and Biogeography* **32**, 198–205 (2023).

51. Hoeks, S. *HomeRange: This Package Provides Access to the HomeRange Dataset*. (2023).

52. IUCN. *The IUCN Red List of Threatened Species. Version 1.19 (May 2021)*. https://www.iucnredlist.org (2021).

53. Zeileis, A. *et al.* betareg: Beta Regression. (2021).

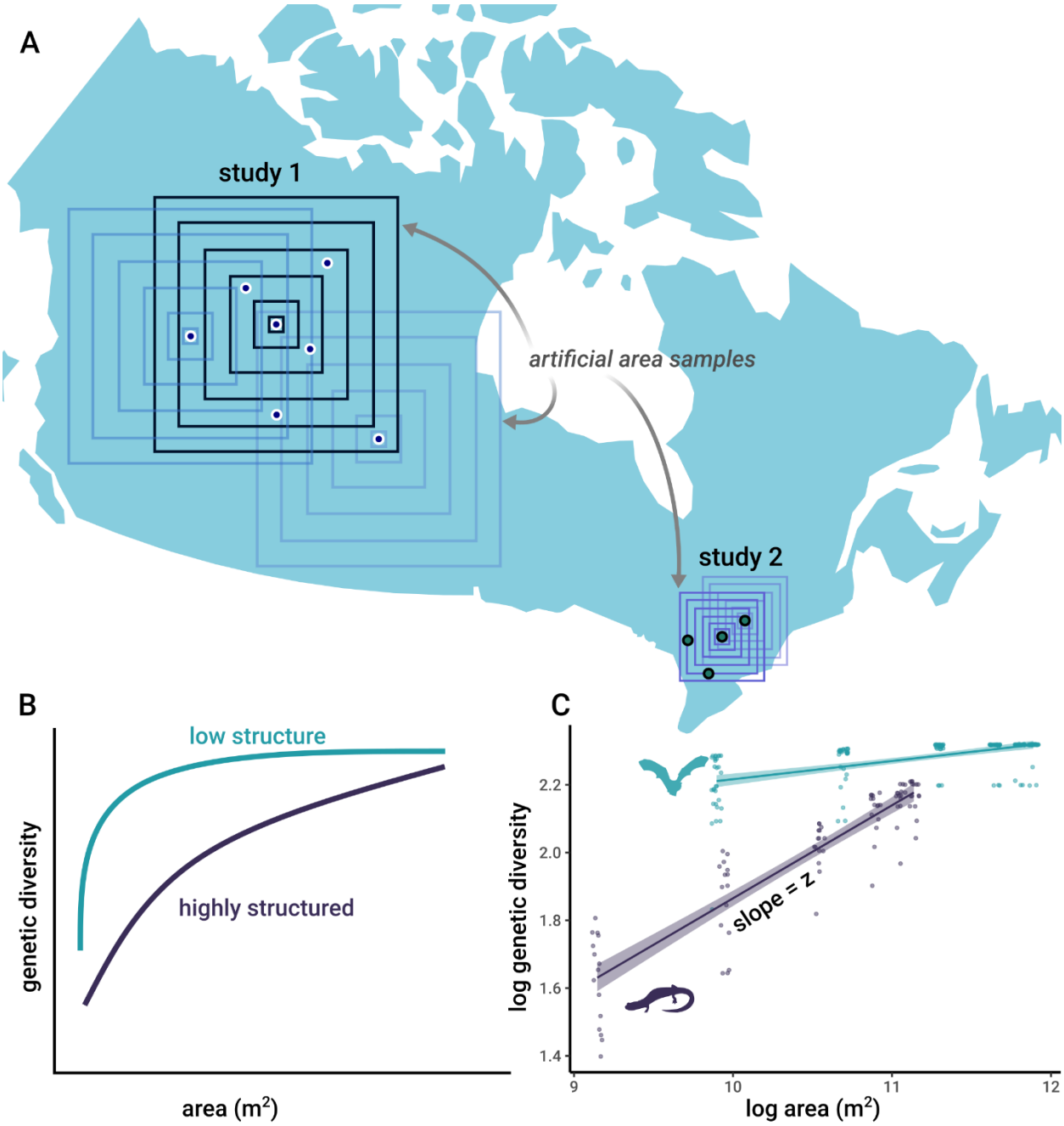

Figure 1. GDAR sampling design and predictions for two hypothetical studies. **A)** For each sample location within a study, we assessed genetic diversity as aggregates of all samples contained within each of 6 concentric quadrats of increasing size. **B)** We then constructed a study's GDAR as the average relationship with area across all its samples assessed in this way, with an estimated scaling exponent, *z*, describing the relationship between area and genetic diversity in log-log space. In species with little genetic structuring (low F_{ST}), alleles are more evenly spread over the landscape and even small areas can harbor large proportions of the alleles present in the entire study sample. Thus, we expect GDARs will more rapidly level off (shallow slope, smaller z) compared to species that are highly genetically structured (high F_{ST}, steep slope, high z). **C)** These predictions are demonstrated in two species with contrasting movement

abilities, the little brown bat (*Myotis lucifugus*) and the Mount Lyell salamander (*Hydromantes platycephalus*). In this example, genetic diversity is measured using allele count. Shaded regions are 95% confidence intervals of the fitted line. Due to its flight ability, we predict that the little brown bat should exhibit less population structure than a comparatively less vagile salamander species due to higher possibility of gene flow.

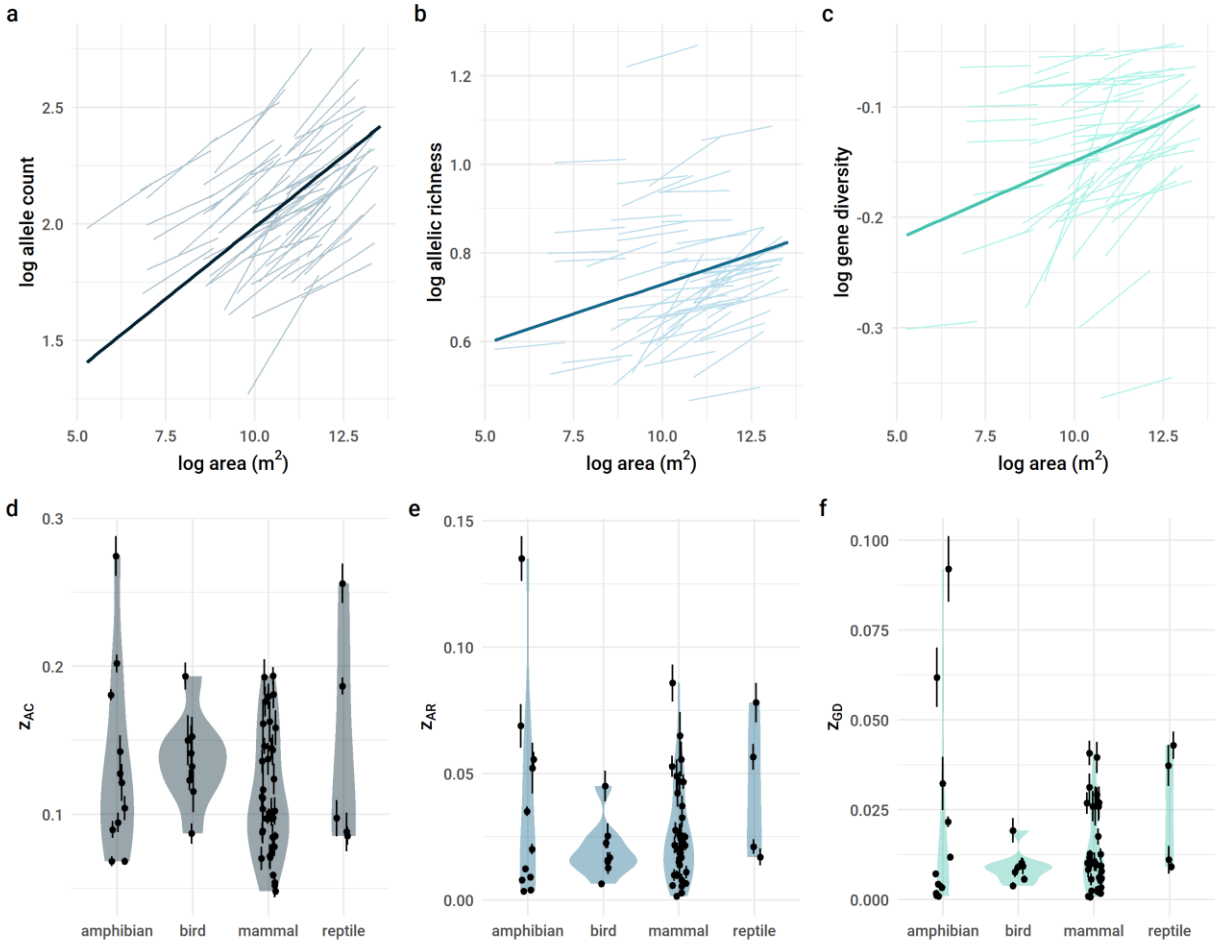

Figure 2. (**A-C**) Genetic diversity—area relationships in terrestrial vertebrates assessed across three genetic metrics. Lighter lines are log diversity vs. log area for each dataset. Dark lines depict the overall relationship across all datasets. The slope of each line is the scaling exponent *z*. (**D-F**) Plots of *z* values for each genetic metric (z_{AC} = allele count, z_{AR} = allelic richness, z_{GD} = gene diversity) by vertebrate class. Points represent estimated *z* values and lines denote the standard error.

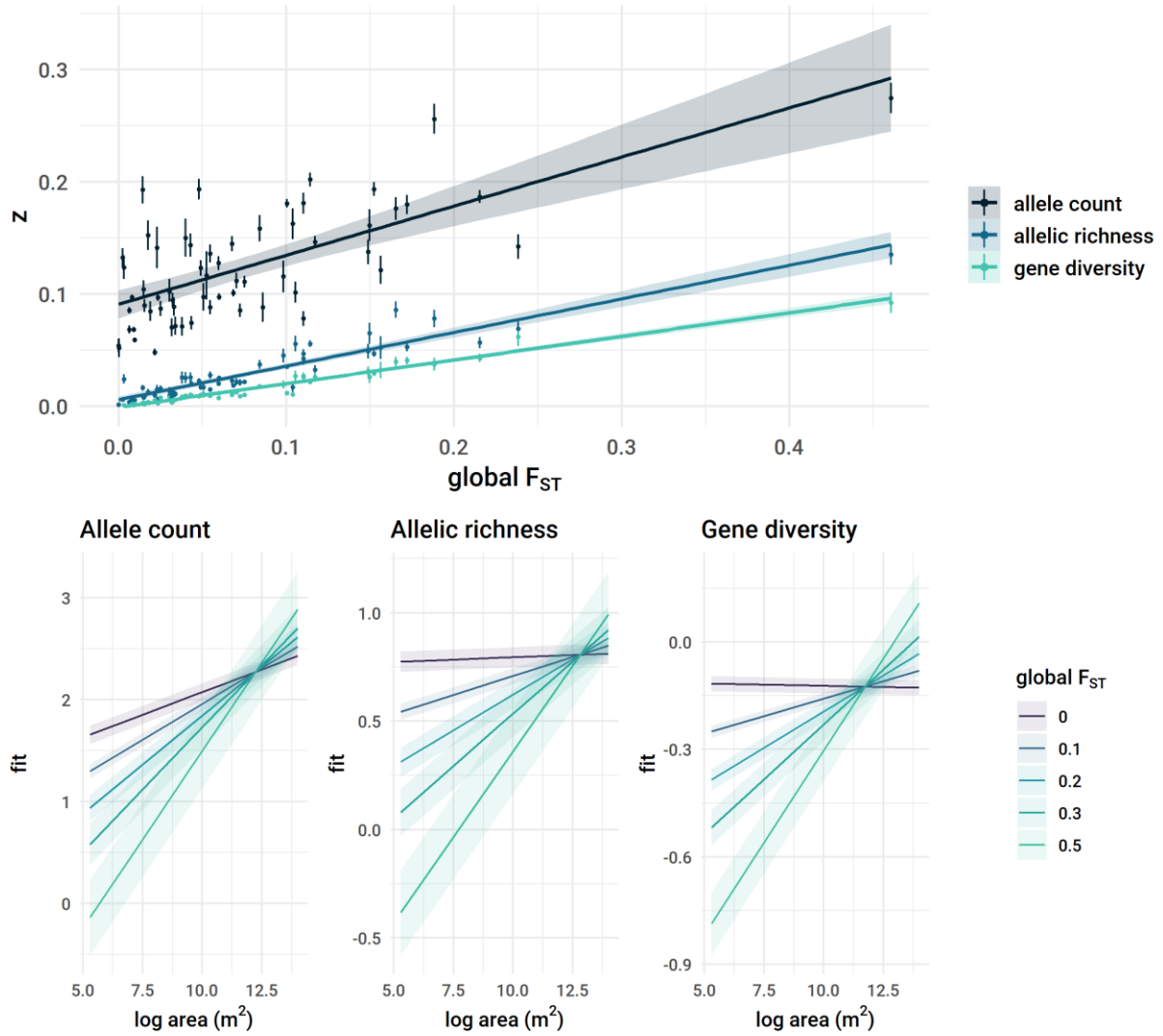

Figure 3. The effect of area on genetic diversity depends on population differentiation (measured with global F_{ST}). **(Top)** The top plot shows the strong correlation between study-specific *z* values and F_{ST} for all metrics of genetic diversity. Each point represents a single genetic dataset (some species are represented by multiple datasets), and lines denote the standard error of *z* estimates. **(Bottom)** Models fitted to the 51 species that included the main effects and interaction of log area and F_{ST} as predictors of genetic diversity. Ribbons denote 95% confidence intervals around the mean effect (solid line). For all diversity metrics, the effect of area strengthens as F_{ST} increases. Gene diversity and allelic richness are unrelated to area when there is no population structure (F_{ST} = 0). The three metrics are shown in order of decreasing sensitivity to sample size: allele counts, rarefied allelic richness, and gene diversity.

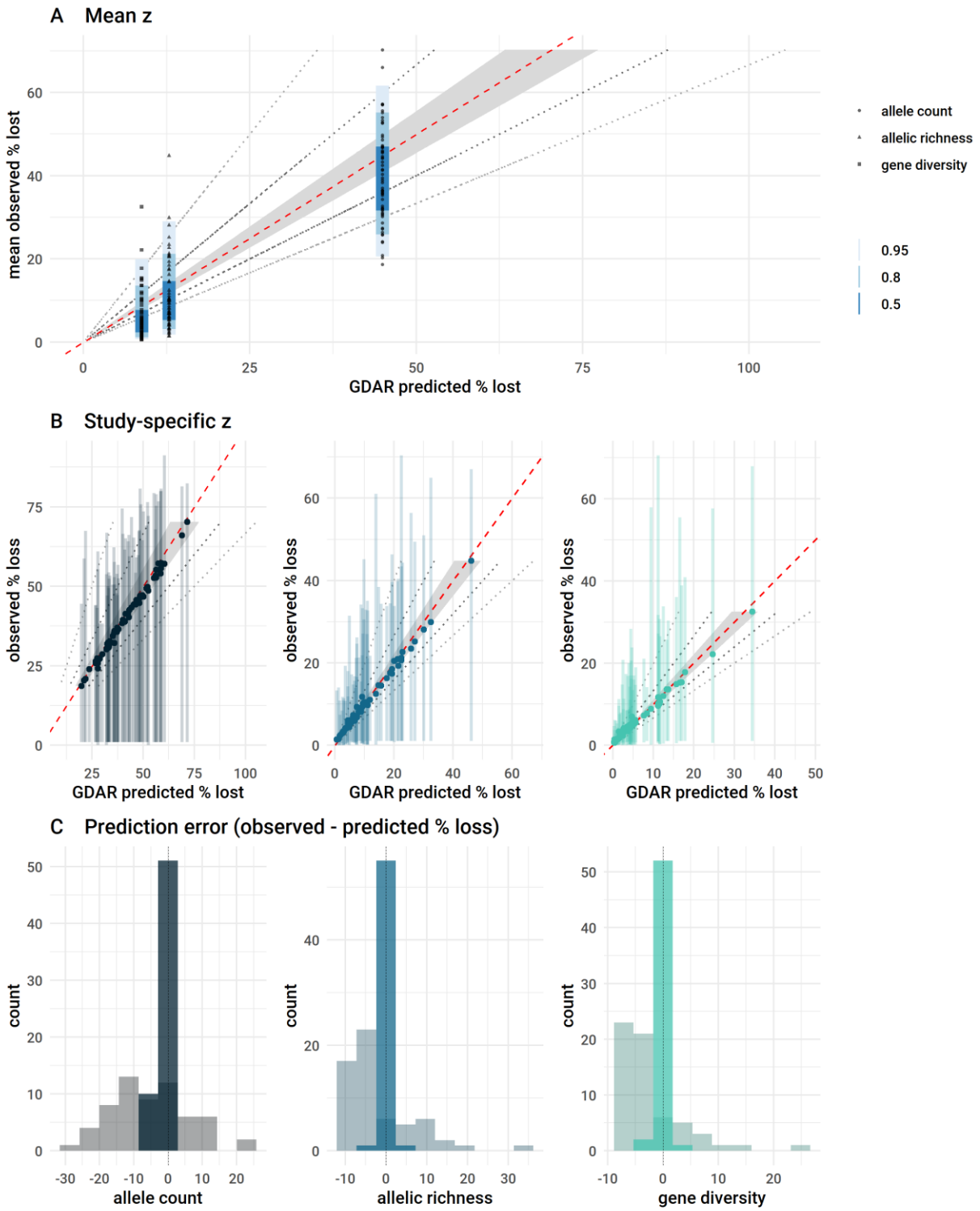

Figure 4. Observed versus predicted change in genetic diversity. **(A-B)** Each point represents the average percent decrease of alleles, allelic richness, or gene diversity after removing 99% of area for each dataset. Red dashed lines depict 100% correlation, grey bands show 10% intervals above or below observed loss, dark and light grey dotted lines show 25% and 50% intervals

around observed loss. **(A)** Predicted vs. observed genetic diversity change from GDARs using the mean *z* value across all studies for each genetic metric (see Table S2). Colored slabs show the distribution of data within 95%, 80%, and 50% quantiles. **(B)** Predicted genetic diversity change from GDAR using study-specific *z* values. Lines flanking points show the range of observed percent genetic diversity loss for each study. **(C)** Histograms show the spread of prediction residuals (the difference between mean observed diversity loss and predicted diversity loss) for each diversity metric. Prediction errors using study level *z* values are shown by more opaque bars, and more transparent bars show the distribution of prediction error using average *z* values. Dashed vertical lines indicate 0 prediction error.

Supplementary information for: Variability, drivers, and utility of genetic diversity-area relationships in terrestrial vertebrates

Chloé Schmidt, Sean Hoban, Deborah M. Leigh, Walter Jetz, Colin J. Garroway

Contents:

Tables S1 – S5

Figures S1 – S4

Table S1. Data summary. The number of sites, total individuals across all sites, estimated global F_{ST}, estimated z values for each genetic metric, and references are given for each dataset (rows). NA values for *z* indicate that the effect of area on genetic diversity was not significant and corresponding datasets were thus omitted from further analyses of *z*.

class	species	sites	individuals	global F_{ST}	zAC	zAR	zGD	references
amphibian	*Ambystoma maculatum*	56	1292	0.0092	0.07	0.00	0.00	[1,2]
amphibian	*Lithobates sylvaticus*	39	888	0.0064	0.07	0.00	0.00	[1,2]
amphibian	*Lithobates sylvaticus*	29	766	0.0598	0.13	0.02	0.01	[3,4]
amphibian	*Ambystoma maculatum*	19	489	0.1564	0.12	0.05	0.03	[5,6]
amphibian	*Ascaphus montanus*	100	1968	0.1143	0.20	0.06	0.02	[7,8]
amphibian	*Ambystoma barbouri*	76	1601	0.1005	0.18	0.03	0.01	[9,10]
amphibian	*Plethodon albagula*	21	343	0.0149	0.10	0.01	0.00	[11,12]
amphibian	*Ambystoma maculatum*	22	626	0.0324	0.09	0.01	0.00	[13,14]
amphibian	*Lithobates sylvaticus*	22	469	0.0156	0.09	0.01	0.00	[13,14]
amphibian	*Rana draytonii*	17	298	0.2384	0.14	0.07	0.06	[15,16]
amphibian	*Hydromantes platycephalus*	15	195	0.4605	0.27	0.14	0.09	[17,18]
bird	*Poecile atricapillus*	32	911	0.0480	0.19	0.02	0.01	[19,20]
bird	*Campylorhynchus brunneicapillus*	12	363	0.0984	0.12	0.05	0.02	[21,22]
bird	*Geospiza fortis*	11	202	0.0401	0.15	0.03	0.01	[23,24]
bird	*Geospiza fuliginosa*	11	198	0.0229	0.14	0.02	0.01	[23,24]
bird	*Geospiza fuliginosa*	21	517	0.0025	0.13	0.01	NA	[25,26]
bird	*Aphelocoma californica*	30	463	0.0492	0.12	0.02	0.01	[27,28]
bird	*Poecile hudsonicus*	13	260	0.0176	0.15	0.01	0.00	[29,30]
bird	*Strix occidentalis*	17	423	0.0251	0.09	0.02	0.01	[31]
mammal	*Sus scrofa*	18	551	0.1040	0.16	0.02	0.01	[32,33]
mammal	*Capreolus capreolus*	13	371	0.1489	0.14	0.05	0.03	[34,35]
mammal	*Pekania pennanti*	34	722	0.0685	0.10	0.02	0.01	[36,37]
mammal	*Nyctalus leisleri*	14	183	0.0190	0.08	NA	NA	[38,39]
mammal	*Myotis lucifugus*	15	735	0.0005	0.05	NA	NA	[40,41]
mammal	*Vicugna vicugna*	14	374	0.1498	0.16	0.06	0.03	[42,43]
mammal	*Tamiasciurus douglasii*	14	186	0.0305	0.10	0.01	0.01	[44,45]
mammal	*Tamiasciurus hudsonicus*	12	188	0.0525	0.12	NA	NA	[44,45]

mammal	*Lepus americanus*	39	853	0.1524	0.19	0.05	0.03	[46,47]
mammal	*Ursus arctos*	16	831	0.1055	0.10	0.06	0.03	[48,49]
mammal	*Ursus maritimus*	11	318	0.0435	0.07	0.02	0.01	[48,49]
mammal	*Myotis lucifugus*	21	1054	0.0145	0.19	0.02	0.00	[50,51]
mammal	*Ovis canadensis*	14	579	0.1102	0.08	0.04	0.03	[52,53]
mammal	*Meles meles*	30	675	0.1721	0.18	0.05	0.04	[54,55]
mammal	*Microtus arvalis*	53	855	0.0064	0.09	0.00	0.00	[56,57]
mammal	*Canis latrans*	41	303	0.0236	0.10	0.01	0.00	[58,59]
mammal	*Rousettus aegyptiacus*	34	490	0.0705	0.11	0.02	0.01	[60,61]
mammal	*Myotis lucifugus*	29	1310	0.0000	0.05	0.00	NA	[62,63]
mammal	*Myotis septentrionalis*	15	896	0.0032	0.12	0.02	0.00	[62,63]
mammal	*Martes americana*	29	653	0.0217	0.05	0.01	0.01	[64,65]
mammal	*Lemmus lemmus*	13	276	0.0304	0.10	0.01	0.01	[66,67]
mammal	*Odocoileus hemionus*	60	1714	0.1173	0.15	0.03	0.03	[68,69]
mammal	*Rangifer tarandus*	18	634	0.0319	0.07	0.01	0.00	[70,71]
mammal	*Lynx canadensis*	28	702	0.0097	0.06	0.01	0.00	[72,73]
mammal	*Felis silvestris*	15	620	0.0841	0.16	0.04	0.02	[74,75]
mammal	*Alces alces*	16	694	0.0429	0.14	0.03	0.01	[76,77]
mammal	*Ursus maritimus*	14	2232	0.0332	0.09	0.01	0.01	[78,79]
mammal	*Ursus americanus*	28	504	0.1104	0.18	0.05	0.03	[80,81]
mammal	*Myotis escalerai*	15	442	0.0378	0.07	0.03	0.01	[82,83]
mammal	*Lynx rufus*	52	1646	0.0600	0.10	0.03	0.01	[84,85]
mammal	*Odocoileus virginianus*	64	2069	0.0081	0.10	0.01	0.00	[86,87]
mammal	*Rangifer tarandus*	27	508	0.0752	0.11	0.02	0.01	[88,89]
mammal	*Rhinolophus ferrumequinum*	27	950	0.0339	0.07	0.01	0.01	[90,91]
mammal	*Rangifer tarandus*	27	802	0.0676	0.14	0.02	0.01	[92,93]
mammal	*Miniopterus schreibersii*	22	312	0.0548	0.09	0.01	0.01	[94,95]
mammal	*Sorex antinorii*	17	213	0.0546	0.14	0.03	0.01	[96,97]
mammal	*Cervus elaphus*	27	638	0.1654	0.18	0.09	0.04	[98,99]
reptile	*Gopherus polyphemus*	46	933	0.2153	0.19	0.06	0.04	[100,101]
reptile	*Amblyrhynchus cristatus*	13	467	0.0860	0.09	NA	NA	[102,103]
reptile	*Liolaemus tenius*	15	127	0.1883	0.26	0.08	0.04	[104,105]

reptile	*Dipsosaurus dorsalis*	19	308	0.0725	0.09	0.02	0.01	[106,107]
reptile	*Uma inornata*	13	268	0.0507	0.10	0.02	0.01	[108,109]

References

1. Coster, S. S., Babbitt, K. J., Cooper, A. & Kovach, A. I. Data from: Limited influence of local and landscape factors on finescale gene flow in two pond-breeding amphibians. *Dryad* (2015) doi:10.5061/dryad.4903q.
2. Coster, S. S., Babbitt, K. J., Cooper, A. & Kovach, A. I. Limited influence of local and landscape factors on finescale gene flow in two pond-breeding amphibians. *Molecular Ecology* **24**, 742–758 (2015).
3. Duncan, S. I., Crespi, E. J., Mattheus, N. M. & Rissler, L. J. History matters more when explaining genetic diversity within the context of the core-periphery hypothesis. *Molecular Ecology* **24**, 4323–4336 (2015).
4. Duncan, S. I., Crespi, E. J., Mattheus, N. M. & Rissler, L. J. Data from: History matters more when explaining genetic diversity within the context of the core-periphery hypothesis. *Dryad* (2015) doi:10.5061/dryad.fp1k7.
5. Johnson, B. B., White, T. A., Phillips, C. A. & Zamudio, K. R. Data from: Asymmetric introgression in a spotted salamander hybrid zone. *Dryad* (2015) doi:10.5061/dryad.v23r2.
6. Johnson, B. B., White, T. A., Phillips, C. A. & Zamudio, K. R. Asymmetric Introgression in a Spotted Salamander Hybrid Zone. *Journal of Heredity* 608–617 (2015) doi:10.1093/jhered/esv042.
7. Metzger, G., Espindola, A., Waits, L. P. & Sullivan, J. Genetic structure across broad spatial and temporal scales: Rocky Mountain tailed frogs (*Ascaphus montanus*; Anura: Ascaphidae) in the inland temperate rainforest. *Journal of Heredity* 700–710 (2015) doi:10.1093/jhered/esv061.
8. Metzger, G., Espindola, A., Waits, L. P. & Sullivan, J. Data from: Genetic structure across broad spatial and temporal scales: Rocky Mountain tailed frogs (Ascaphus montanus;

Anura: Ascaphidae) in the inland temperate rainforest. *Dryad* (2015) doi:10.5061/dryad.2pb57.

9. Micheletti, S. J. & Storfer, A. Data from: An approach for identifying cryptic barriers to gene flow that limit species' geographic ranges. *Dryad* (2016) doi:10.5061/dryad.c6kj2.
10. Micheletti, S. J. & Storfer, A. An approach for identifying cryptic barriers to gene flow that limit species' geographic ranges. *Molecular Ecology* **26**, 490–504 (2017).
11. Peterman, W. E., Connette, G. M., Semlitsch, R. D. & Eggert, L. S. Ecological resistance surfaces predict fine-scale genetic differentiation in a terrestrial woodland salamander. *Molecular Ecology* **23**, 2402–2413 (2014).
12. Peterman, W. E., Connette, G. M., Semlitsch, R. D. & Eggert, L. S. Data from: Ecological resistance surfaces predict fine scale genetic differentiation in a terrestrial woodland salamander Dryad. *Dryad* (2014) doi:10.5061/dryad.m4f17.
13. Richardson, J. L. Data from: Divergent landscape effects on population connectivity in two co-occurring amphibian species. *Dryad* (2012) doi:10.5061/dryad.51b94.
14. Richardson, J. L. Divergent landscape effects on population connectivity in two co-occurring amphibian species. *Molecular Ecology* **21**, 4437–4451 (2012).
15. Richmond, J. Q., Barr, K. R., Backlin, A. R., Vandergast, A. G. & Fisher, R. N. Evolutionary dynamics of a rapidly receding southern range boundary in the threatened California Red-Legged Frog (Rana draytonii). *Evolutionary Applications* **6**, 808–822 (2013).
16. Richmond, J. Q., Barr, K. R., Backlin, A. R., Vandergast, A. G. & Fisher, R. N. Data from: Evolutionary dynamics of a rapidly receding southern range boundary in the threatened California Red-Legged Frog (Rana draytonii). *Dryad* (2013).

17. Rovito, S. M. & Schoville, S. D. Testing models of refugial isolation, colonization and population connectivity in two species of montane salamanders. *Heredity* **119**, 265–274 (2017).
18. Rovito, S. M. & Schoville, S. D. Data from: Testing models of refugial isolation, colonization and population connectivity in two species of montane salamanders. *Dryad* (2017) doi:10.5061/dryad.c197n.
19. Adams, R. V. & Burg, T. M. Data from: Influence of ecological and geological features on rangewide patterns of genetic structure in a widespread passerine. *Heredity* (2014) doi:10.5061/dryad.k086v.
20. Adams, R. V. & Burg, T. M. Influence of ecological and geological features on rangewide patterns of genetic structure in a widespread passerine. *Heredity* **114**, 143–154 (2015).
21. Barr, K. R. *et al.* Habitat fragmentation in coastal southern California disrupts genetic connectivity in the cactus wren (Campylorhynchus brunneicapillus). *Molecular Ecology* **24**, 2349–2363 (2015).
22. Barr, K. R. *et al.* Data from: Habitat fragmentation in coastal southern California disrupts genetic connectivity in the Cactus Wren (Campylorhynchus brunneicapillus). *Molecular Ecology* (2015) doi:10.5061/dryad.j5h92.
23. Farrington, H. L., Lawson, L. P., Clark, C. M. & Petren, K. The Evolutionary History of Darwin's Finches: Speciation, Gene Flow, and Introgression in a Fragmented Landscape. *Evolution* **68**, 2932–2944 (2014).
24. Farrington, H. L., Lawson, L. P., Clark, C. M. & Petren, K. Data from: The evolutionary history of Darwin's finches: speciation, gene flow, and introgression in a fragmented landscape. 227028 bytes (2014) doi:10.5061/DRYAD.J92FS.

25. Galligan, T. H. *et al.* Panmixia supports divergence with gene flow in Darwin's small ground finch, Geospiza fuliginosa, on Santa Cruz, Galápagos Islands. *Molecular Ecology* **21**, 2106–2115 (2012).
26. Galligan, T. H. *et al.* Data from: Panmixia supports divergence with gene flow in Darwin's small ground finch, Geospiza fuliginosa, on Santa Cruz, Galápagos Islands. 45489 bytes (2012) doi:10.5061/DRYAD.4SB063BN.
27. Gowen, F. C. *et al.* Speciation in Western Scrub-Jays, Haldane's rule, and genetic clines in secondary contact. *BMC Evolutionary Biology* **14**, 1–15 (2014).
28. Gowen, F. C. *et al.* Data from: Speciation in Western Scrub-Jays, Haldane's rule, and genetic clines in secondary contact. *BMC Evolutionary Biology* (2014) doi:10.5061/dryad.57f48.
29. Lait, L. A. & Burg, T. M. When east meets west: Population structure of a high-latitude resident species, the boreal chickadee (Poecile hudsonicus). *Heredity* **111**, 321–329 (2013).
30. Lait, L. A. & Burg, T. M. Data from: When east meets west: population structure of a high-latitude resident species, the boreal chickadee (Poecile hudsonicus). *Heredity* (2013) doi:10.5061/dryad.82hs7.
31. Miller, M. P., Davis, R. J., Mullins, T. D., Haig, S. M. & Forsman, E. D. Microsatellite markers, habitat quality, and sample location data for Northern Spotted Owls (Strix occidentalis caurina). (2017) doi:10.5066/F7J67FVW.
32. Alexandri, P. *et al.* Distinguishing migration events of different timing for wild boar in the Balkans. *Journal of Biogeography* **44**, 259–270 (2017).
33. Alexandri, P. *et al.* Data from: Distinguishing migration events of different timing for wild boar in the Balkans. 38412420 bytes (2017) doi:10.5061/DRYAD.T722H.

34. Baker, K. H. & Rus Hoelzel, A. Data from: Evolution of population genetic structure of the British roe deer by natural and anthropogenic processes (Capreolus capreolus). 131072 bytes (2013) doi:10.5061/DRYAD.V90P5.

35. Baker, K. H. & Rus Hoelzel, A. Evolution of population genetic structure of the British roe deer by natural and anthropogenic processes (*Capreolus capreolus*). *Ecol Evol* **3**, 89–102 (2013).

36. Bertrand, P., Bowman, J., Dyer, R., Manseau, M. & PJ, W. Sex-specific graphs: Relating group-specific topology to demographic and landscape data. *Molecular Ecology* **26**, 3898–3912 (2017).

37. Bertrand, P., Bowman, J., Dyer, R., Manseau, M. & PJ, W. Data from: Sex-specific graphs: Relating group-specific topology to demographic and landscape data. *Molecular Ecology* (2017) doi:10.5061/dryad.167d5.

38. Boston, E. S. M., Montgomery, W. I., Hynes, R. & Prodöhl, P. A. New insights on postglacial colonization in western Europe: the phylogeography of the Leisler's bat (*Nyctalus leisleri*). *Proc. R. Soc. B.* **282**, 20142605 (2015).

39. Boston, E. S. M., Montgomery, W. I., Hynes, R. & Prodöhl, P. A. Data from: New insights on postglacial colonisation in Western Europe: the phylogeography of the Leisler's bat (Nyctalus leisleri). 34926 bytes (2015) doi:10.5061/DRYAD.6G6R6.

40. Burns, L. E., Frasier, T. R. & Broders, H. G. Genetic connectivity among swarming sites in the wide ranging and recently declining little brown bat (Myotis lucifugus). *Ecology and Evolution* **4**, 4130–4149 (2014).

41. Burns, L. E., Frasier, T. R. & Broders, H. G. Data from: Genetic connectivity among swarming sites in the wide ranging and recently declining little brown bat (Myotis lucifugus). *Ecology and Evolution* (2014) doi:10.5061/dryad.hs37s.

42. Casey, C. S. *et al.* Comparing genetic diversity and demographic history in co-distributed wild South American camelids. *Heredity* **121**, 387–400 (2018).

43. Casey, C. S. *et al.* Data from: Comparing genetic diversity and demographic history in co-distributed wild South American camelids. 59614 bytes (2018) doi:10.5061/DRYAD.G8D77FT.

44. Chavez, A. S., Saltzberg, C. J. & Kenagy, G. J. Genetic and phenotypic variation across a hybrid zone between ecologically divergent tree squirrels (Tamiasciurus). *Molecular Ecology* **20**, 3350–3366 (2011).

45. Chavez, A. S., Saltzberg, C. J. & Kenagy, G. J. Data from: Genetic and phenotypic variation across a hybrid zone between ecologically divergent tree squirrels (Tamiasciurus). *Molecular Ecology* (2011) doi:10.5061/dryad.195qg.

46. Cheng, E., Hodges, K. E., Melo-Ferreira, J., Alves, P. C. & Mills, L. S. Conservation implications of the evolutionary history and genetic diversity hotspots of the snowshoe hare. *Molecular Ecology* **23**, 2929–2942 (2014).

47. Cheng, E., Hodges, K. E., Melo-Ferreira, J., Alves, P. C. & Mills, L. S. Data from: Conservation implications of the evolutionary history and genetic diversity hotspots of the snowshoe hare. *Molecular Ecology* (2014) doi:10.5061/dryad.dh63p.

48. Cronin, M. A. & MacNeil, M. D. Genetic relationships of extant brown bears (Ursus arctos) and polar bears (Ursus maritimus). *Journal of Heredity* **103**, 873–881 (2012).

49. Cronin, M. A. & MacNeil, M. D. Data from: Genetic relationships of extant brown bears (Ursus arctos) and polar bears (Ursus maritimus). *Journal of Heredity* (2012) doi:10.5061/dryad.q30rt.

50. Davy, C. M. *et al.* Prelude to a panzootic: gene flow and immunogenetic variation in northern little brown myotis vulnerable to bat white-nose syndrome. *FACETS* **2**, 690–714 (2017).

51. Davy, C. M. *et al.* Data from: Prelude to a panzootic: gene flow and immunogenetic variation in northern little brown myotis vulnerable to bat white-nose syndrome. *FACETS* (2017) doi:10.5061/dryad.h7n25.

52. Epps, C. W., Crowhurst, R. S. & Nickerson, B. S. Assessing changes in functional connectivity in a desert bighorn sheep metapopulation after two generations. *Molecular Ecology* **27**, 2334–2346 (2018).

53. Epps, C. W., Crowhurst, R. S. & Nickerson, B. S. Data from: Assessing changes in functional connectivity in a desert bighorn sheep metapopulation after two generations. *Molecular Ecology* (2018) doi:10.5061/dryad.mp71t50.

54. Frantz, A. C. *et al.* Revisiting the phylogeography and demography of European badgers (Meles meles) based on broad sampling, multiple markers and simulations. *Heredity* **113**, 443–453 (2014).

55. Frantz, A. C. *et al.* Data from: Re-visiting the phylogeography and demography of European badgers (Meles meles) based on broad sampling, multiple markers and simulations. 140089 bytes (2014) doi:10.5061/DRYAD.5NM5G.

56. Gauffre, B. *et al.* Short-term variations in gene flow related to cyclic density fluctuations in the common vole. *Molecular Ecology* **23**, 3214–3225 (2014).

57. Gauffre, B. *et al.* Data from: Short-term variations in gene flow related to cyclic density fluctuations in the common vole. 197880 bytes (2014) doi:10.5061/DRYAD.JF7SN.

58. Heppenheimer, E. *et al.* Demographic history influences spatial patterns of genetic diversityin recently expanded coyote (Canis latrans) populations. *Heredity* 1–13 (2017) doi:10.1038/s41437-017-0014-5.

59. Heppenheimer, E. *et al.* Data from: Demographic history influences spatial patterns of genetic diversity in recently expanded coyote (Canis latrans) populations. 92698 bytes (2017) doi:10.5061/DRYAD.2T965.

60. Hulva, P. *et al.* Data from: Environmental margin and island evolution in Middle Eastern populations of the Egyptian fruit bat. 228070 bytes (2012) doi:10.5061/DRYAD.K68K8.

61. Hulva, P. *et al.* Environmental margin and island evolution in M iddle E astern populations of the E gyptian fruit bat. *Molecular Ecology* **21**, 6104–6116 (2012).

62. Johnson, L. N. L. *et al.* Population Genetic Structure Within and among Seasonal Site Types in the Little Brown Bat (Myotis lucifugus) and the Northern Long-Eared Bat (M. septentrionalis). *PLOS ONE* **10**, 1–18 (2015).

63. Johnson, L. N. L. *et al.* Data from: Population genetic structure within and among seasonal site types in the little brown bat (Myotis lucifugus) and the northern long-eared bat (M. septentrionalis). *PLOS ONE* (2015) doi:10.5061/dryad.47nm0.

64. Koen, E. L., Bowman, J. & Wilson, P. J. Data from: Node-based measures of connectivity in genetic networks. *Molecular Ecology Resources* (2015) doi:10.5061/dryad.4tg23.

65. Koen, E. L., Bowman, J. & Wilson, P. J. Node-based measures of connectivity in genetic networks. *Molecular Ecology Resources* **16**, 69–79 (2016).

66. Lagerholm, V. K. *et al.* Data from: Run to the hills: gene flow among mountain areas leads to low genetic differentiation in the Norwegian lemming. 70687 bytes (2016) doi:10.5061/DRYAD.KR966.

67. Lagerholm, V. K. *et al.* Run to the hills: gene flow among mountain areas leads to low genetic differentiation in the Norwegian lemming. *Biological Journal of the Linnean Society* **121**, 1–14 (2017).

68. Latch, E. K., Reding, D. M., Heffelfinger, J. R., Alcalá-Galván, C. H. & Rhodes, O. E. Range-wide analysis of genetic structure in a widespread, highly mobile species (Odocoileus hemionus) reveals the importance of historical biogeography. *Molecular Ecology* **23**, 3171–3190 (2014).

69. Latch, E. K., Reding, D. M., Heffelfinger, J. R., Alcalá-Galván, C. H. & Rhodes, O. E. Data from: Range-wide analysis of genetic structure in a widespread, highly mobile species (Odocoileus hemionus) reveals the importance of historical biogeography. *Molecular Ecology* (2014) doi:10.5061/dryad.ns2jn.

70. Mager, K. H., Colson, K. E., Groves, P. & Hundertmark, K. J. Population structure over a broad spatial scale driven by nonanthropogenic factors in a wide-ranging migratory mammal, Alaskan caribou. *Molecular Ecology* **23**, 6045–6057 (2014).

71. Mager, K. H., Colson, K. E., Groves, P. & Hundertmark, K. J. Data from: Population structure over a broad spatial scale driven by non-anthropogenic factors in a wide-ranging migratory mammal, Alaskan caribou. *Molecular Ecology* (2014) doi:10.5061/dryad.3hp5v.

72. Marrotte, R. R. *et al.* Multi-species genetic connectivity in a terrestrial habitat network. *Movement Ecology* **5**, 1–11 (2017).

73. Marrotte, R. R. *et al.* Data from: Multi-species genetic connectivity in a terrestrial habitat network. *Movement Ecology* (2017) doi:10.5061/dryad.qn4kq.

74. Mattucci, F., Oliveira, R., Lyons, L. A., Alves, P. C. & Randi, E. European wildcat populations are subdivided into five main biogeographic groups: consequences of Pleistocene climate changes or recent anthropogenic fragmentation? *Ecology and Evolution* **6**, 3–22 (2016).

75. Mattucci, F., Oliveira, R., Lyons, L. A., Alves, P. C. & Randi, E. Data from: European wildcat populations are subdivided into five main biogeographic groups: consequences of Pleistocene climate changes or recent anthropogenic fragmentation? 681984 bytes (2016) doi:10.5061/DRYAD.KB13M.

76. Niedziałkowska, M. *et al.* Data from: The contemporary genetic pattern of European moose is shaped by postglacial recolonization, bottlenecks, and the geographical barrier of the Baltic Sea. 102689 bytes (2015) doi:10.5061/DRYAD.0TC6Q.

77. Niedziałkowska, M. *et al.* The contemporary genetic pattern of European moose is shaped by postglacial recolonization, bottlenecks, and the geographical barrier of the Baltic Sea. *Biol. J. Linn. Soc.* **117**, 879–894 (2016).

78. Peacock, E. *et al.* Implications of the circumpolar genetic structure of polar bears for their conservation in a rapidly warming Arctic. *PLoS ONE* **10**, 1–30 (2015).

79. Peacock, E. *et al.* Data from: Implications of the circumpolar genetic structure of polar bears for their conservation in a rapidly warming Arctic. 595858 bytes (2015) doi:10.5061/DRYAD.V2J1R.

80. Puckett, E. E., Etter, P. D., Johnson, E. A. & Eggert, L. S. Phylogeographic analyses of American black bears (Ursus americanus) suggest four glacial refugia and complex patterns of postglacial admixture. *Molecular Biology and Evolution* **32**, 2338–2350 (2015).

81. Puckett, E. E., Etter, P. D., Johnson, E. A. & Eggert, L. S. Data from: Phylogeographic analyses of American black bears (Ursus americanus) suggest four glacial refugia and complex patterns of post-glacial admixture. *Molecular Biology and Evolution* (2015) doi:10.5061/dryad.dc02b.

82. Razgour, O., Salicini, I., Ibáñez, C., Randi, E. & Juste, J. Unravelling the evolutionary history and future prospects of endemic species restricted to former glacial refugia. *Molecular Ecology* **24**, 5267–5283 (2015).

83. Razgour, O., Salicini, I., Ibáñez, C., Randi, E. & Juste, J. Data from: Unravelling the evolutionary history and future prospects of endemic species restricted to former glacial refugia. 2802205 bytes (2015) doi:10.5061/DRYAD.V1V47.

84. Reding, D. M., Bronikowski, A. M., Johnson, W. E. & Clark, W. R. Pleistocene and ecological effects on continental-scale genetic differentiation in the bobcat (Lynx rufus). *Molecular Ecology* **21**, 3078–3093 (2012).

85. Reding, D. M., Bronikowski, A. M., Johnson, W. E. & Clark, W. R. Data from: Pleistocene and ecological effects on continental-scale genetic differentiation in the bobcat (Lynx rufus). *Molecular Ecology* (2012) doi:10.5061/dryad.d3t16pd2.

86. Robinson, S. J., Samuel, M. D., Lopez, D. L. & Shelton, P. The walk is never random: Subtle landscape effects shape gene flow in a continuous white-tailed deer population in the Midwestern United States. *Molecular Ecology* **21**, 4190–4205 (2012).

87. Robinson, S. J., Samuel, M. D., Lopez, D. L. & Shelton, P. Data from: The walk is never random: subtle landscape effects shape gene flow in a continuous white-tailed deer population in the Midwestern United States. *Molecular Ecology* (2012) doi:10.5061/dryad.p7639.

88. Serrouya, R. *et al.* Population size and major valleys explain microsatellite variation better than taxonomic units for caribou in western Canada. *Molecular Ecology* **21**, 2588–2601 (2012).

89. Serrouya, R. *et al.* Data from: Population size and major valleys explain microsatellite variation better than taxonomic units for caribou in western Canada. 114056 bytes (2012) doi:10.5061/DRYAD.250C3S47.

90. Tournayre, O. *et al.* Integrating population genetics to define conservation units from the core to the edge of *Rhinolophus ferrumequinum* western range. *Ecology and Evolution* **9**, 12272–12290 (2019).

91. Tournayre, O. *et al.* Data from: Integrating population genetics to define conservation units from the core to the edge of Rhinolophus ferrumequinum western range. 104872 bytes (2020) doi:10.5061/DRYAD.R44T5DK.

92. Weckworth, B. V., Musiani, M., McDevitt, A. D., Hebblewhite, M. & Mariani, S. Reconstruction of caribou evolutionary history in Western North America and its implications for conservation. *Molecular Ecology* **21**, 3610–3624 (2012).

93. Weckworth, B. V., Musiani, M., McDevitt, A. D., Hebblewhite, M. & Mariani, S. Data from: Reconstruction of caribou evolutionary history in Western North America and its implications for conservation. *Molecular Ecology* (2012) doi:10.5061/dryad.gn22271h.

94. Witsenburg, F. *et al.* How a haemosporidian parasite of bats gets around: the genetic structure of a parasite, vector and host compared. *Molecular Ecology* **24**, 926–940 (2015).

95. Witsenburg, F. *et al.* Data from: How a haemosporidian parasite of bats gets around: the genetic structure of a parasite, vector and host compared. 418639 bytes (2015) doi:10.5061/DRYAD.2M1P0.

96. Yannic, G., Basset, P., Büchi, L., Hausser, J. & Broquet, T. Data from: Scale-specific sex-biased dispersal in the Valais shrew unveiled by genetic variation on the Y chromosome, autosomes, and mitochondrial DNA. 86016 bytes (2011) doi:10.5061/DRYAD.8K3423TS.

97. Yannic, G., Basset, P., Büchi, L., Hausser, J. & Broquet, T. Scale-specific sex-biased dispersal in the Valais shrew unveiled by genetic variation on the Y chromosome, autosomes, and mitochondrial DNA. *Evolution* **66**, 1737–1750 (2012).

98. Zachos, F. E. *et al.* Genetic Structure and Effective Population Sizes in European Red Deer (Cervus elaphus) at a Continental Scale: Insights from Microsatellite DNA. *Journal of Heredity* **107**, 318–326 (2016).

99. Zachos, F. E. *et al.* Data from: Genetic structure and effective population sizes in European red deer (Cervus elaphus) at a continental scale: insights from microsatellite DNA. 98504 bytes (2016) doi:10.5061/DRYAD.1V6P1.

100. Gaillard, D. *et al.* Range-wide and regional patterns of population structure and genetic diversity in the gopher tortoise. *Journal of Fish and Wildlife Management* **8**, 497–512 (2017).

101. Gaillard, D. *et al.* Data from: Range-wide and regional patterns of population structure and genetic diversity in the gopher tortoise. 2527036 bytes (2017) doi:10.5061/DRYAD.NK064.

102. MacLeod, A. *et al.* Hybridization masks speciation in the evolutionary history of the Galápagos marine iguana. *Proceedings of the Royal Society B: Biological Sciences* **282**, 20150425 (2015).
103. MacLeod, A. *et al.* Data from: Hybridization masks speciation in the evolutionary history of the Galápagos marine iguana. 19278179 bytes (2015) doi:10.5061/DRYAD.PP6BM.
104. Muñoz-Mendoza, C. *et al.* Geography and past climate changes have shaped the evolution of a widespread lizard from the Chilean hotspot. *Molecular Phylogenetics and Evolution* **116**, 157–171 (2017).
105. Muñoz-Mendoza, C. *et al.* Data from: Geography and past climate changes have shaped the evolution of a widespread lizard from the Chilean hotspot. 273270 bytes (2017) doi:10.5061/DRYAD.JK183.
106. Valdivia-Carrillo, T., García-De León, F. J., Blázquez, Ma. C., Gutiérrez-Flores, C. & González Zamorano, P. Phylogeography and Ecological Niche Modeling of the Desert Iguana (Dipsosaurus dorsalis, Baird & Girard 1852) in the Baja California Peninsula. *Journal of Heredity* **108**, 640–649 (2017).
107. Valdivia-Carrillo, T., García-De León, F. J., Blázquez, Ma. C., Gutiérrez-Flores, C. & González Zamorano, P. Data from: Phylogeography and ecological niche modelling of the desert iguana (Dipsosaurus dorsalis, Baird & Girard 1852) in the Baja California Peninsula. 13137255 bytes (2017) doi:10.5061/DRYAD.6R7QN.
108. Vandergast, A. G. *et al.* Drifting to oblivion? Rapid genetic differentiation in an endangered lizard following habitat fragmentation and drought. *Diversity and Distributions* **22**, 344–357 (2016).

109. Vandergast, A. G. *et al.* Dryad Data -- Drifting to oblivion? Rapid genetic differentiation in an endangered lizard following habitat fragmentation and drought. (2016) doi:10.5061/dryad.30t5b.

Table S2. GDAR scaling exponents (z-values) for terrestrial vertebrates summarized across taxonomic groups (overall values) and for each taxonomic class. Means and standard deviations of z-values are given for allele counts (z_{AC}), allelic richness (z_{AR}), and gene diversity GDARs (z_{GD}).

	z_{AC}	z_{AR}	z_{GD}
overall	0.12 ± 0.05	0.03 ± 0.02	0.02 ± 0.02
amphibian	0.13 ± 0.06	0.04 ± 0.04	0.02 ± 0.03
bird	0.14 ± 0.03	0.02 ± 0.01	0.01 ± 0.00
mammal	0.11 ± 0.04	0.03 ± 0.02	0.01 ± 0.01
reptile	0.14 ± 0.08	0.04 ± 0.03	0.03 ± 0.02

Table S3. Comparison of area effect sizes between models with area alone, and global F_{ST} and an area*F_{ST} interaction as predictors. Effect sizes and standard errors are given for area, F_{ST}, and the interaction between area and F_{ST} where applicable. All effects were significant ($p<0.05$) in all models. The area effect is strongly reduced when F_{ST} and their interaction are included in the model. For gene diversity and allelic richness, when populations are panmictic ($F_{ST} = 0$), the effect of area is negligible (bold values). The coefficient for the interaction terms are orders of magnitude larger than the area effect, demonstrating that the effect of area is strongly mediated by population structure (see also Figure S2 for plotted interaction effects). We show the effect size of F_{ST} only for complete understanding of the magnitude of the interactive effect with area. We caution against causal interpretations of F_{ST} on genetic diversity because genetic diversity (alpha diversity) and genetic differentiation (beta diversity) reflect two measures of diversity that influence each other and are products of the same processes.

genetic metric	model	area	F_{ST}	area*F_{ST} interaction
gene diversity	area	0.01 ± 0.0003	--	--
	interaction	**-0.001 ± 0.0004**	-2.44 ± 0.11	0.21 ± 0.004
allelic richness	area	0.02 ± 0.0005	--	--
	interaction	**0.004 ± 0.0007**	-3.95 ± 0.24	0.31 ± 0.007
allele count	area	0.13 ± 0.001	--	--
	interaction	0.09 ± 0.001	-6.33 ± 0.46	0.50 ± 0.01

Table S4. Model summaries for relationships between F_{ST}, *z* values derived from allele count (zAC), allelic richness (zAR), and gene diversity (zGD), and predictor variables including: home range size (km^2), species range size (km^2), species body mass (g), and the area of the spatial extent of the sample locations in each dataset (km^2). All predictors were log-transformed prior to analysis. Because F_{ST} is bounded by 0 and 1, we used a beta regression and report pseudo-R^2 to summarize explained variation. *Z* values are not bounded by 0 and 1 thus we used linear regressions with normally distributed errors and report adjusted R^2 (R^2_{adj}), which corrects for the number of predictors included in the model, to summarize explained variation. Estimated slopes for each predictor are given with 95% confidence intervals. Relationships were typically stronger in the F_{ST} model compared to *z* models, where predictor effects tended to be small.

	predictor	**estimate**	**95% CI**
F_{ST}	home range	-0.19	-0.34 – -0.04
pseudo R^2 = 0.52	range size	-0.44	-0.89 – 0.01
	body mass	0.30	0.14 – 0.45
	sampled area size	0.20	0.10 – 0.30
zAC	home range	-0.02	-0.03 – -0.01
R^2_{adj} = 0.39	range size	0.01	-0.02 – 0.04
	body mass	0.01	-0.00 – 0.02
	sampled area size	0.01	0.00 – 0.02
zAR	home range	0.00	-0.01 – -0.00
R^2_{adj} = 0.38	range size	-0.01	-0.03 – -0.00
	body mass	0.01	0.00 – 0.01
	sampled area size	0.00	0.00 – 0.01
zGD	home range	0.00	-0.01 – -0.00
R^2_{adj} = 0.42	range size	-0.01	-0.01 – 0.00
	body mass	0.00	0.00 – 0.01
	sampled area size	0.00	0.00 – 0.00

Table S5. F_{ST} estimates from the MacroPopGen database and associated trait data.

species	F_{ST}	mass (g)	species range size (km2)	home range size (km2)	sample area (km2)
Alces alces	0.14	461900.76	23096275.49	40.49	175366.25
Alces alces	0.10	461900.76	23096275.49	40.49	1771220.04
Bison bison	0.12	624577.07	140673.07	605.92	2570587.13
Chrysocyon brachyurus	0.13	23325.00	4335910.28	54.07	3007362.49
Ctenomys minutus	0.20	92.00	54952.67	0.00	1164.51
Cynomys ludovicianus	0.12	797.05	1820824.74	0.00	319.71
Cynomys parvidens	0.29	899.98	31805.77	0.00	13315.57
Didelphis virginiana	0.07	2442.08	6033226.94	0.44	1098.05
Gulo gulo	0.07	12792.49	24394376.49	553.13	10655064.79
Lepus americanus	0.18	1568.42	9597267.58	0.08	19945447.02
Lontra canadensis	0.07	8087.42	19086449.84	0.17	191718.98
Lycalopex vetulus	0.03	4233.47	1782063.08	3.85	2323208.40
Lynx rufus	0.07	6374.47	9879514.31	19.88	9189982.82
Lynx rufus	0.10	6374.47	9879514.31	19.88	10394522.78
Lynx rufus	0.02	6374.47	9879514.31	19.88	168693.39
Marmota flaviventris	0.13	3709.73	1718256.72	0.04	159109.65
Martes americana	0.06	873.69	7637869.53	4.36	11660211.07
Martes americana	0.25	873.69	7637869.53	4.36	6760157.05
Pekania pennanti	0.14	3750.00	3711380.88	26.97	5743415.25
Microtus californicus	0.22	57.42	287643.37	0.00	76221.24
Ochotona princeps	0.22	157.63	894661.41	0.00	1434.21
Odocoileus virginianus	0.01	75901.25	14410636.17	1.39	1048733.76
Ondatra zibethicus	0.18	991.31	14688578.52	0.01	11328640.61
Oreamnos americanus	0.19	72105.40	801852.34	39.50	4725770.76
Ovis canadensis	0.16	74644.87	532974.92	19.56	63031.27
Ovis canadensis	0.26	74644.87	532974.92	19.56	1837485.48
Ovis dalli	0.16	70194.13	816225.07	7.84	2537227.55
Panthera onca	0.11	83943.09	9026158.26	161.37	26153976.40
Panthera onca	0.10	83943.09	9026158.26	161.37	26001315.13
Panthera onca	0.04	83943.09	9026158.26	161.37	367694.81
Peromyscus leucopus	0.04	18.07	5831351.77	0.00	64.76
Peromyscus leucopus	0.02	18.07	5831351.77	0.00	69760.20
Peromyscus maniculatus	0.16	19.98	13030881.66	0.00	71652.19
Puma concolor	0.03	53954.05	21145707.25	219.93	1502430.99
Puma concolor	0.09	53954.05	21145707.25	219.93	802285.37
Puma concolor	0.09	53954.05	21145707.25	219.93	49202.25
Puma concolor	0.09	53954.05	21145707.25	219.93	920939.26
Rangifer tarandus	0.35	109088.50	18660769.81	426.50	514089.62
Rangifer tarandus	0.04	109088.50	18660769.81	426.50	2002962.38
Rangifer tarandus	0.09	109088.50	18660769.81	426.50	1494784.44
Rangifer tarandus	0.13	109088.50	18660769.81	426.50	15220188.89

Rattus norvegicus	0.07	282.89	18826152.77	0.02	63.83
Tamias ruficaudus	0.08	60.06	147850.63	0.00	72050.94
Tamias striatus	0.05	90.50	4197616.69	0.00	24743.56
Urocitellus brunneus	0.26	300.00	1286.80	0.01	31682.52
Ursus americanus	0.23	110500.00	10469239.77	131.07	481369.34
Ursus americanus	0.11	110500.00	10469239.77	131.07	62483.39
Ursus arctos	0.15	196287.50	24216958.81	337.72	3104094.30
Ursus arctos	0.05	196287.50	24216958.81	337.72	706656.94
Ursus maritimus	0.03	371703.81	22605603.23	78541.43	9409086.03
Vicugna vicugna	0.14	47499.61	618703.14	0.03	469293.97
Vulpes velox	0.08	2088.00	599398.12	11.80	956737.27

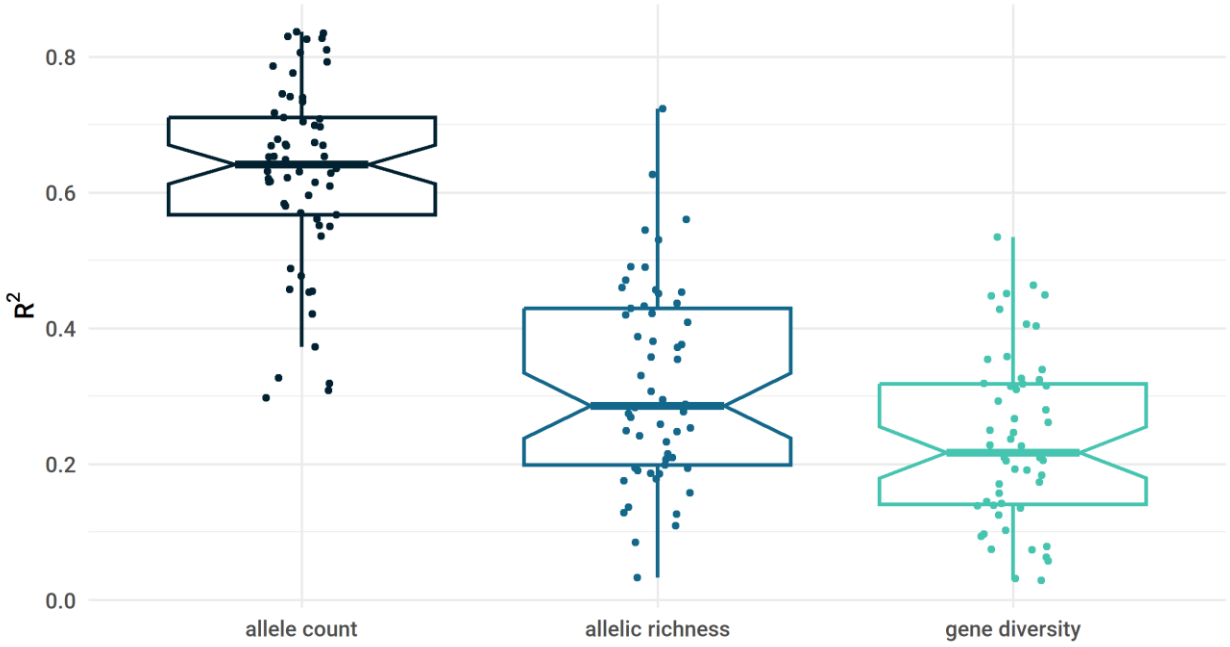

Figure S1. Box plots of variance in genetic diversity explained by area (R^2) for each genetic metric. Points are the R^2 of a simple linear model of the log-log relationship between each genetic metric (x axis) and area for each dataset. As expected, the variance in diversity explained by area is higher in genetic diversity metrics that are more strongly affected by sample size. This general pattern was consistent across all taxonomic groups.

Figure S2. Genetic diversity vs area plotted on a log-log scale for all 61 datasets. Red-shaded regions are 95% confidence intervals for the effect of area on genetic diversity. The slopes of these relationships are the scaling exponents *z* (values are reported in each plot title; they are NA when the relationship was not significant). Plots for allele count, allelic richness, and gene diversity are shown consecutively: note the genetic metric on the y axis. Point color denotes sample size, with lighter colors indicating greater numbers of individuals sampled.

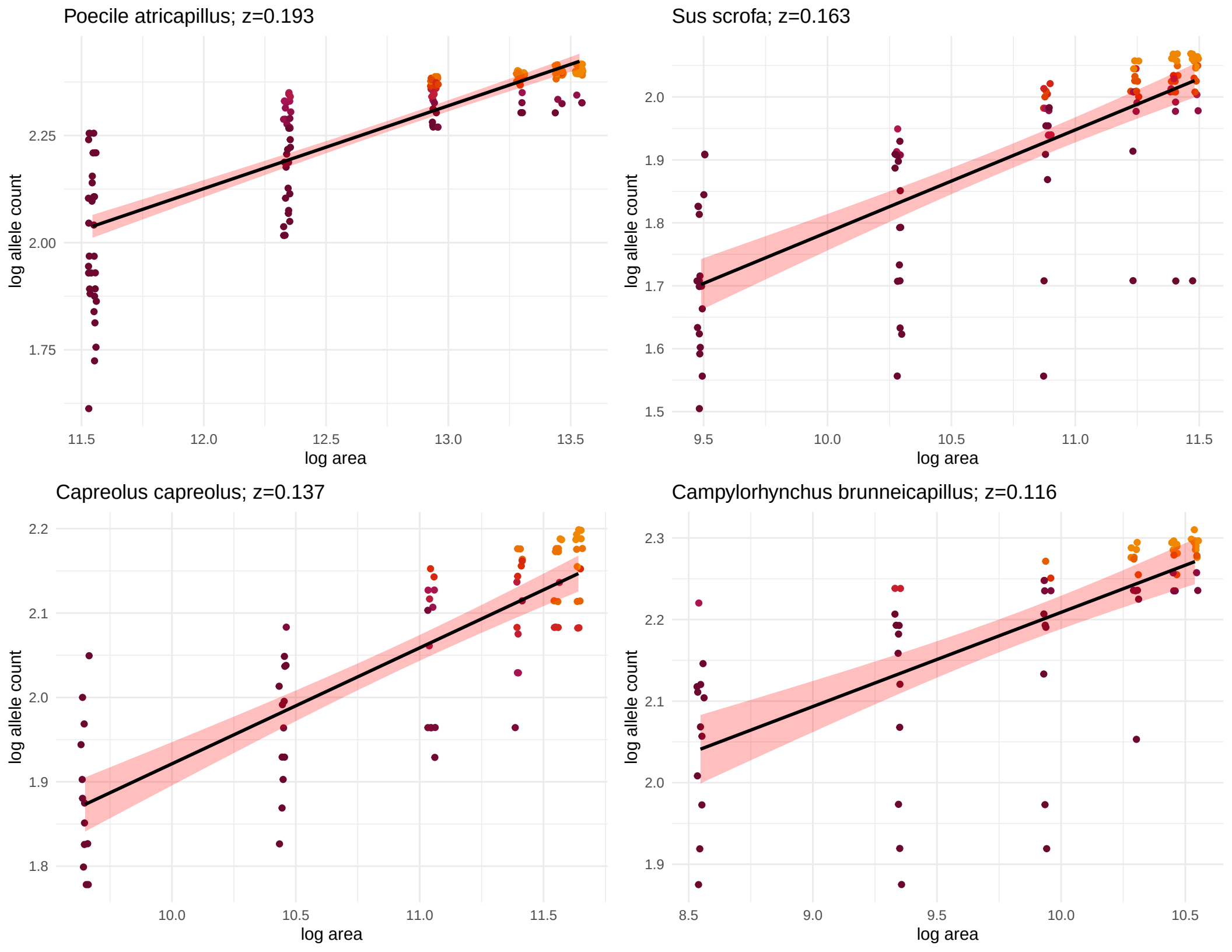
Poecile atricapillus; z=0.193
log allele count
log area
2.25
2.00
1.75
11.5
12.0
12.5
13.0
13.5
Sus scrofa; z=0.163
log allele count
log area
2.0
1.9
1.8
1.7
1.6
1.5
9.5
10.0
10.5
11.0
11.5
Capreolus capreolus; z=0.137
log allele count
log area
2.2
2.1
2.0
1.9
1.8
10.0
10.5
11.0
11.5
Campylorhynchus brunneicapillus; z=0.116
log allele count
log area
2.3
2.2
2.1
2.0
1.9
8.5
9.0
9.5
10.0
10.5

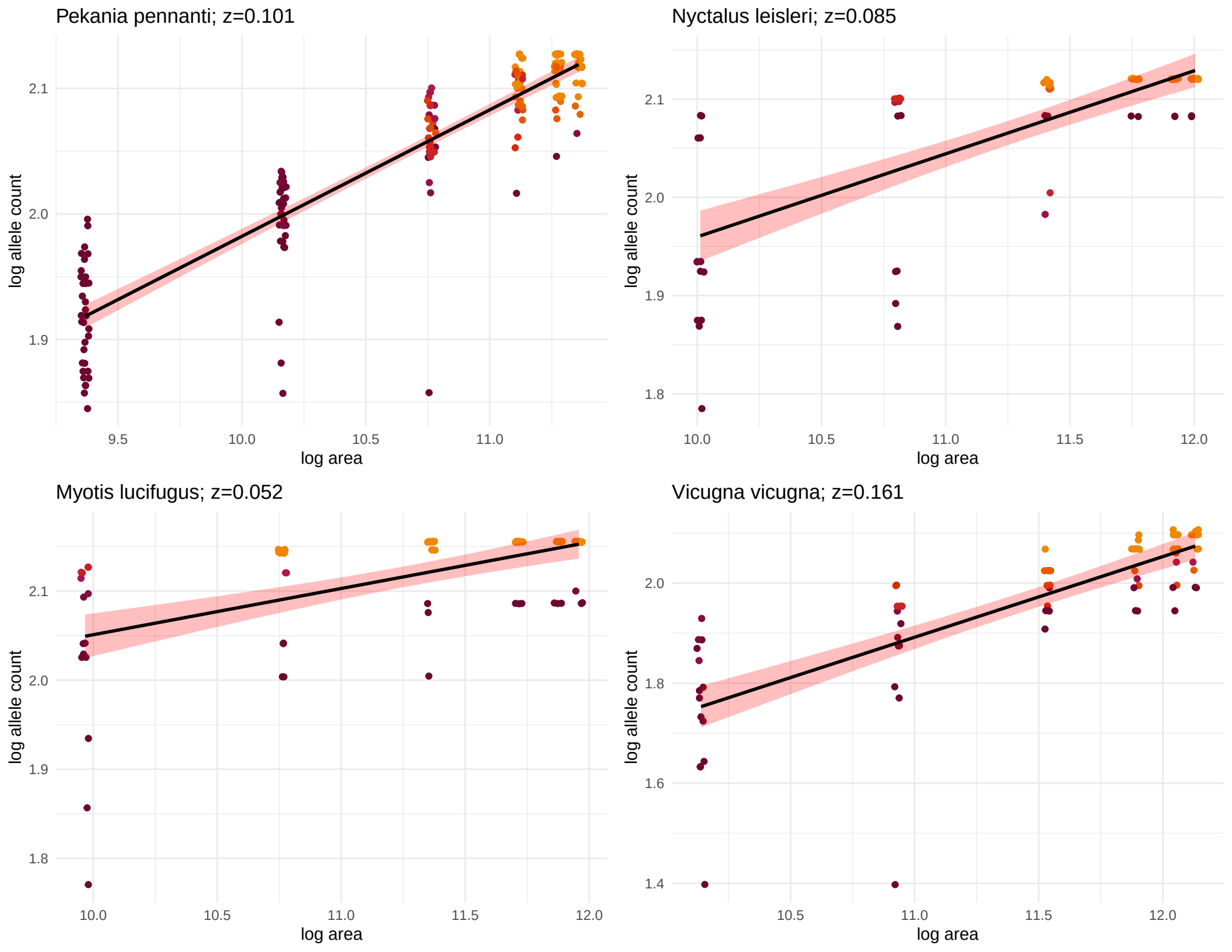
Pekania pennanti; z=0.101
Nyctalus leisleri; z=0.085
Myotis lucifugus; z=0.052
Vicugna vicugna; z=0.161
log allele count
log area
2.1
2.0
1.9
1.8
1.6
1.4
9.5
10.0
10.5
11.0
11.5
12.0

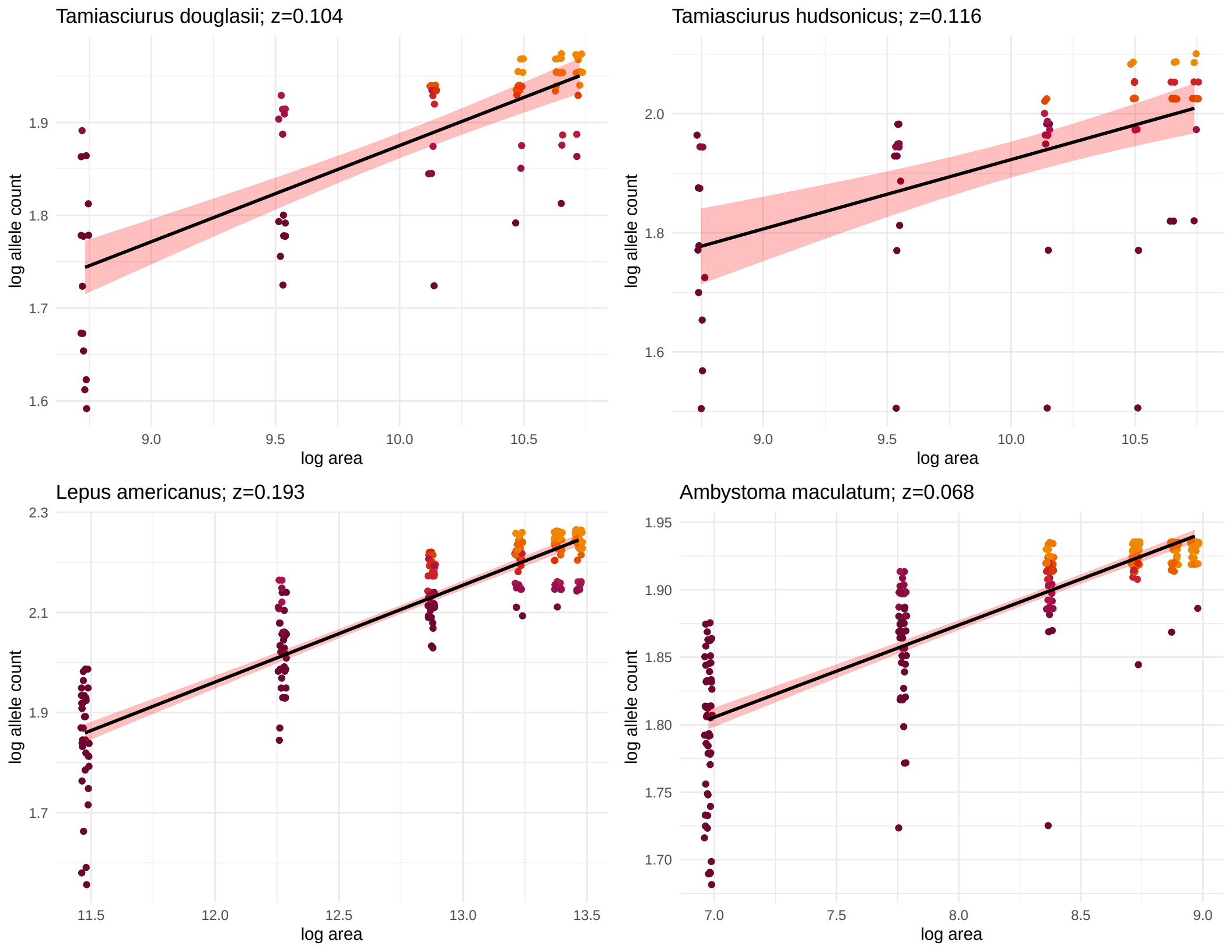
Tamiasciurus douglasii; z=0.104
log allele count
log area
1.6
1.7
1.8
1.9
9.0
9.5
10.0
10.5
Tamiasciurus hudsonicus; z=0.116
log allele count
log area
1.6
1.8
2.0
9.0
9.5
10.0
10.5
Lepus americanus; z=0.193
log allele count
log area
1.7
1.9
2.1
2.3
11.5
12.0
12.5
13.0
13.5
Ambystoma maculatum; z=0.068
log allele count
log area
1.70
1.75
1.80
1.85
1.90
1.95
7.0
7.5
8.0
8.5
9.0

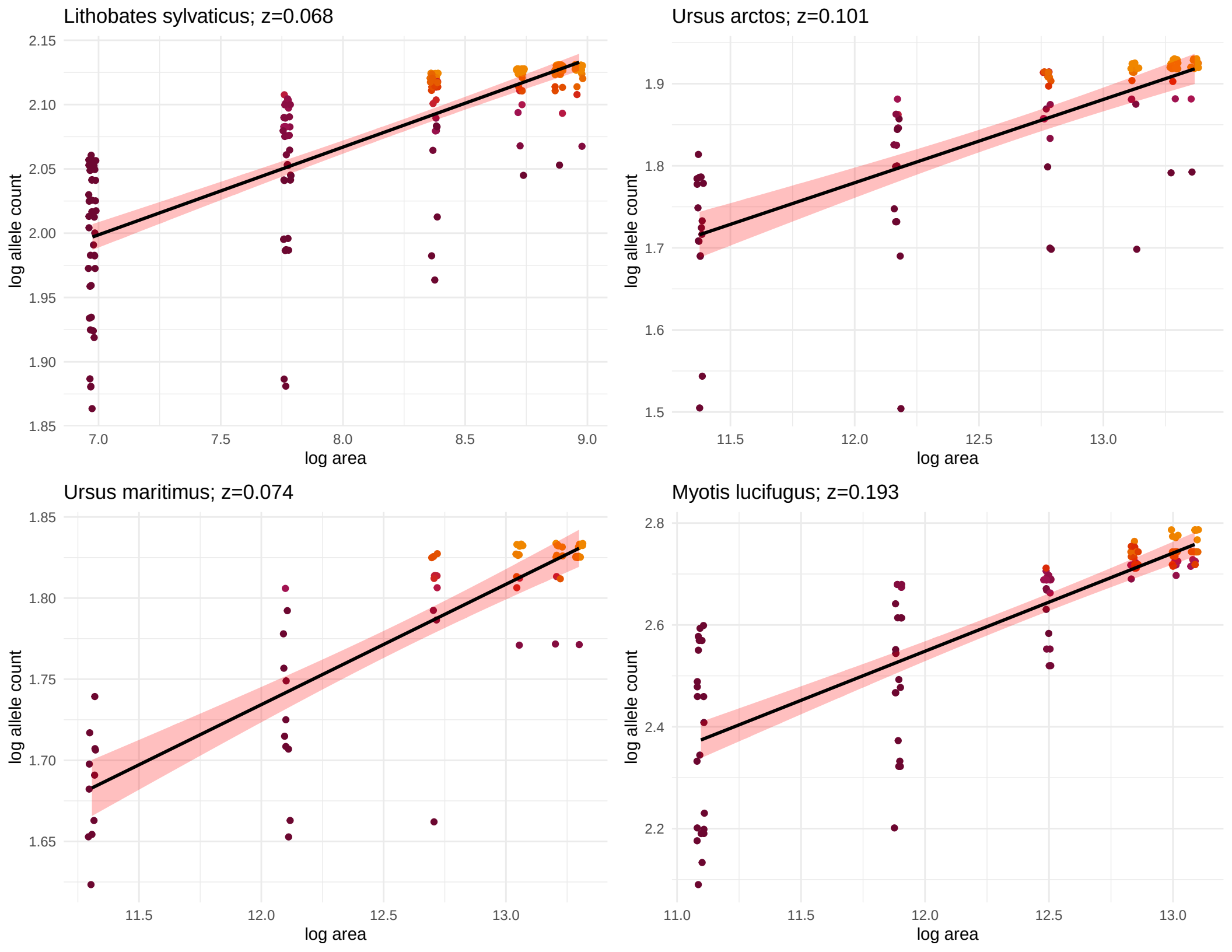
Lithobates sylvaticus; z=0.068
Ursus arctos; z=0.101
Ursus maritimus; z=0.074
Myotis lucifugus; z=0.193
log allele count
log area
2.15
2.10
2.05
2.00
1.95
1.90
1.85
7.0
7.5
8.0
8.5
9.0
1.9
1.8
1.7
1.6
1.5
11.5
12.0
12.5
13.0
1.80
1.75
1.70
1.65
2.8
2.6
2.4
2.2
11.0

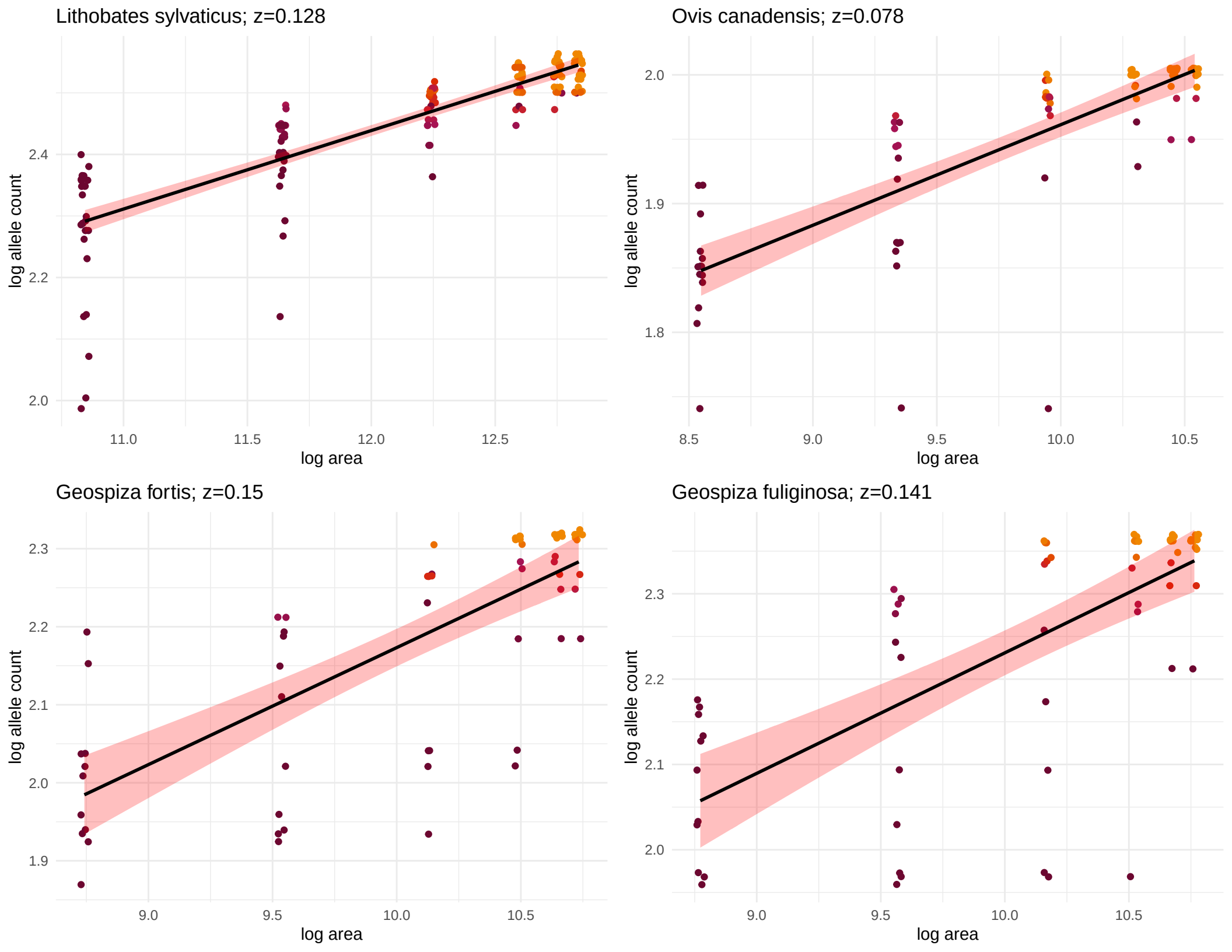
Lithobates sylvaticus; z=0.128
log allele count
log area
Ovis canadensis; z=0.078
log allele count
log area
Geospiza fortis; z=0.15
log allele count
log area
Geospiza fuliginosa; z=0.141
log allele count
log area

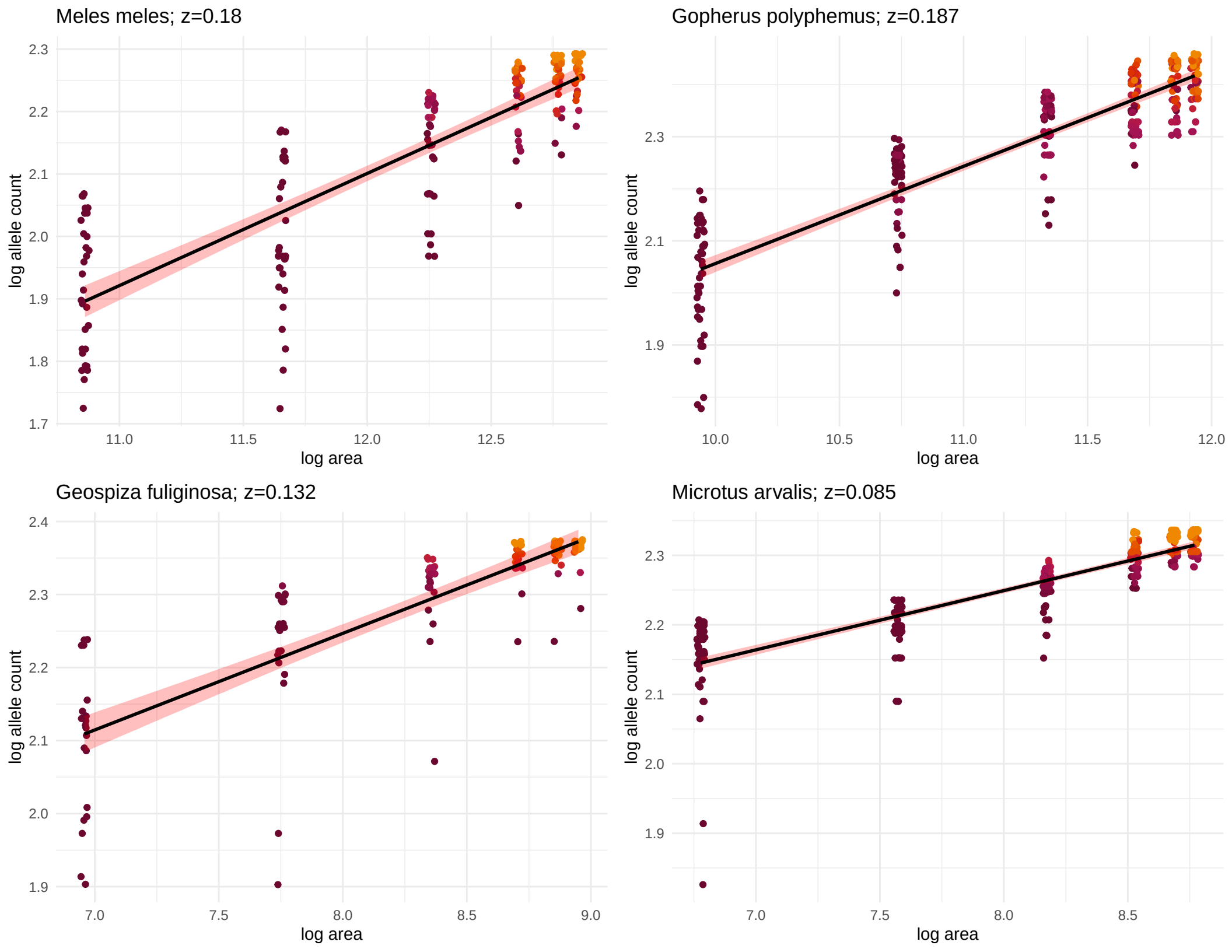
Meles meles; z=0.18
log allele count
log area
Gopherus polyphemus; z=0.187
log allele count
log area
Geospiza fuliginosa; z=0.132
log allele count
log area
Microtus arvalis; z=0.085
log allele count
log area

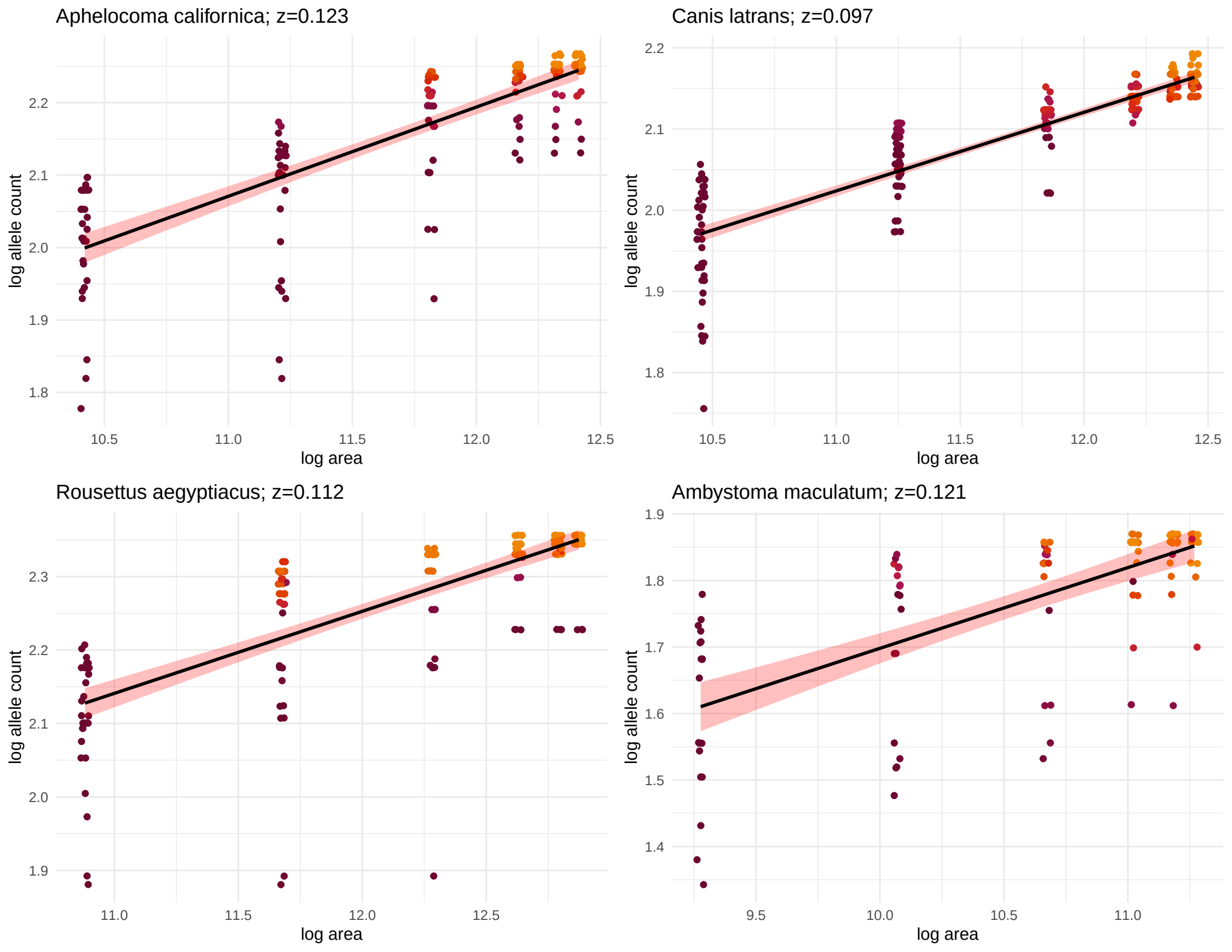
Aphelocoma californica; z=0.123
Canis latrans; z=0.097
Rousettus aegyptiacus; z=0.112
Ambystoma maculatum; z=0.121
log allele count
log area

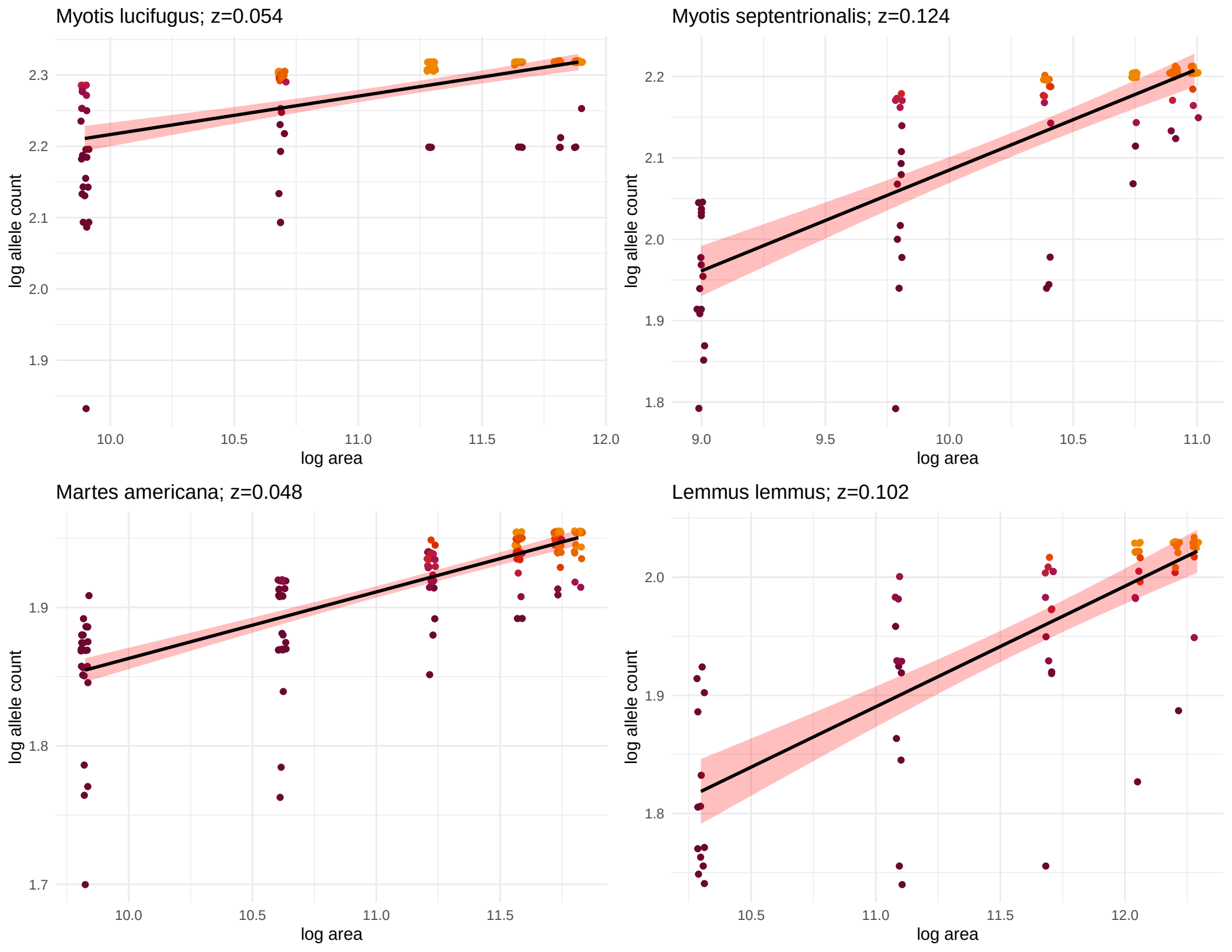
Myotis lucifugus; z=0.054
log allele count
log area
2.3
2.2
2.1
2.0
1.9
10.0
10.5
11.0
11.5
12.0
Myotis septentrionalis; z=0.124
log allele count
log area
2.2
2.1
2.0
1.9
1.8
9.0
9.5
10.0
10.5
11.0
Martes americana; z=0.048
log allele count
log area
1.9
1.8
1.7
10.0
10.5
11.0
11.5
Lemmus lemmus; z=0.102
log allele count
log area
2.0
1.9
1.8
10.5
11.0
11.5
12.0

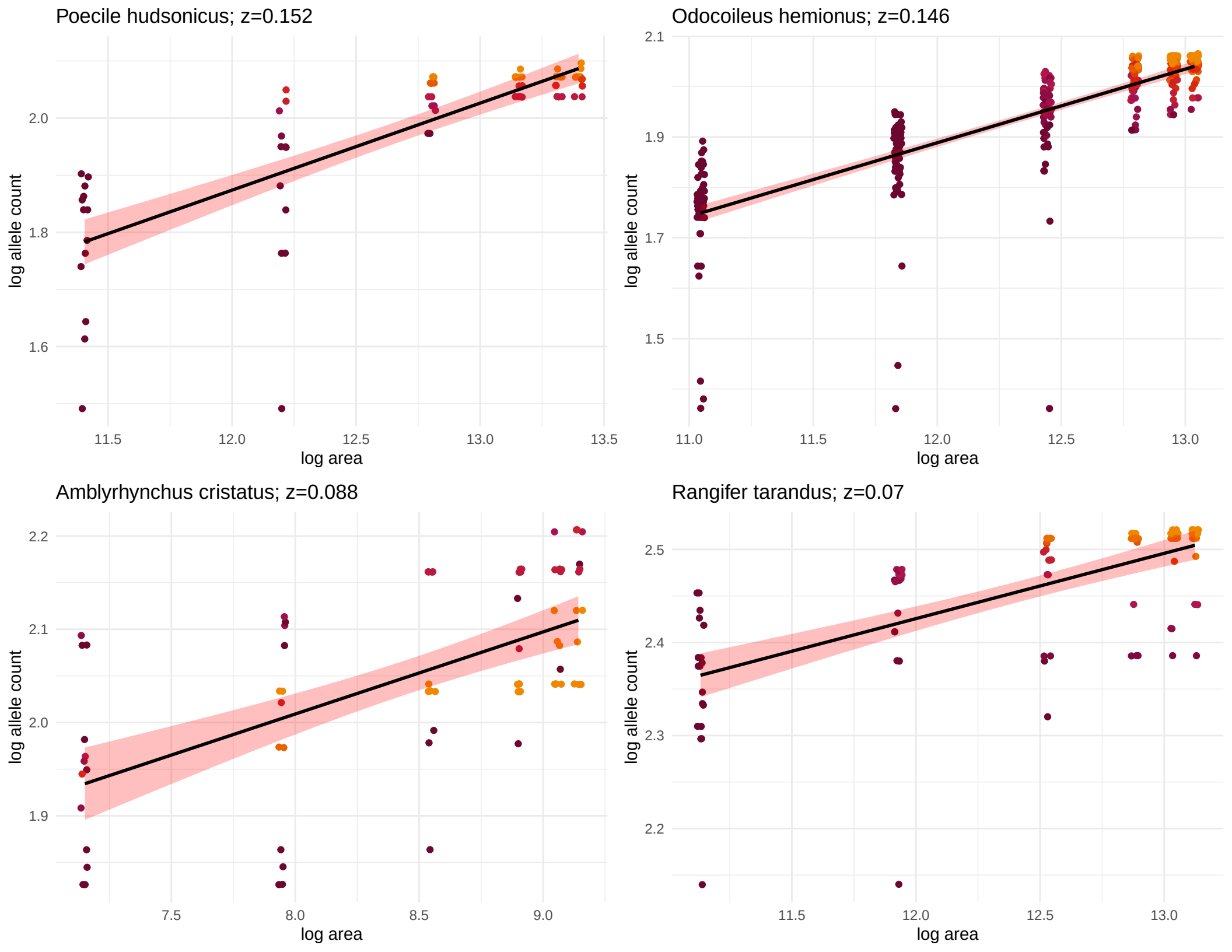
Poecile hudsonicus; z=0.152
log allele count
log area
2.0
1.8
1.6
11.5
12.0
12.5
13.0
13.5
Odocoileus hemionus; z=0.146
log allele count
log area
2.1
1.9
1.7
1.5
11.0
11.5
12.0
12.5
13.0
Amblyrhynchus cristatus; z=0.088
log allele count
log area
2.2
2.1
2.0
1.9
7.5
8.0
8.5
9.0
Rangifer tarandus; z=0.07
log allele count
log area
2.5
2.4
2.3
2.2
11.5
12.0
12.5
13.0

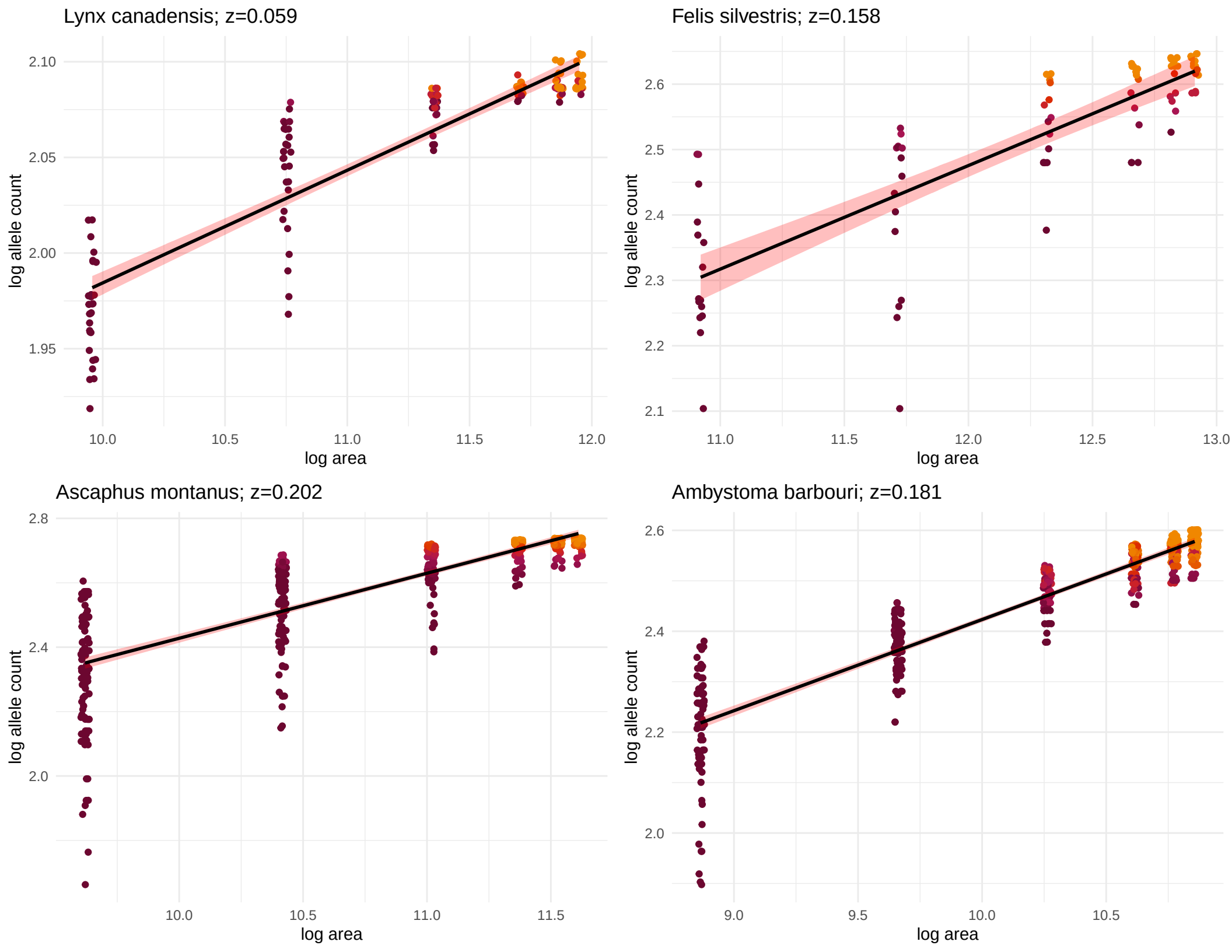
Lynx canadensis; z=0.059
log allele count
log area
2.10
2.05
2.00
1.95
10.0
10.5
11.0
11.5
12.0
Felis silvestris; z=0.158
log allele count
log area
2.6
2.5
2.4
2.3
2.2
2.1
11.0
11.5
12.0
12.5
13.0
Ascaphus montanus; z=0.202
log allele count
log area
2.8
2.4
2.0
10.0
10.5
11.0
11.5
Ambystoma barbouri; z=0.181
log allele count
log area
2.6
2.4
2.2
2.0
9.0
9.5
10.0
10.5

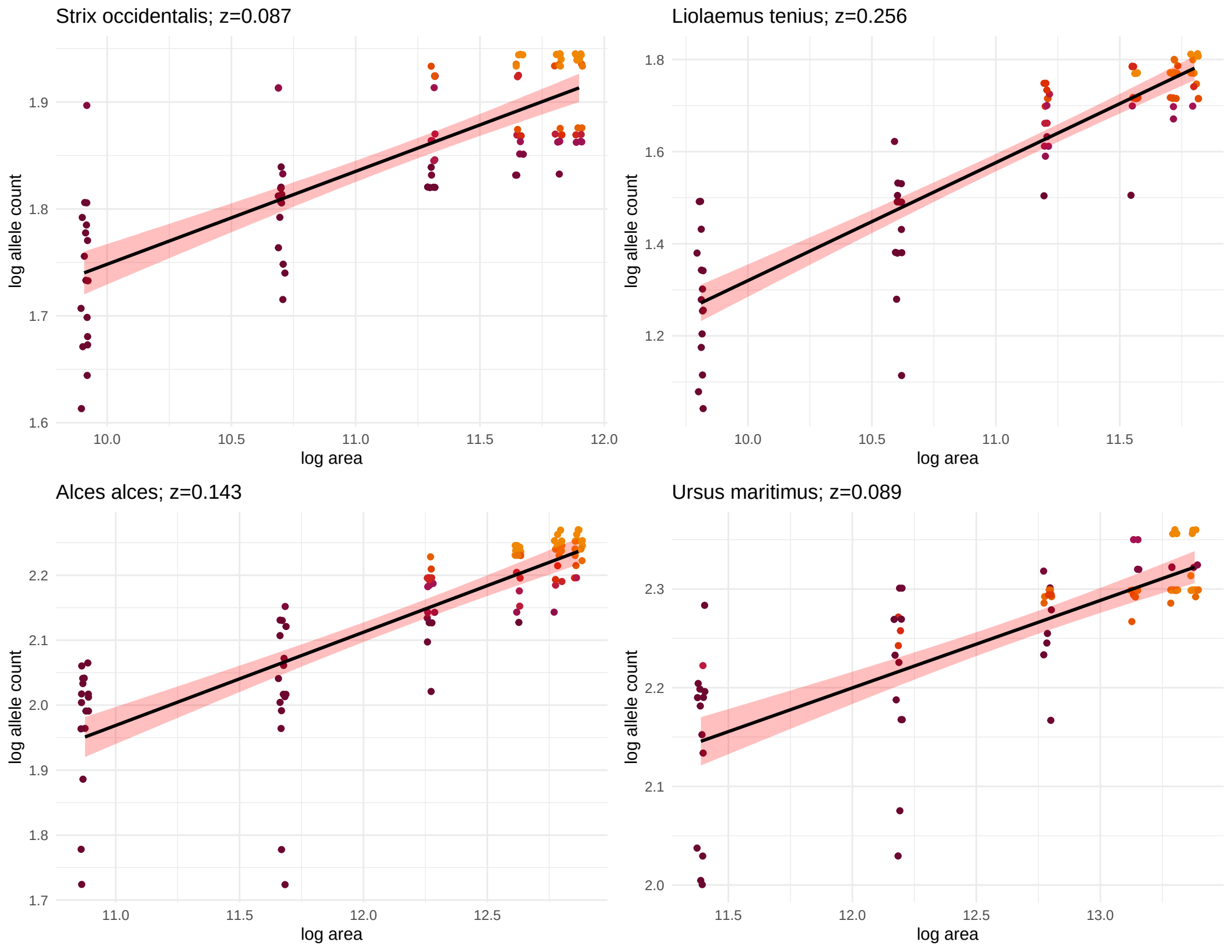
Strix occidentalis; z=0.087
log allele count
log area
1.6
1.7
1.8
1.9
10.0
10.5
11.0
11.5
12.0
Liolaemus tenius; z=0.256
log allele count
log area
1.2
1.4
1.6
1.8
10.0
10.5
11.0
11.5
Alces alces; z=0.143
log allele count
log area
1.7
1.8
1.9
2.0
2.1
2.2
11.0
11.5
12.0
12.5
Ursus maritimus; z=0.089
log allele count
log area
2.0
2.1
2.2
2.3
11.5
12.0
12.5
13.0

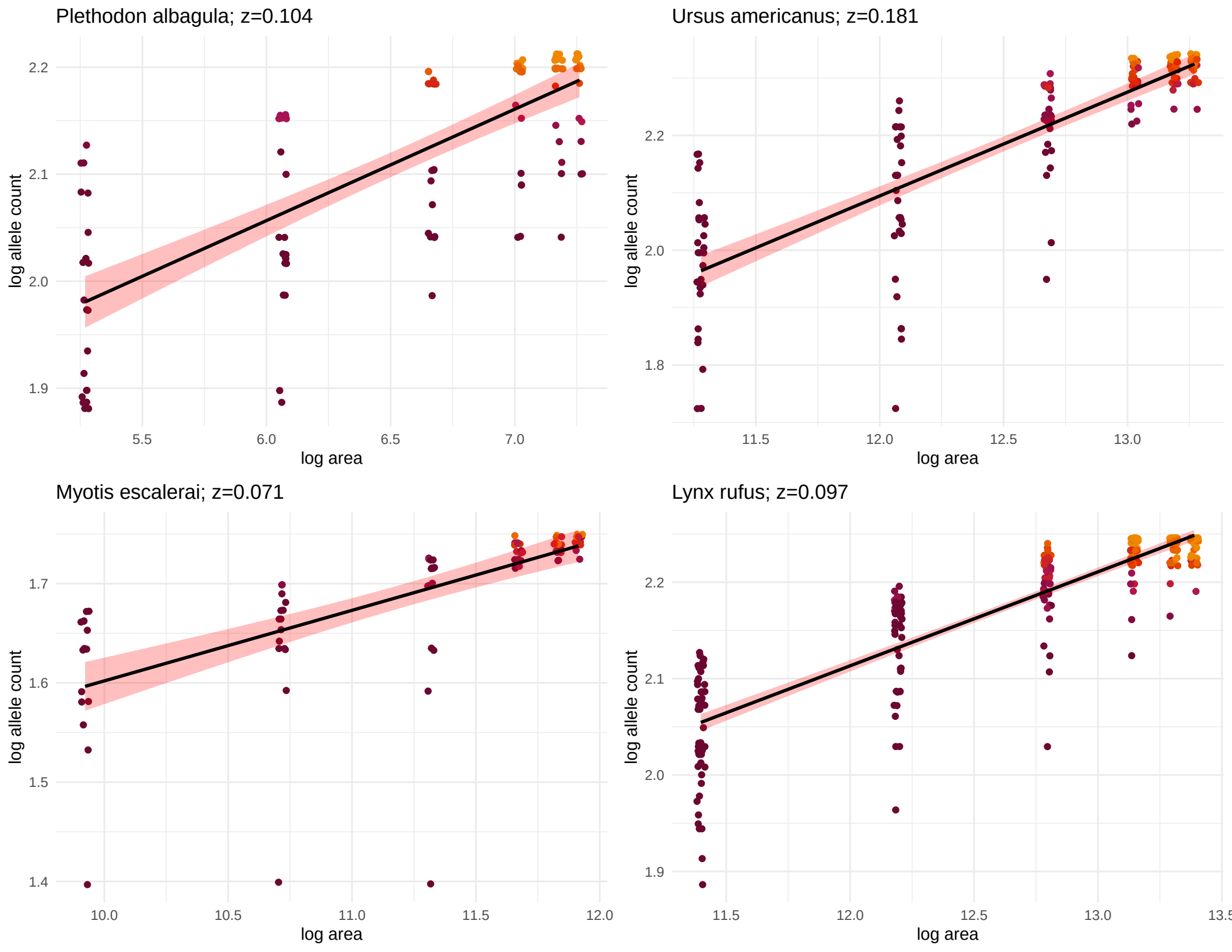
Plethodon albagula; z=0.104
log allele count
log area
2.2
2.1
2.0
1.9
5.5
6.0
6.5
7.0
Ursus americanus; z=0.181
log allele count
log area
2.2
2.0
1.8
11.5
12.0
12.5
13.0
Myotis escalerai; z=0.071
log allele count
log area
1.7
1.6
1.5
1.4
10.0
10.5
11.0
11.5
12.0
Lynx rufus; z=0.097
log allele count
log area
2.2
2.1
2.0
1.9
11.5
12.0
12.5
13.0
13.5

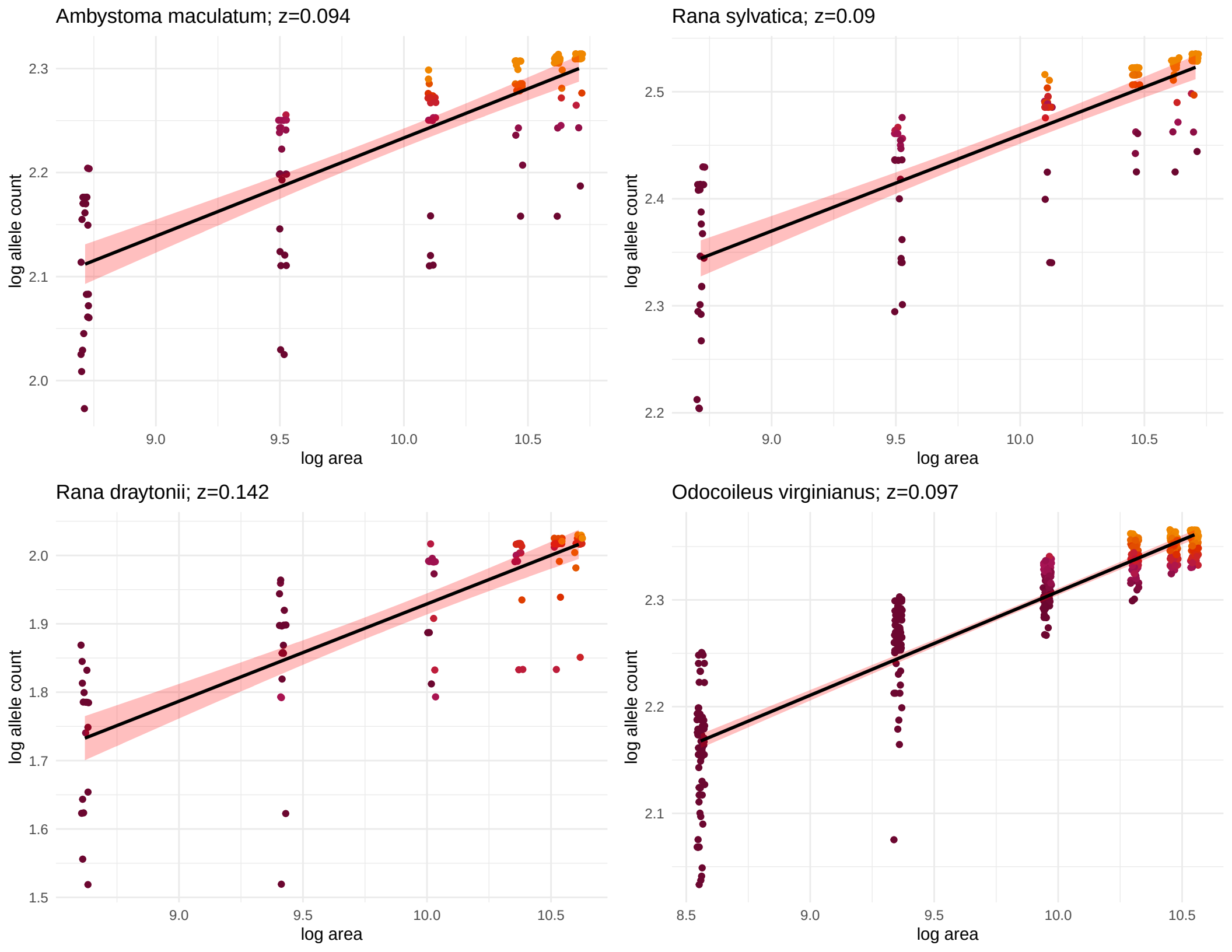
Ambystoma maculatum; z=0.094
Rana sylvatica; z=0.09
Rana draytonii; z=0.142
Odocoileus virginianus; z=0.097
log allele count
log area
2.3
2.2
2.1
2.0
2.5
2.4
2.3
2.2
2.0
1.9
1.8
1.7
1.6
1.5
2.3
2.2
2.1
9.0
9.5
10.0
10.5
8.5

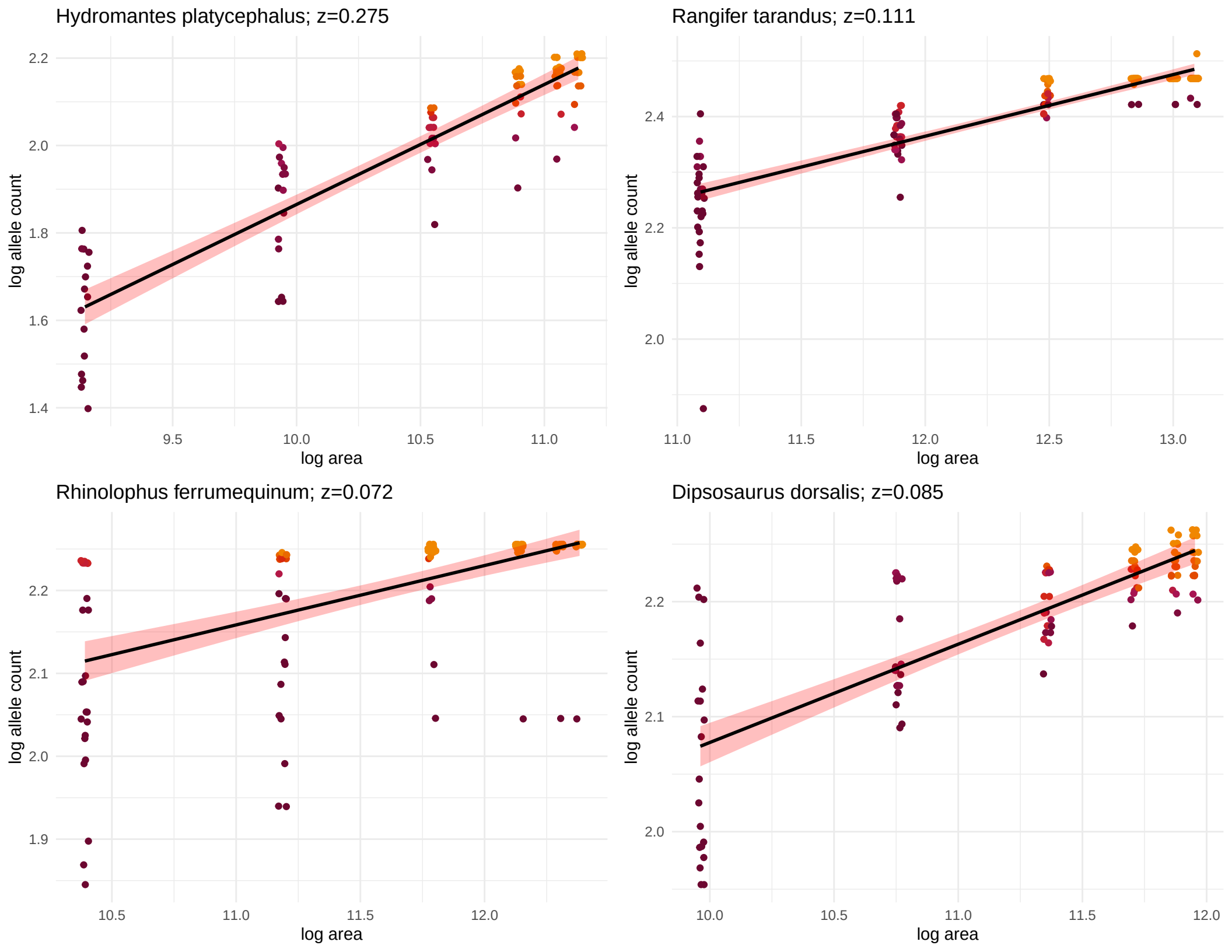
Hydromantes platycephalus; z=0.275
log allele count
log area
Rangifer tarandus; z=0.111
log allele count
log area
Rhinolophus ferrumequinum; z=0.072
log allele count
log area
Dipsosaurus dorsalis; z=0.085
log allele count
log area

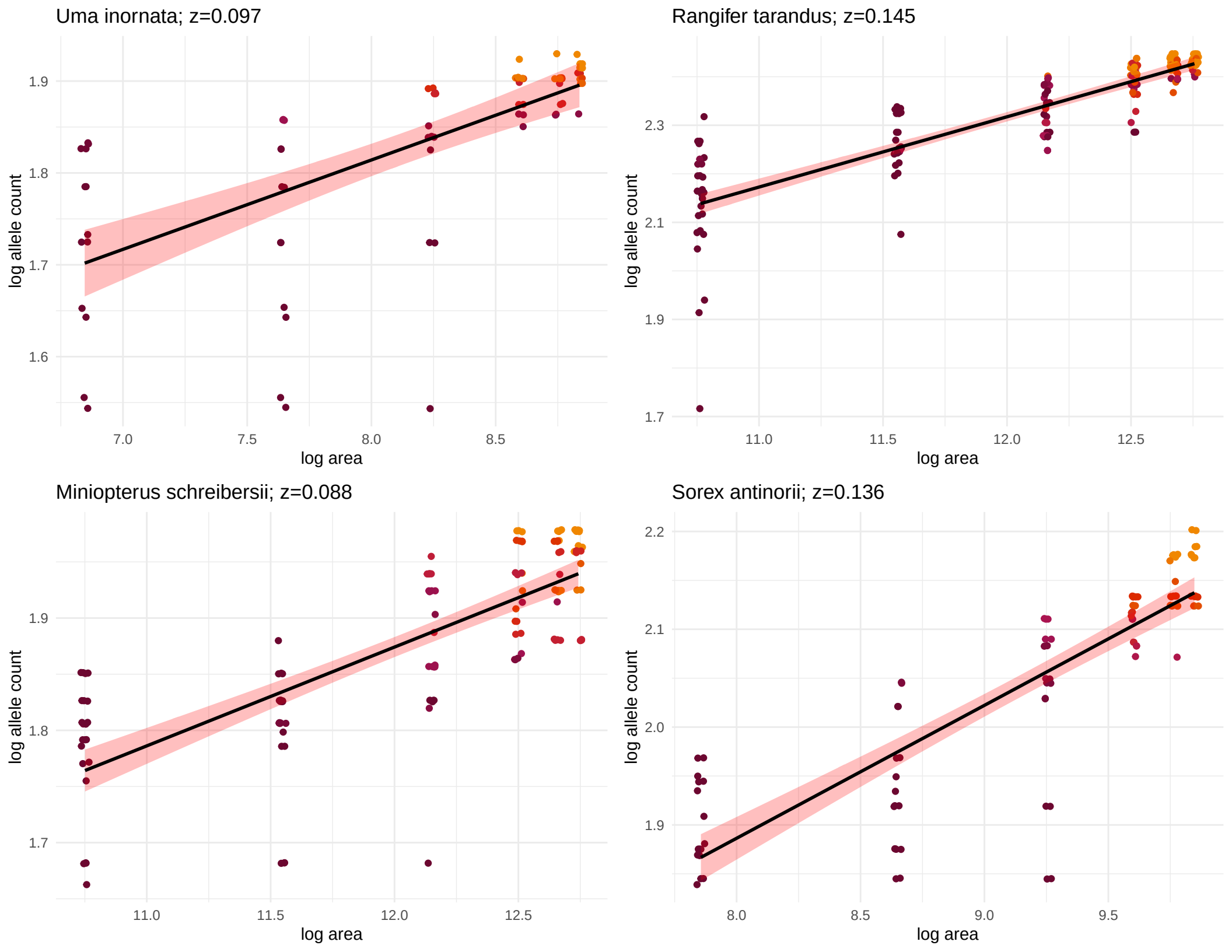
Uma inornata; z=0.097
log allele count
log area
1.9
1.8
1.7
1.6
7.0
7.5
8.0
8.5
Rangifer tarandus; z=0.145
log allele count
log area
2.3
2.1
1.9
1.7
11.0
11.5
12.0
12.5
Miniopterus schreibersii; z=0.088
log allele count
log area
1.9
1.8
1.7
11.0
11.5
12.0
12.5
Sorex antinorii; z=0.136
log allele count
log area
2.2
2.1
2.0
1.9
8.0
8.5
9.0
9.5

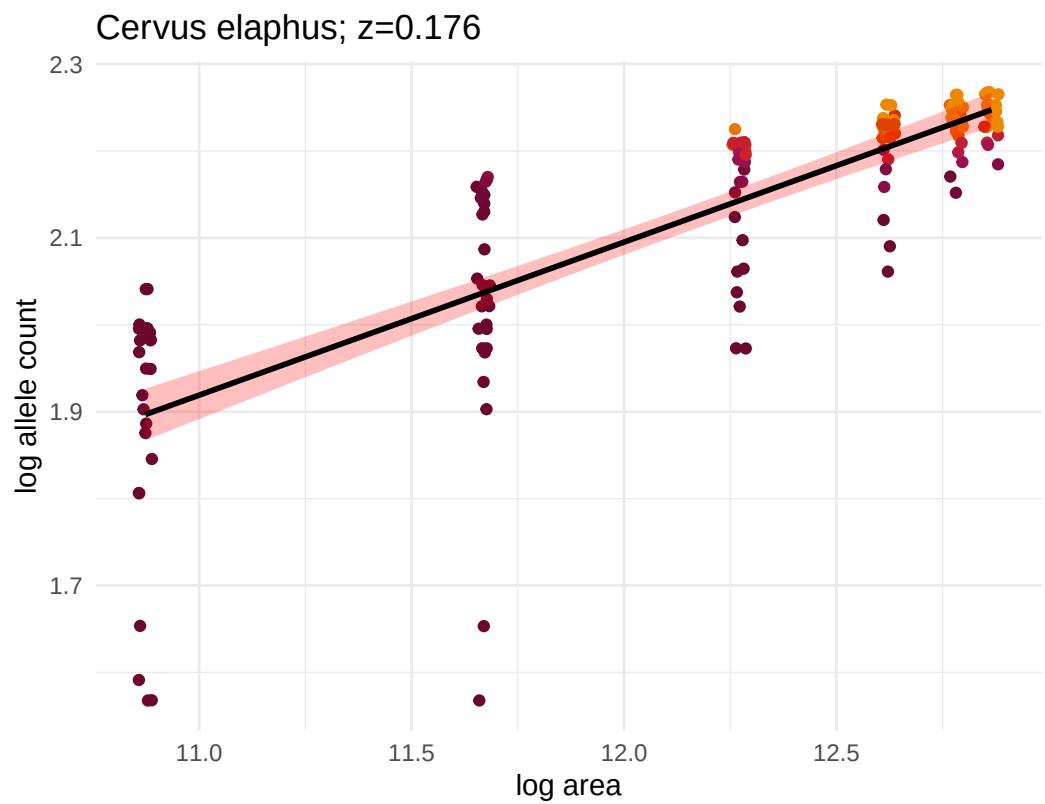
Cervus elaphus; z=0.176
log allele count
2.3
2.1
1.9
1.7
11.0
11.5
12.0
12.5
log area

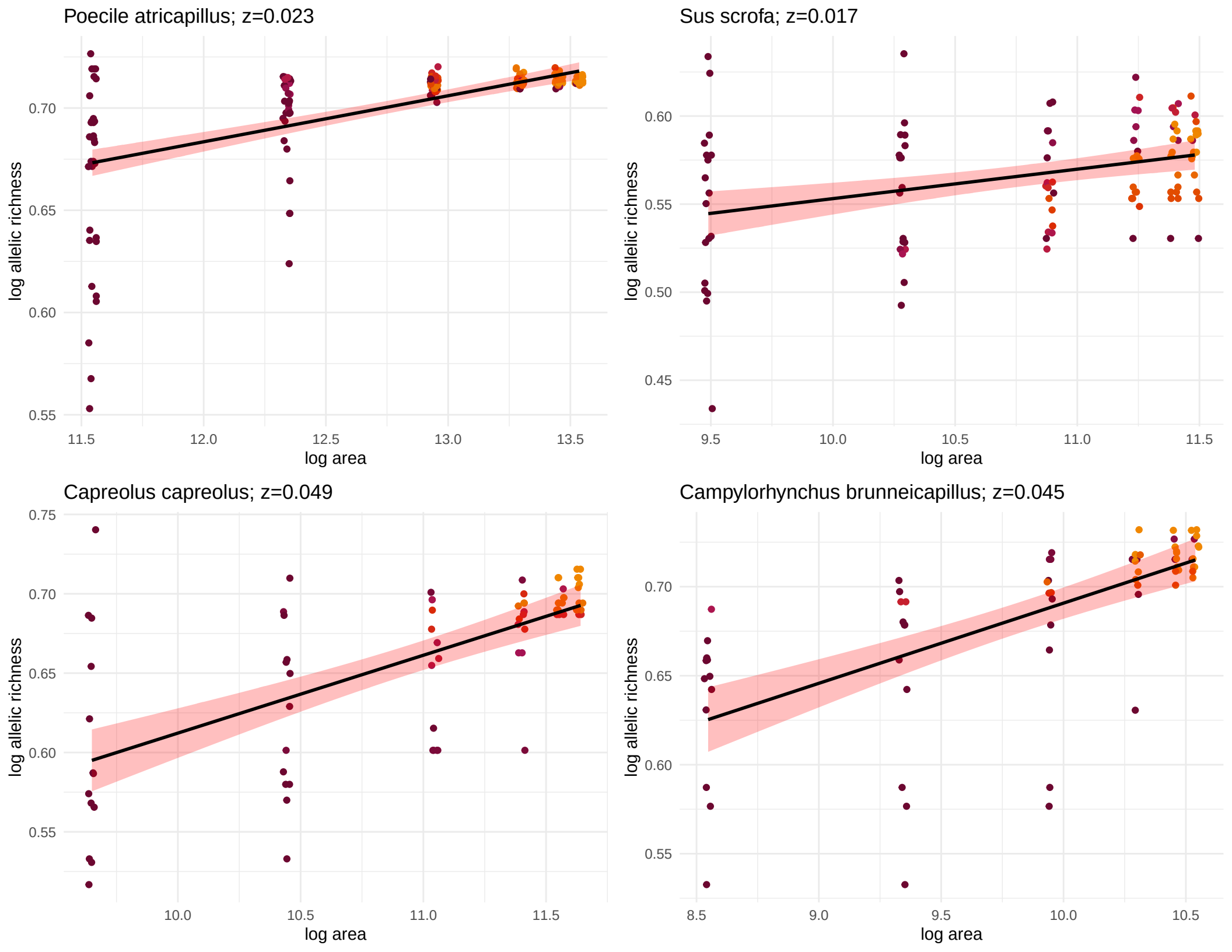
Poecile atricapillus; z=0.023
log allelic richness
log area
0.55
0.60
0.65
0.70
11.5
12.0
12.5
13.0
13.5
Sus scrofa; z=0.017
log allelic richness
log area
0.45
0.50
0.55
0.60
9.5
10.0
10.5
11.0
11.5
Capreolus capreolus; z=0.049
log allelic richness
log area
0.55
0.60
0.65
0.70
0.75
10.0
10.5
11.0
11.5
Campylorhynchus brunneicapillus; z=0.045
log allelic richness
log area
0.55
0.60
0.65
0.70
8.5
9.0
9.5
10.0
10.5

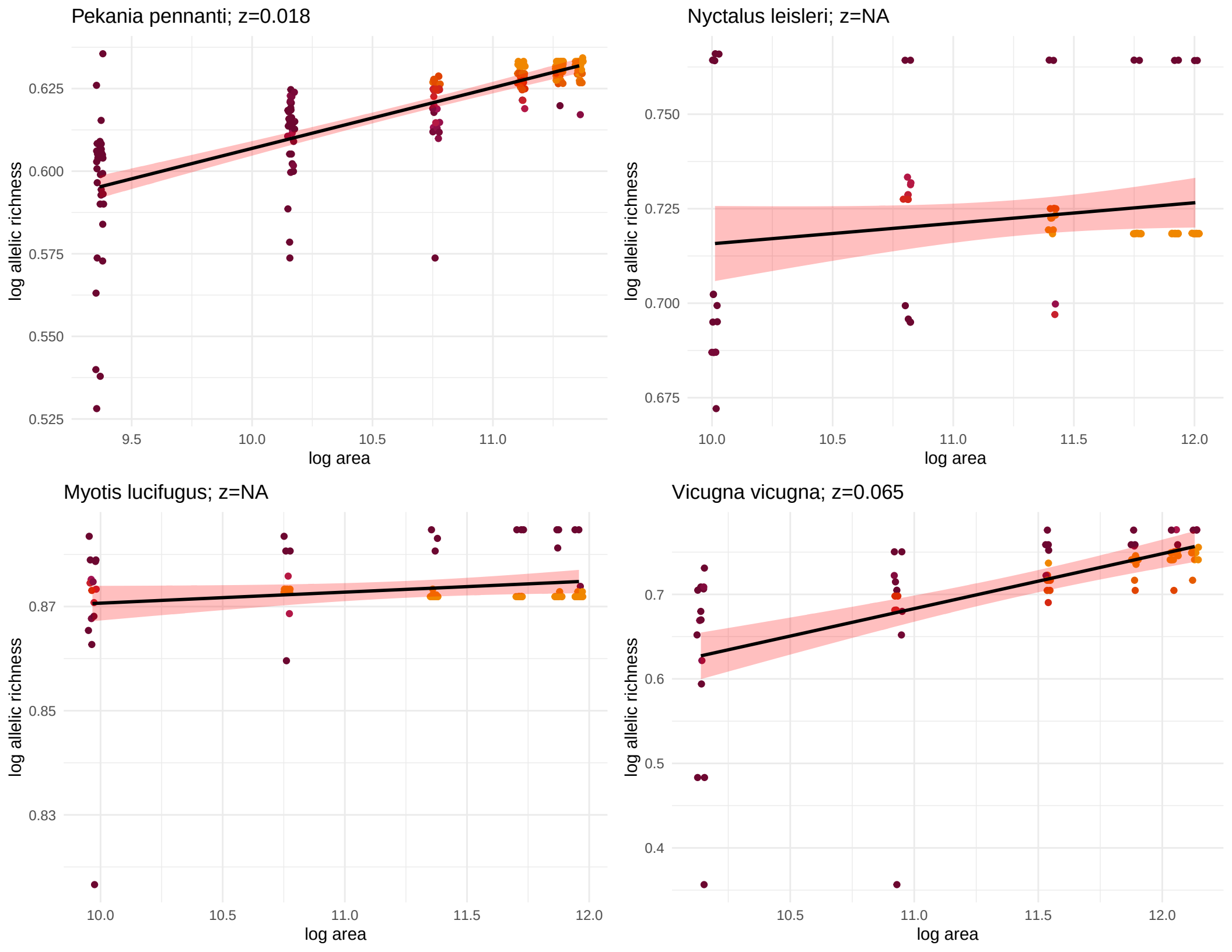
Pekania pennanti; z=0.018
log allelic richness
log area
0.625
0.600
0.575
0.550
0.525
9.5
10.0
10.5
11.0
Nyctalus leisleri; z=NA
log allelic richness
log area
0.750
0.725
0.700
0.675
10.0
10.5
11.0
11.5
12.0
Myotis lucifugus; z=NA
log allelic richness
log area
0.87
0.85
0.83
10.0
10.5
11.0
11.5
12.0
Vicugna vicugna; z=0.065
log allelic richness
log area
0.7
0.6
0.5
0.4
10.5
11.0
11.5
12.0

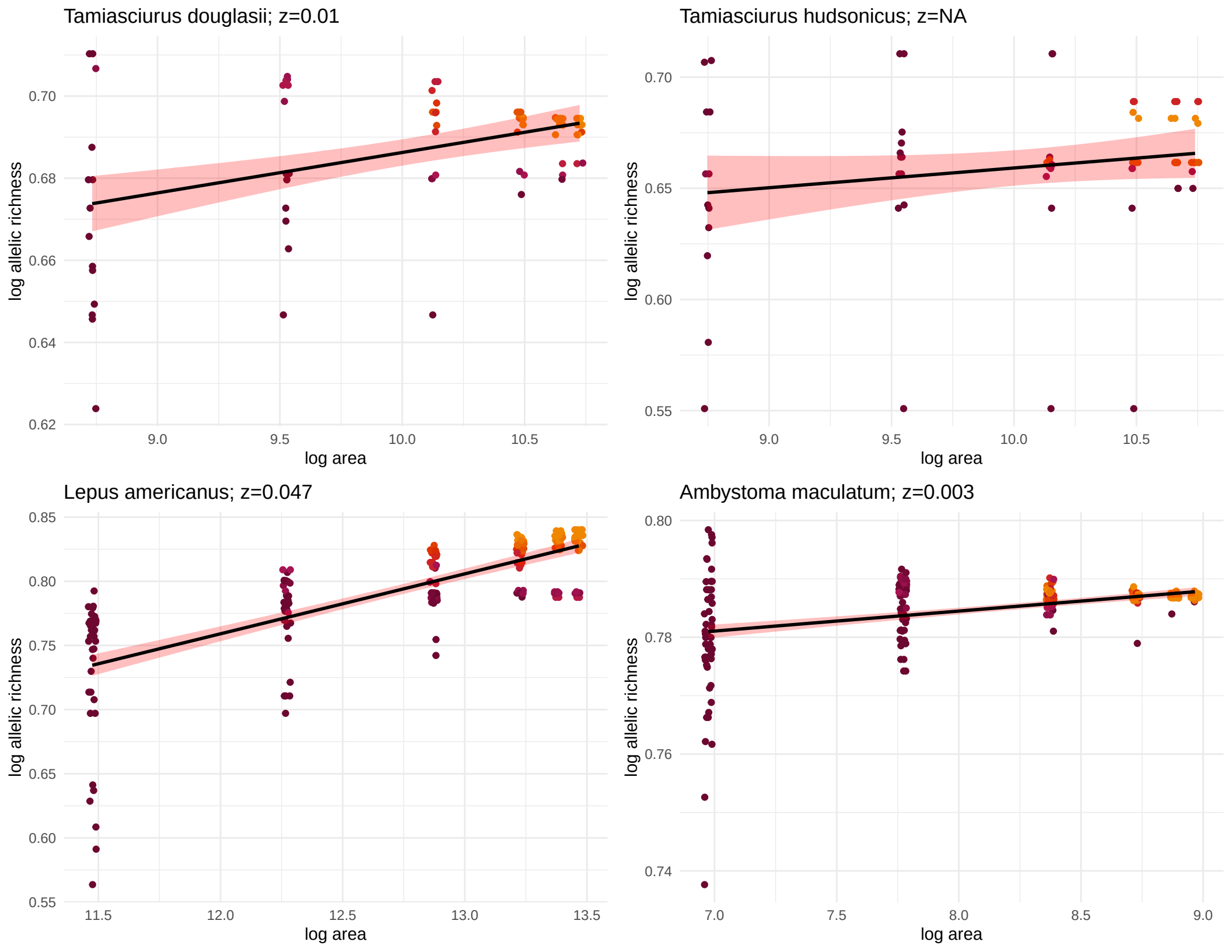
Tamiasciurus douglasii; z=0.01
log allelic richness
log area
0.70
0.68
0.66
0.64
0.62
9.0
9.5
10.0
10.5
Tamiasciurus hudsonicus; z=NA
log allelic richness
log area
0.70
0.65
0.60
0.55
9.0
9.5
10.0
10.5
Lepus americanus; z=0.047
log allelic richness
log area
0.85
0.80
0.75
0.70
0.65
0.60
0.55
11.5
12.0
12.5
13.0
13.5
Ambystoma maculatum; z=0.003
log allelic richness
log area
0.80
0.78
0.76
0.74
7.0
7.5
8.0
8.5
9.0

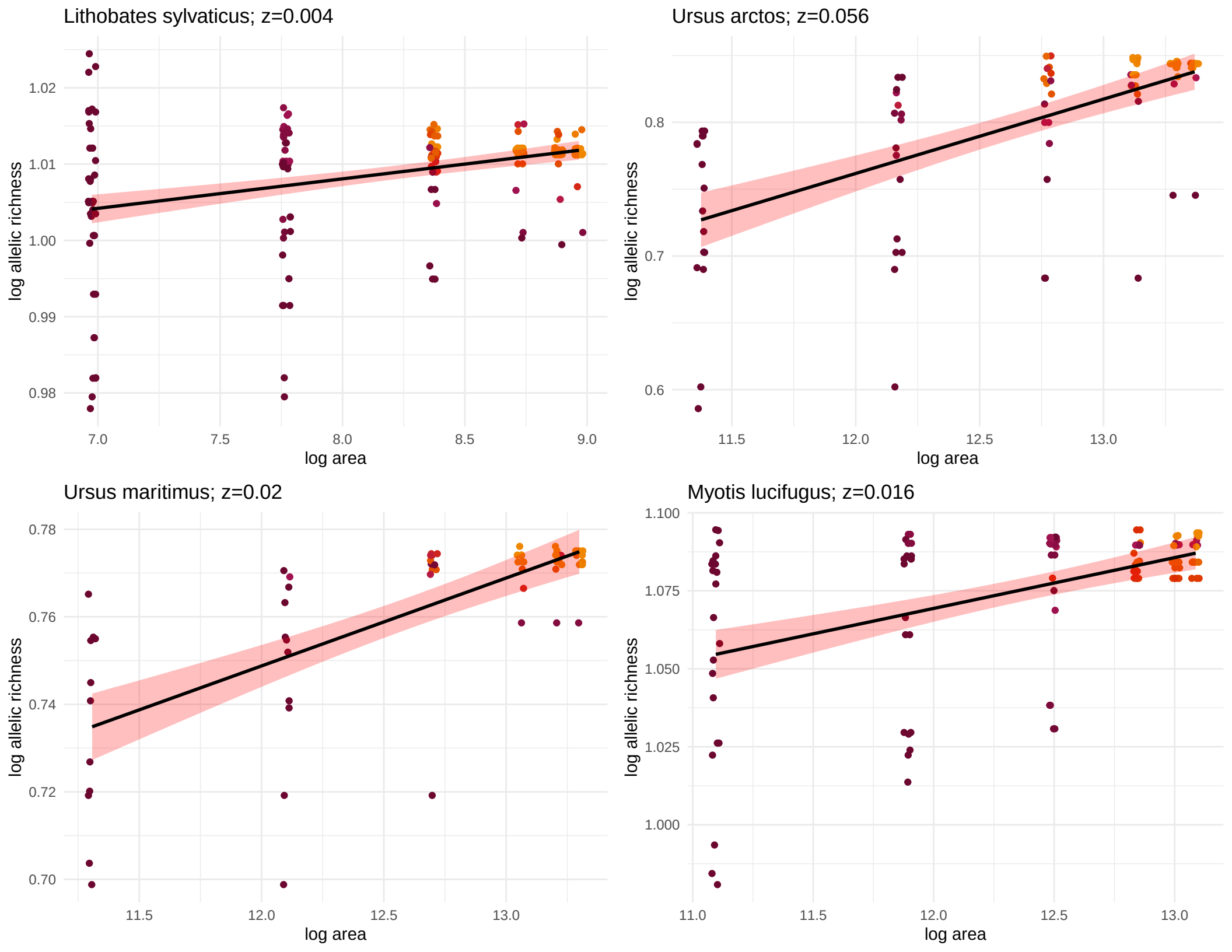
Lithobates sylvaticus; z=0.004
log allelic richness
log area
1.02
1.01
1.00
0.99
0.98
7.0
7.5
8.0
8.5
9.0
Ursus arctos; z=0.056
log allelic richness
log area
0.8
0.7
0.6
11.5
12.0
12.5
13.0
Ursus maritimus; z=0.02
log allelic richness
log area
0.78
0.76
0.74
0.72
0.70
11.5
12.0
12.5
13.0
Myotis lucifugus; z=0.016
log allelic richness
log area
1.100
1.075
1.050
1.025
1.000
11.0
11.5
12.0
12.5
13.0

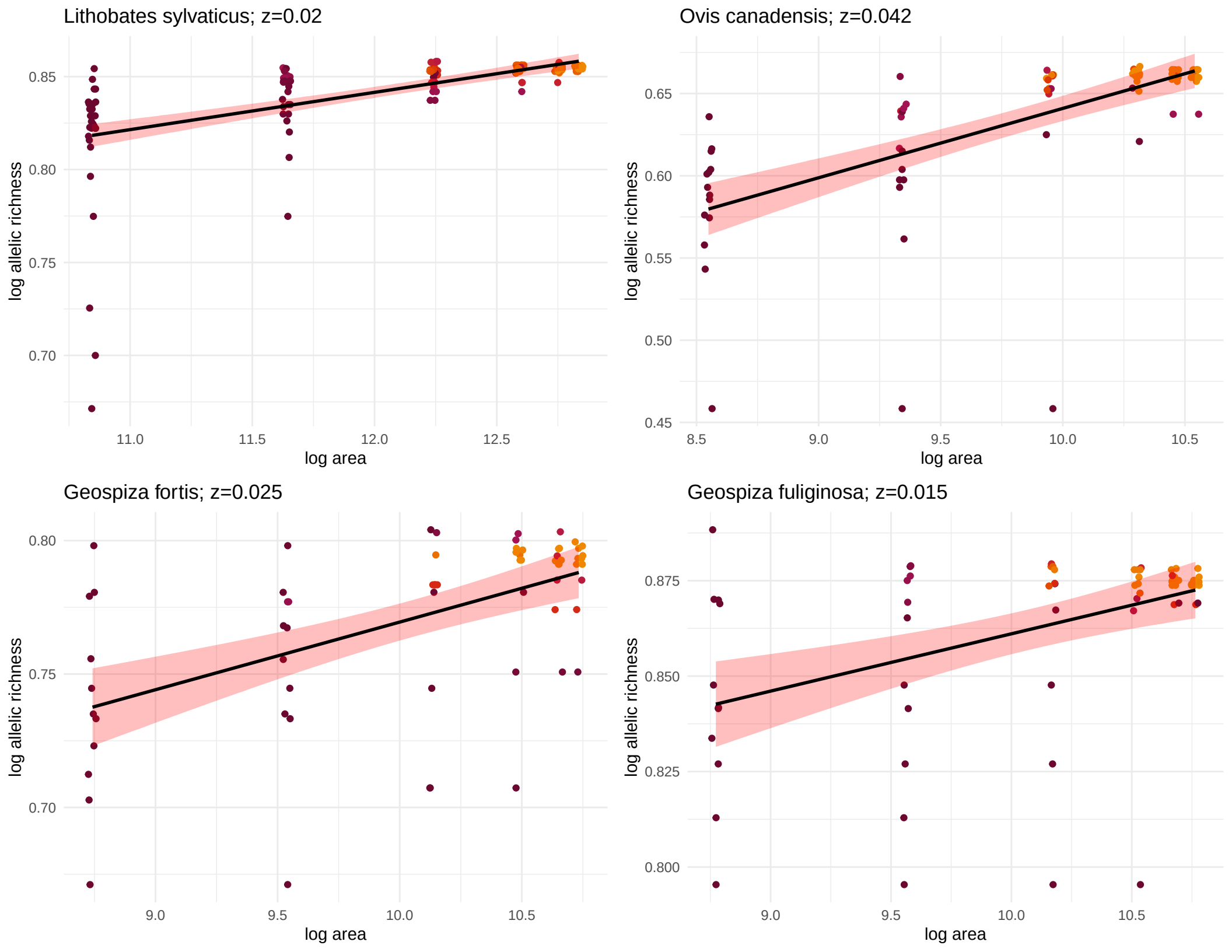
Lithobates sylvaticus; z=0.02
log allelic richness
0.85
0.80
0.75
0.70
11.0
11.5
12.0
12.5
log area
Ovis canadensis; z=0.042
log allelic richness
0.65
0.60
0.55
0.50
0.45
8.5
9.0
9.5
10.0
10.5
log area
Geospiza fortis; z=0.025
log allelic richness
0.80
0.75
0.70
9.0
9.5
10.0
10.5
log area
Geospiza fuliginosa; z=0.015
log allelic richness
0.875
0.850
0.825
0.800
9.0
9.5
10.0
10.5
log area

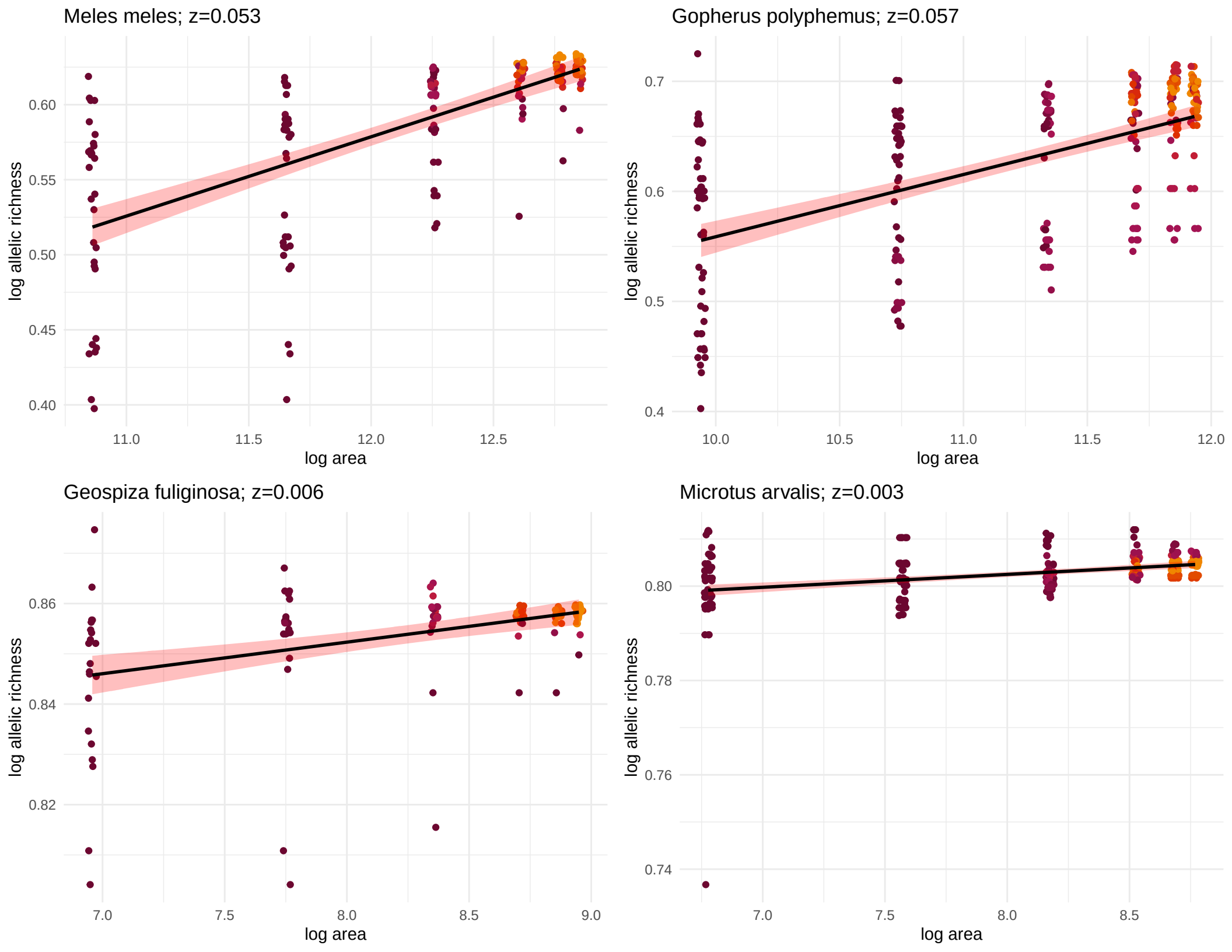
Meles meles; z=0.053
log allelic richness
log area
Gopherus polyphemus; z=0.057
log allelic richness
log area
Geospiza fuliginosa; z=0.006
log allelic richness
log area
Microtus arvalis; z=0.003
log allelic richness
log area

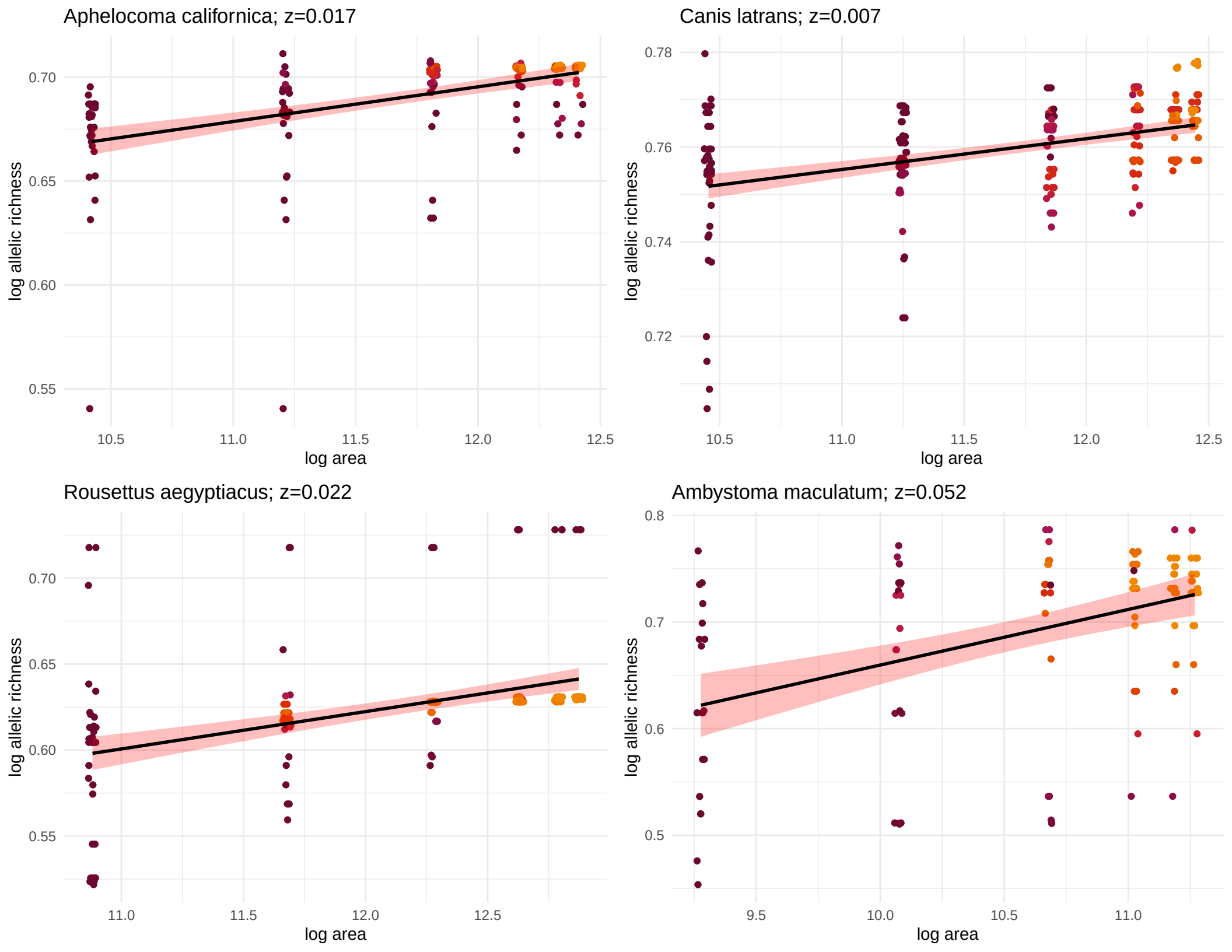
Aphelocoma californica; z=0.017
Canis latrans; z=0.007
Rousettus aegyptiacus; z=0.022
Ambystoma maculatum; z=0.052
log allelic richness
log area
0.55
0.60
0.65
0.70
0.72
0.74
0.76
0.78
0.5
0.6
0.7
0.8
10.5
11.0
11.5
12.0
12.5
9.5
10.0
10.5
11.0

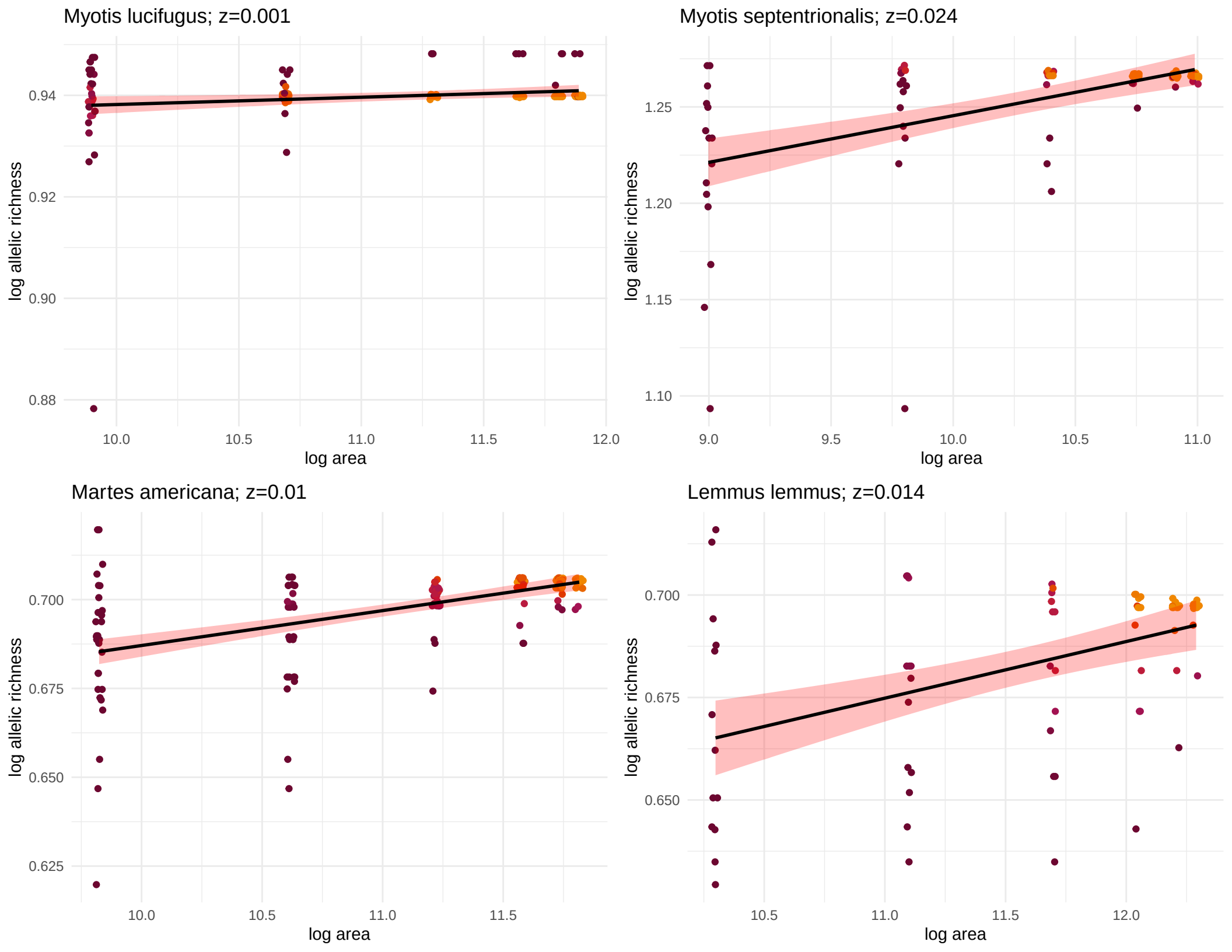
Myotis lucifugus; z=0.001
log allelic richness
0.94
0.92
0.90
0.88
10.0
10.5
11.0
11.5
12.0
log area
Myotis septentrionalis; z=0.024
log allelic richness
1.25
1.20
1.15
1.10
9.0
9.5
10.0
10.5
11.0
log area
Martes americana; z=0.01
log allelic richness
0.700
0.675
0.650
0.625
10.0
10.5
11.0
11.5
log area
Lemmus lemmus; z=0.014
log allelic richness
0.700
0.675
0.650
10.5
11.0
11.5
12.0
log area

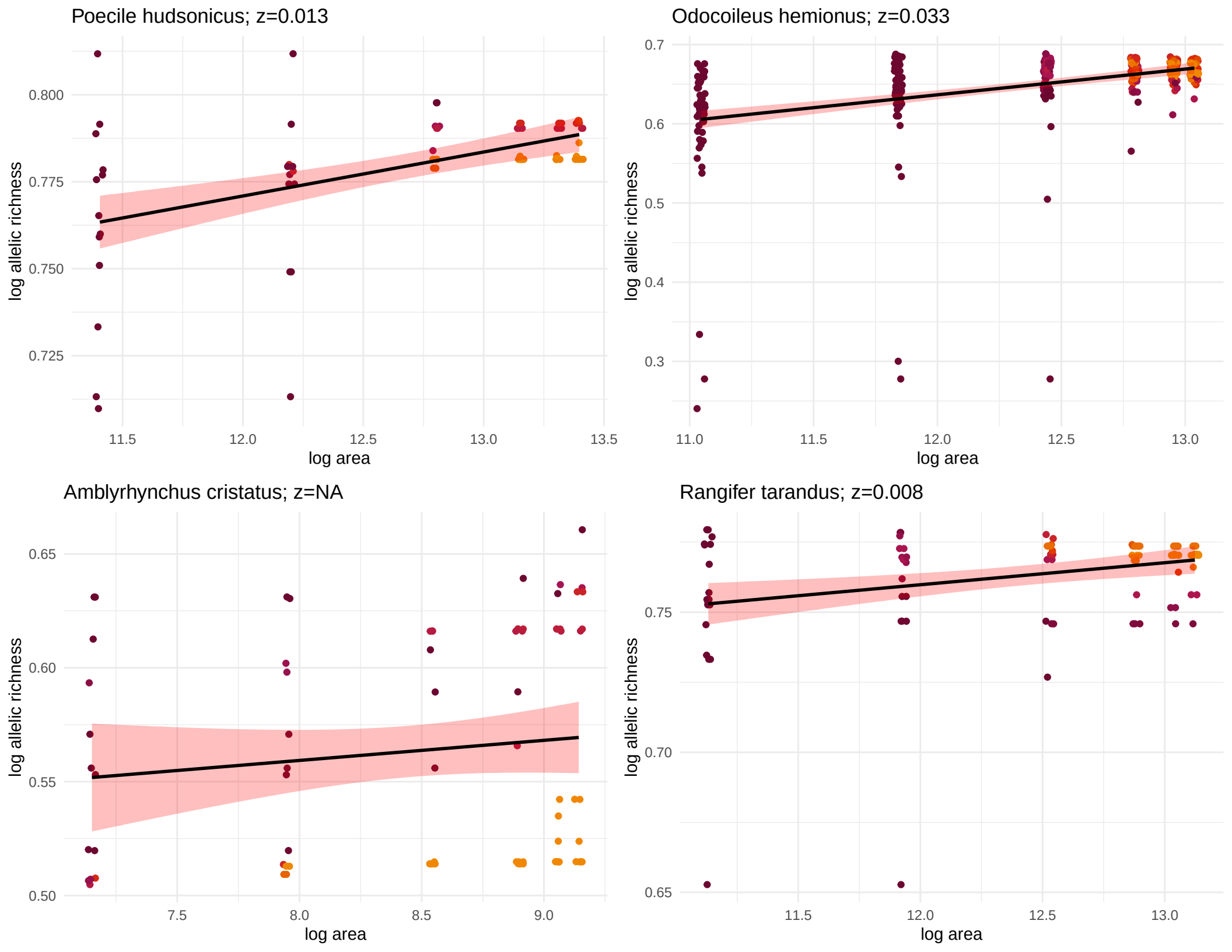
Poecile hudsonicus; z=0.013
log allelic richness
log area
0.800
0.775
0.750
0.725
11.5
12.0
12.5
13.0
13.5
Odocoileus hemionus; z=0.033
log allelic richness
log area
0.7
0.6
0.5
0.4
0.3
11.0
11.5
12.0
12.5
13.0
Amblyrhynchus cristatus; z=NA
log allelic richness
log area
0.65
0.60
0.55
0.50
7.5
8.0
8.5
9.0
Rangifer tarandus; z=0.008
log allelic richness
log area
0.75
0.70
0.65
11.5
12.0
12.5
13.0

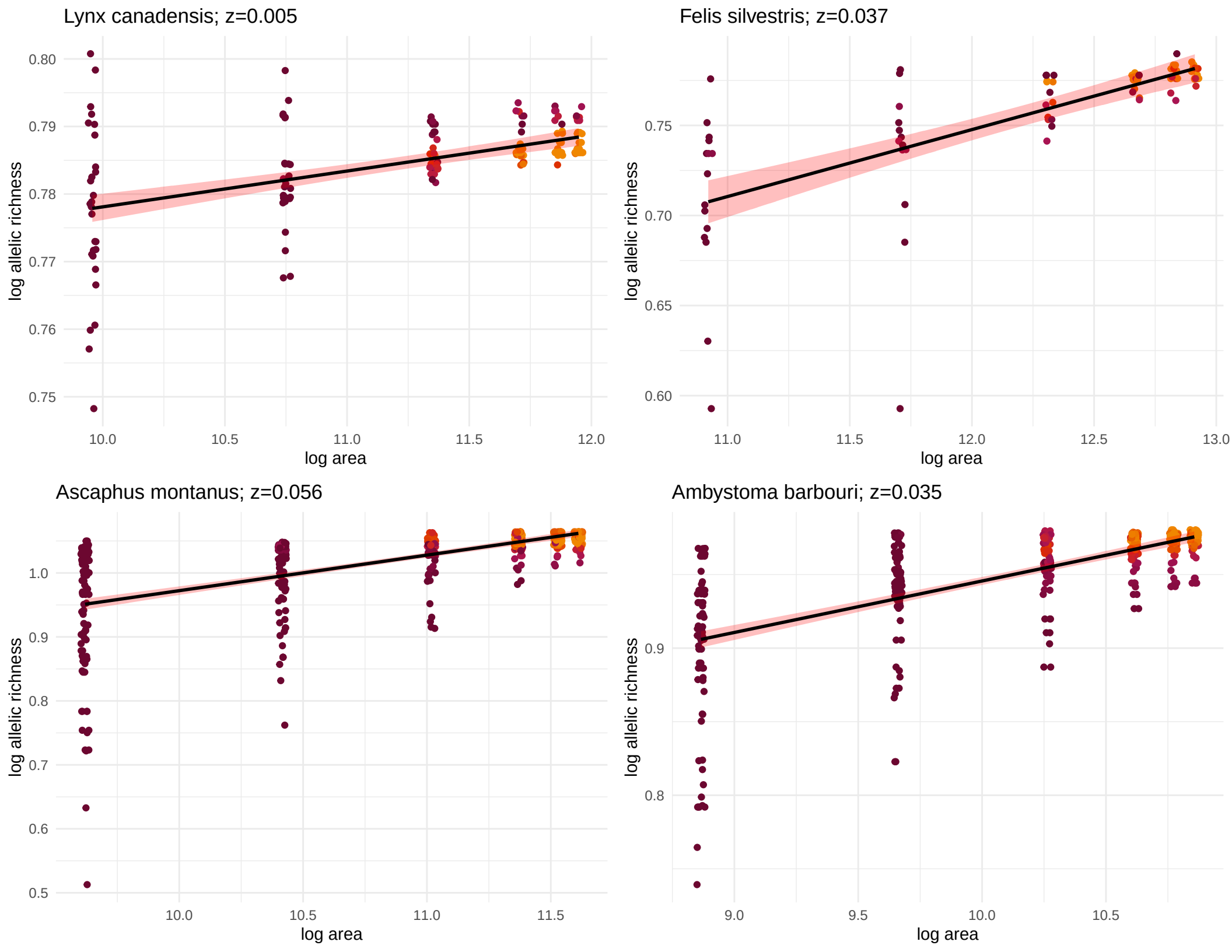
Lynx canadensis; z=0.005
Felis silvestris; z=0.037
Ascaphus montanus; z=0.056
Ambystoma barbouri; z=0.035
log allelic richness
log area

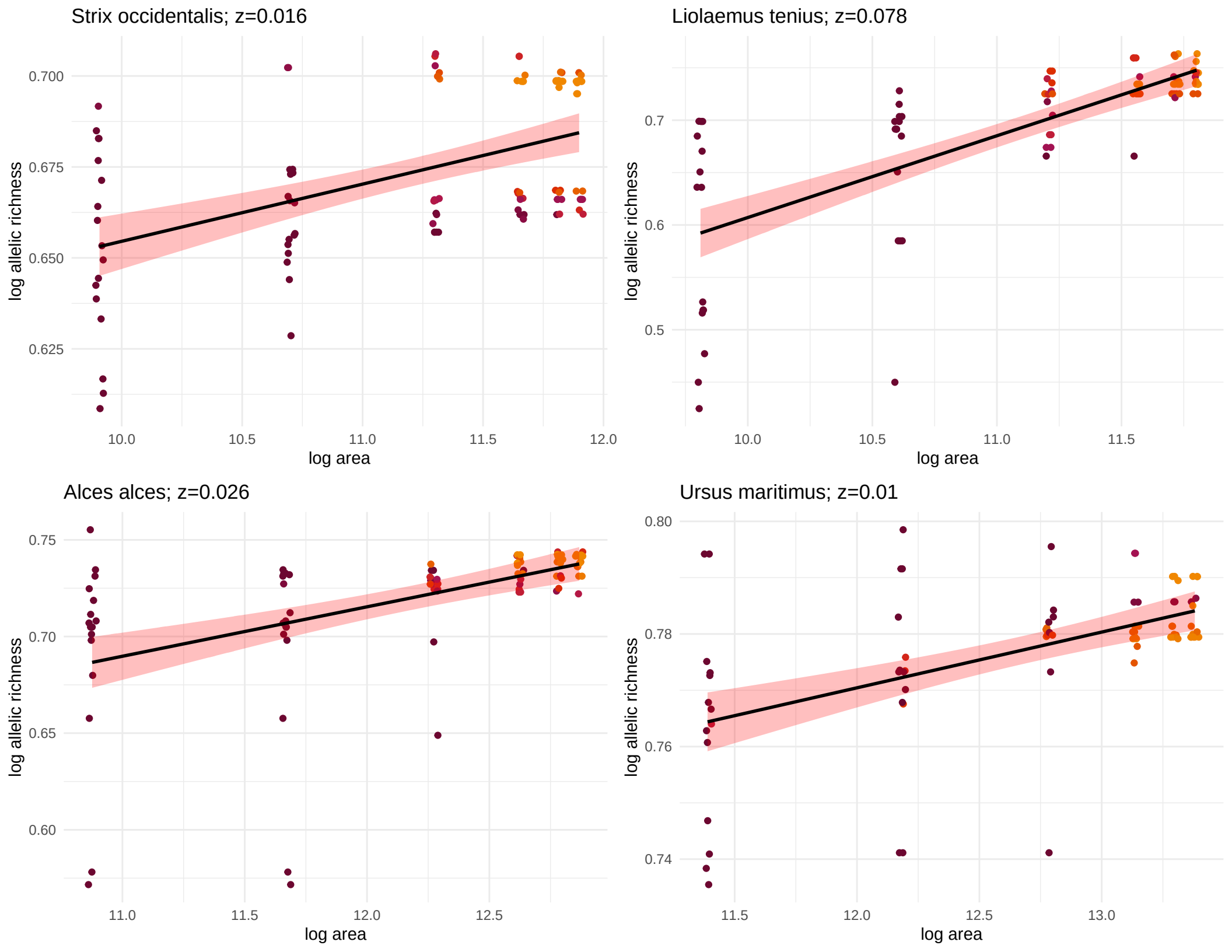
Strix occidentalis; z=0.016
log allelic richness
log area
0.700
0.675
0.650
0.625
10.0
10.5
11.0
11.5
12.0
Liolaemus tenius; z=0.078
log allelic richness
log area
0.7
0.6
0.5
10.0
10.5
11.0
11.5
Alces alces; z=0.026
log allelic richness
log area
0.75
0.70
0.65
0.60
11.0
11.5
12.0
12.5
Ursus maritimus; z=0.01
log allelic richness
log area
0.80
0.78
0.76
0.74
11.5
12.0
12.5
13.0

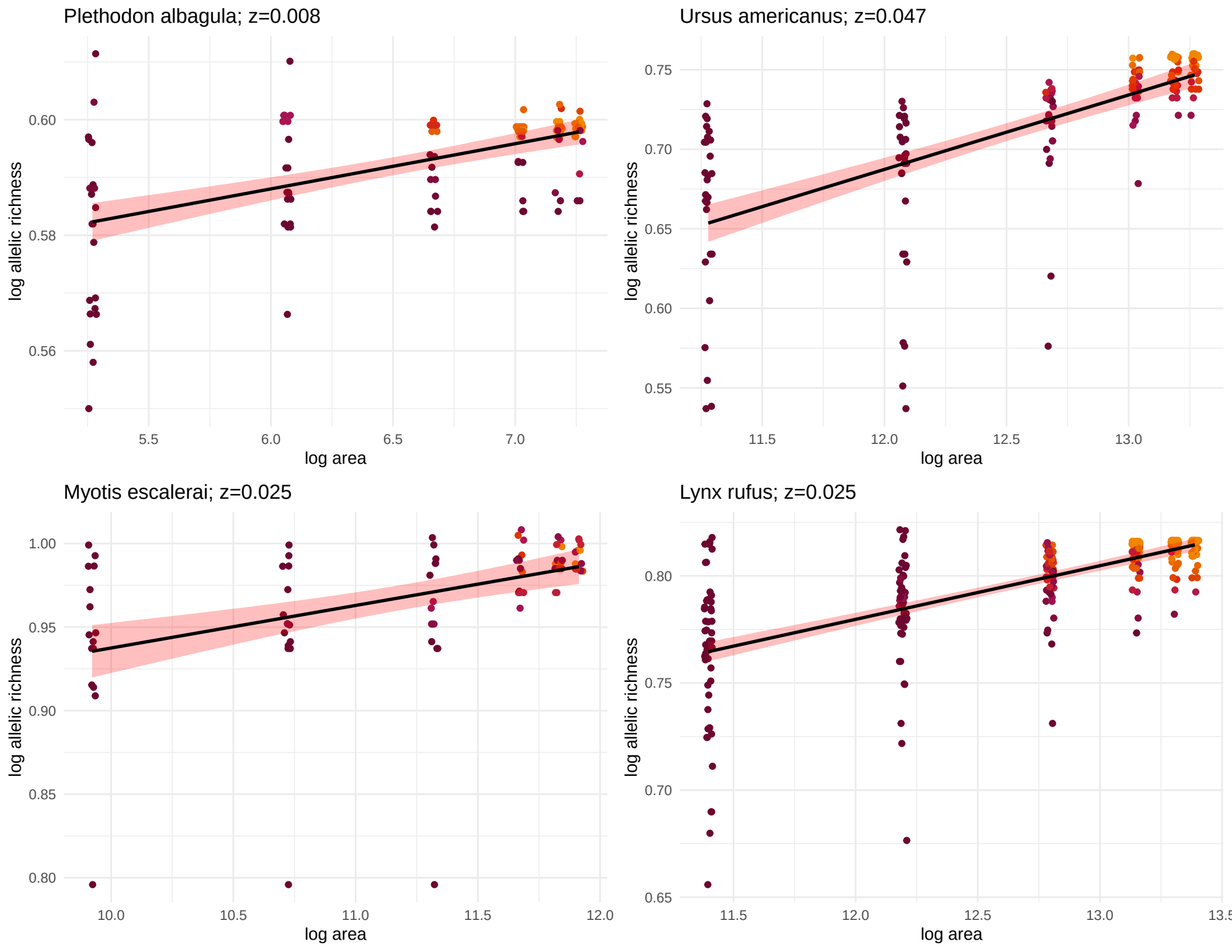
Plethodon albagula; z=0.008
log allelic richness
log area
0.60
0.58
0.56
5.5
6.0
6.5
7.0
Ursus americanus; z=0.047
log allelic richness
log area
0.75
0.70
0.65
0.60
0.55
11.5
12.0
12.5
13.0
Myotis escalerai; z=0.025
log allelic richness
log area
1.00
0.95
0.90
0.85
0.80
10.0
10.5
11.0
11.5
12.0
Lynx rufus; z=0.025
log allelic richness
log area
0.80
0.75
0.70
0.65
11.5
12.0
12.5
13.0
13.5

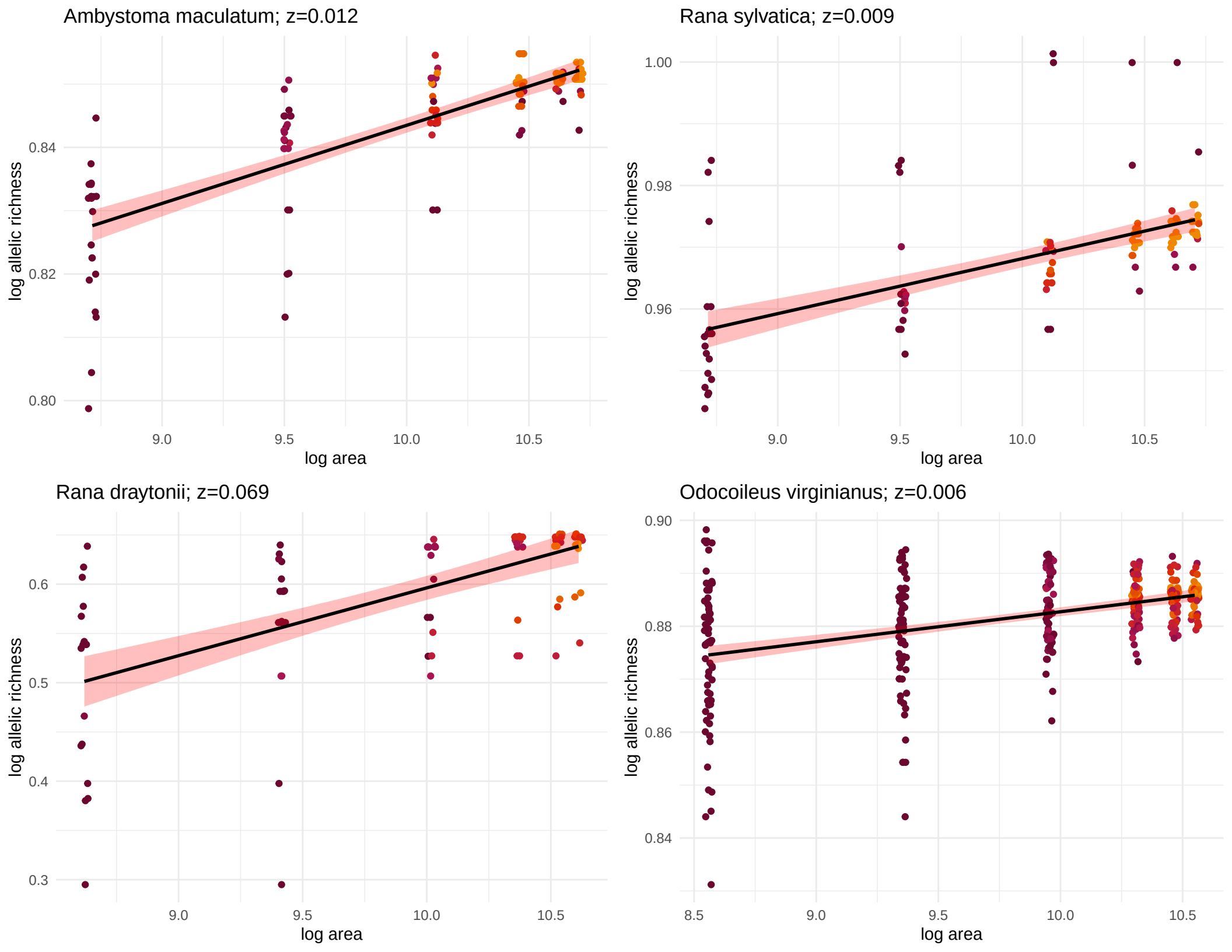
Ambystoma maculatum; z=0.012
log allelic richness
0.84
0.82
0.80
9.0
9.5
10.0
10.5
log area
Rana sylvatica; z=0.009
log allelic richness
1.00
0.98
0.96
9.0
9.5
10.0
10.5
log area
Rana draytonii; z=0.069
log allelic richness
0.6
0.5
0.4
0.3
9.0
9.5
10.0
10.5
log area
Odocoileus virginianus; z=0.006
log allelic richness
0.90
0.88
0.86
0.84
8.5
9.0
9.5
10.0
10.5
log area

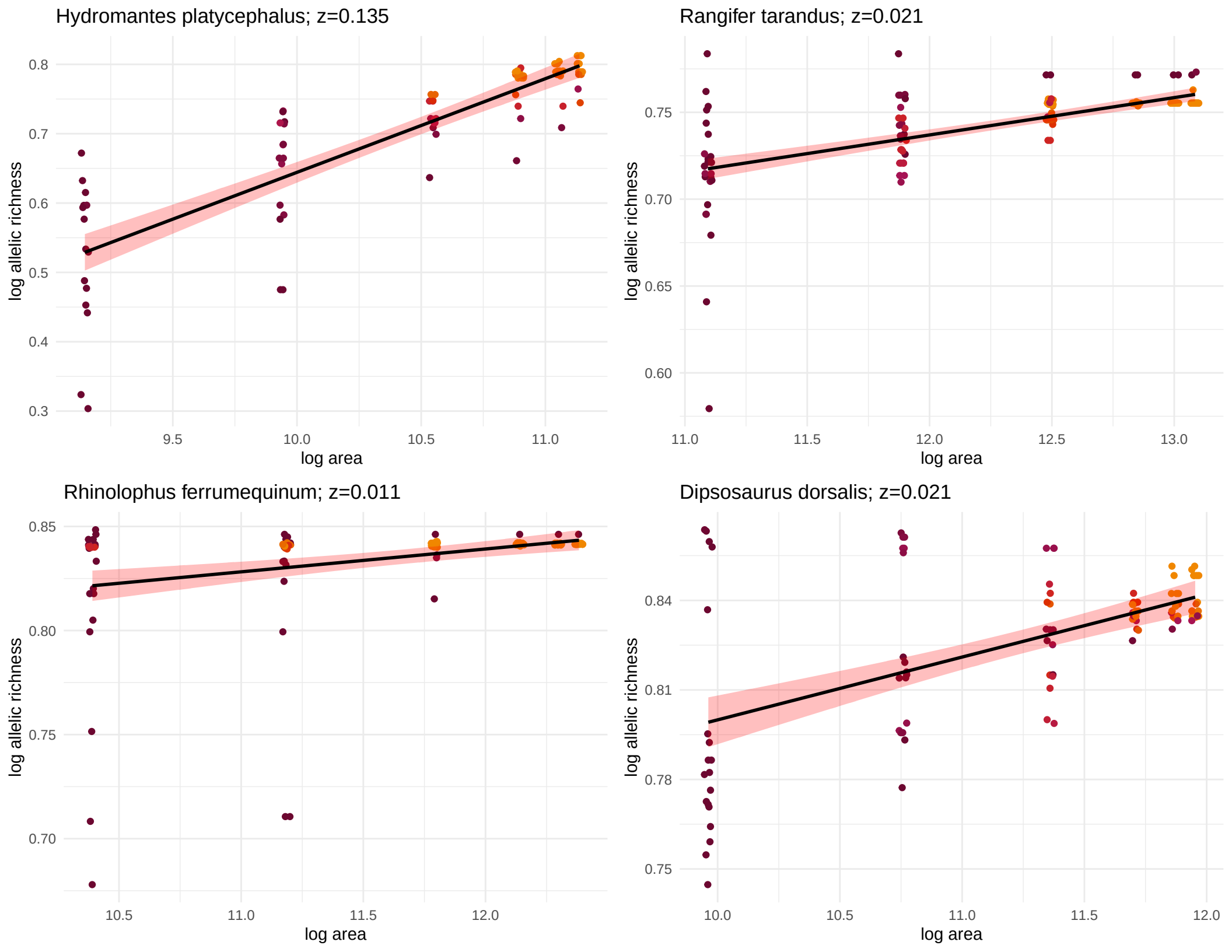
Hydromantes platycephalus; z=0.135
log allelic richness
log area
Rangifer tarandus; z=0.021
log allelic richness
log area
Rhinolophus ferrumequinum; z=0.011
log allelic richness
log area
Dipsosaurus dorsalis; z=0.021
log allelic richness
log area

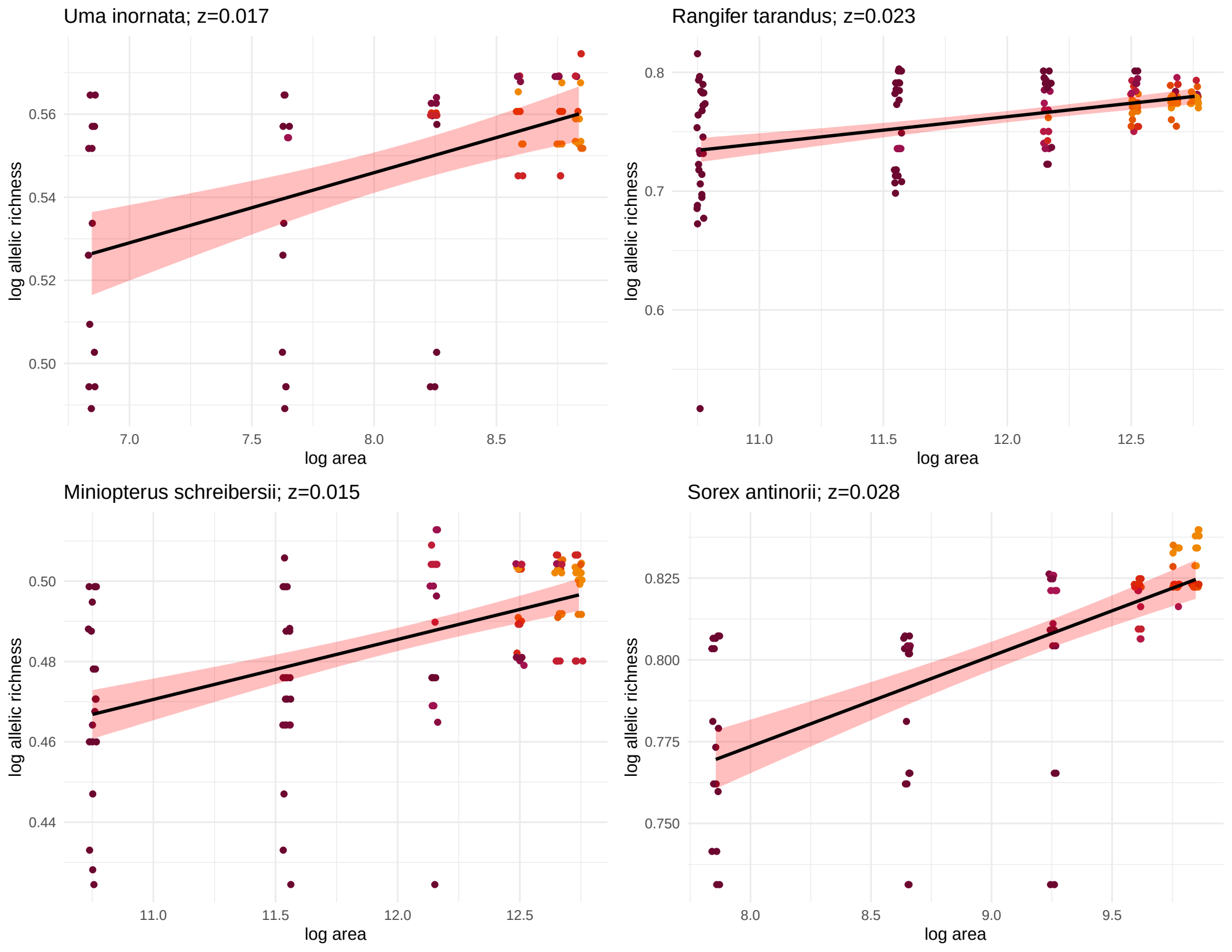
Uma inornata; z=0.017
log allelic richness
0.56
0.54
0.52
0.50
7.0
7.5
8.0
8.5
log area
Rangifer tarandus; z=0.023
log allelic richness
0.8
0.7
0.6
11.0
11.5
12.0
12.5
log area
Miniopterus schreibersii; z=0.015
log allelic richness
0.50
0.48
0.46
0.44
11.0
11.5
12.0
12.5
log area
Sorex antinorii; z=0.028
log allelic richness
0.825
0.800
0.775
0.750
8.0
8.5
9.0
9.5
log area

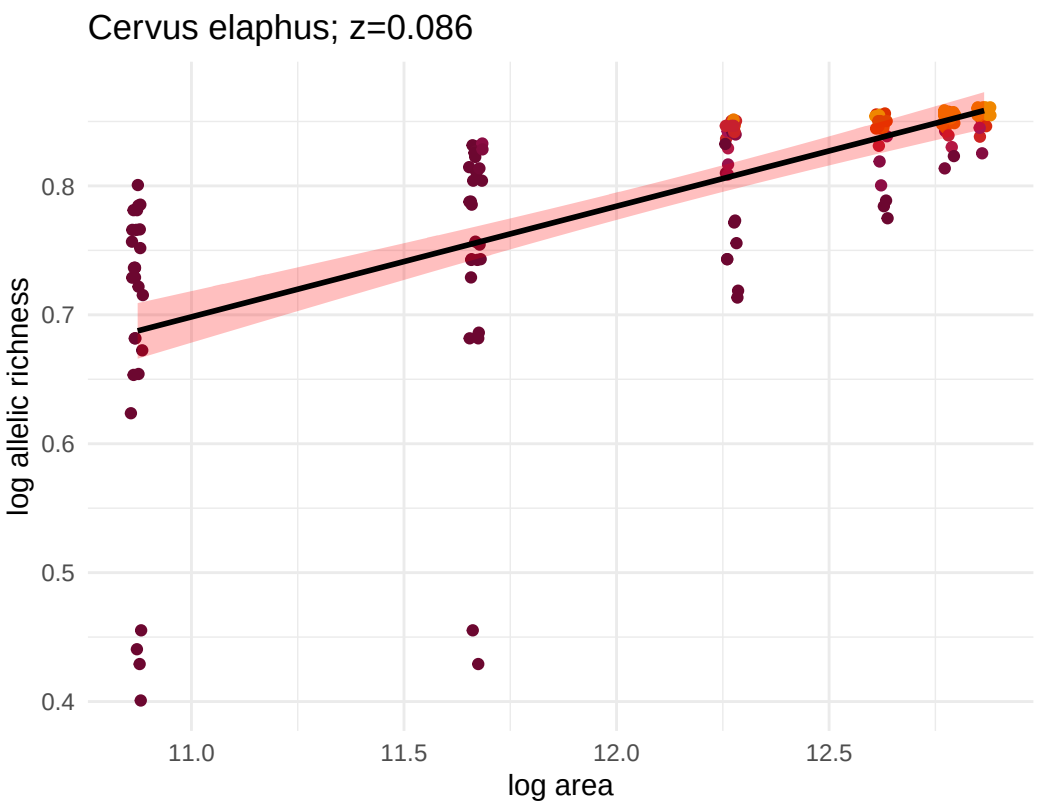
Cervus elaphus; z=0.086
log allelic richness
0.8
0.7
0.6
0.5
0.4
11.0
11.5
12.0
12.5
log area

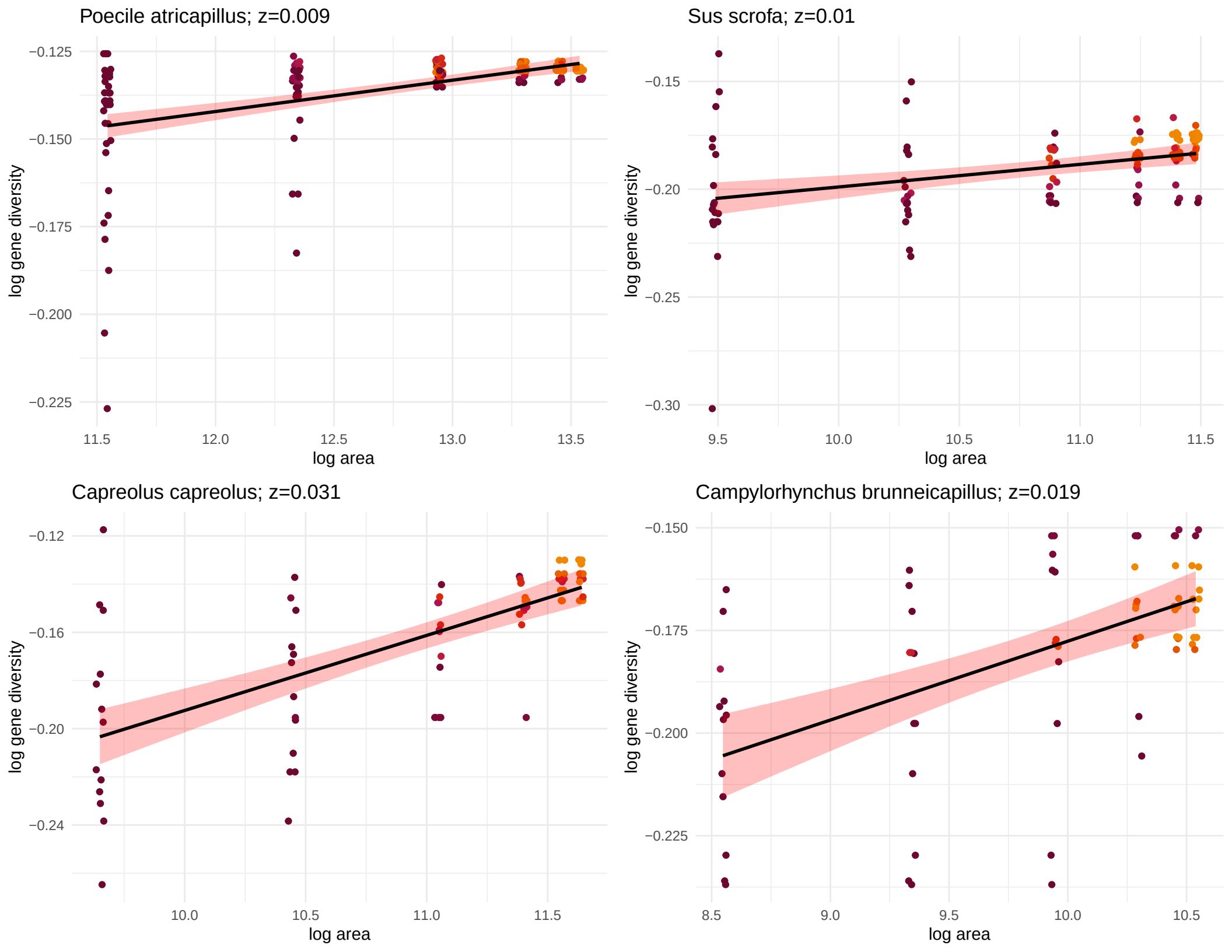
Poecile atricapillus; z=0.009
log gene diversity
−0.125
−0.150
−0.175
−0.200
−0.225
11.5
12.0
12.5
13.0
13.5
log area
Sus scrofa; z=0.01
log gene diversity
−0.15
−0.20
−0.25
−0.30
9.5
10.0
10.5
11.0
11.5
log area
Capreolus capreolus; z=0.031
log gene diversity
−0.12
−0.16
−0.20
−0.24
10.0
10.5
11.0
11.5
log area
Campylorhynchus brunneicapillus; z=0.019
log gene diversity
−0.150
−0.175
−0.200
−0.225
8.5
9.0
9.5
10.0
10.5
log area

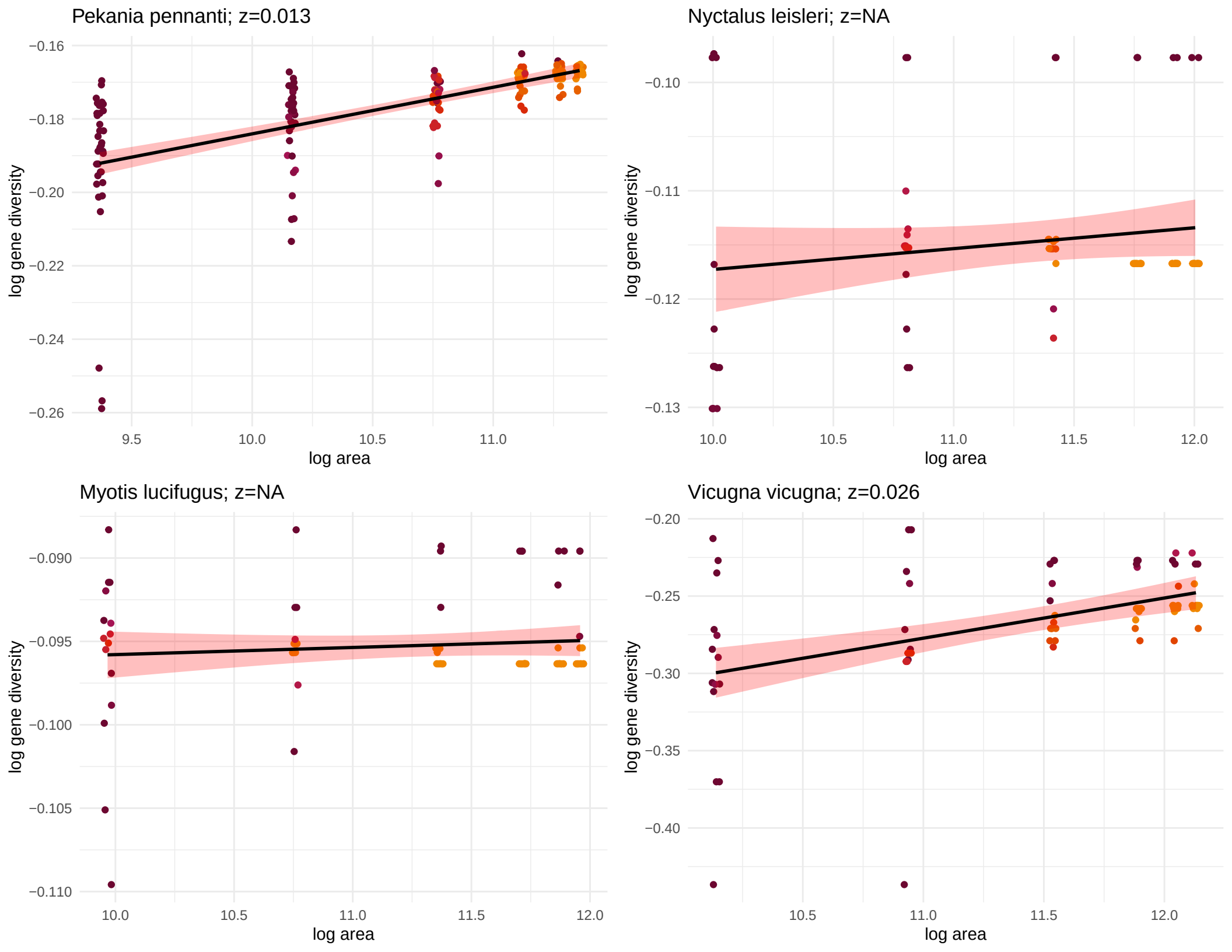
Pekania pennanti; z=0.013
log gene diversity
log area
−0.16
−0.18
−0.20
−0.22
−0.24
−0.26
9.5
10.0
10.5
11.0
Nyctalus leisleri; z=NA
log gene diversity
log area
−0.10
−0.11
−0.12
−0.13
10.0
10.5
11.0
11.5
12.0
Myotis lucifugus; z=NA
log gene diversity
log area
−0.090
−0.095
−0.100
−0.105
−0.110
10.0
10.5
11.0
11.5
12.0
Vicugna vicugna; z=0.026
log gene diversity
log area
−0.20
−0.25
−0.30
−0.35
−0.40
10.5
11.0
11.5
12.0

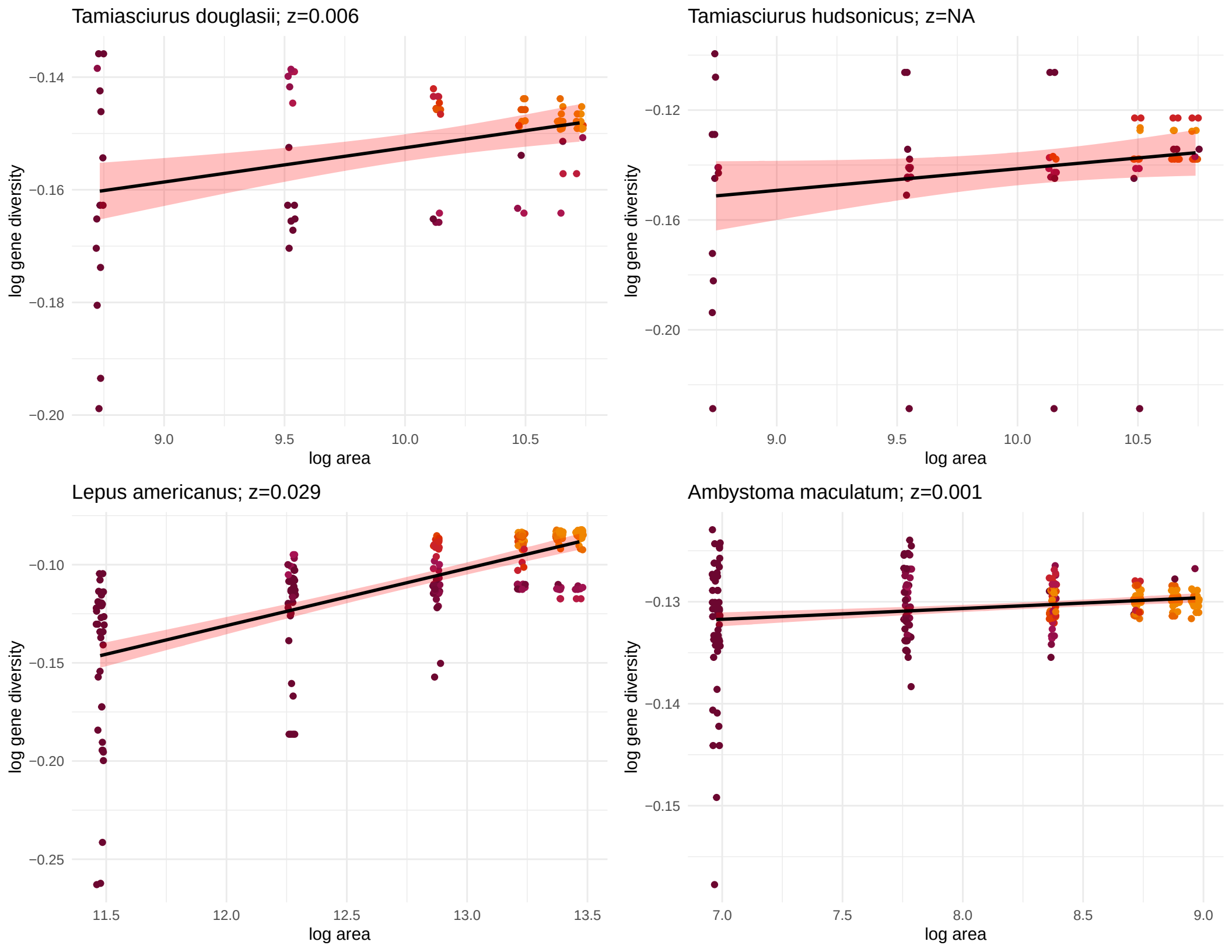
Tamiasciurus douglasii; z=0.006
log gene diversity
−0.14
−0.16
−0.18
−0.20
9.0
9.5
10.0
10.5
log area
Tamiasciurus hudsonicus; z=NA
log gene diversity
−0.12
−0.16
−0.20
9.0
9.5
10.0
10.5
log area
Lepus americanus; z=0.029
log gene diversity
−0.10
−0.15
−0.20
−0.25
11.5
12.0
12.5
13.0
13.5
log area
Ambystoma maculatum; z=0.001
log gene diversity
−0.13
−0.14
−0.15
7.0
7.5
8.0
8.5
9.0
log area

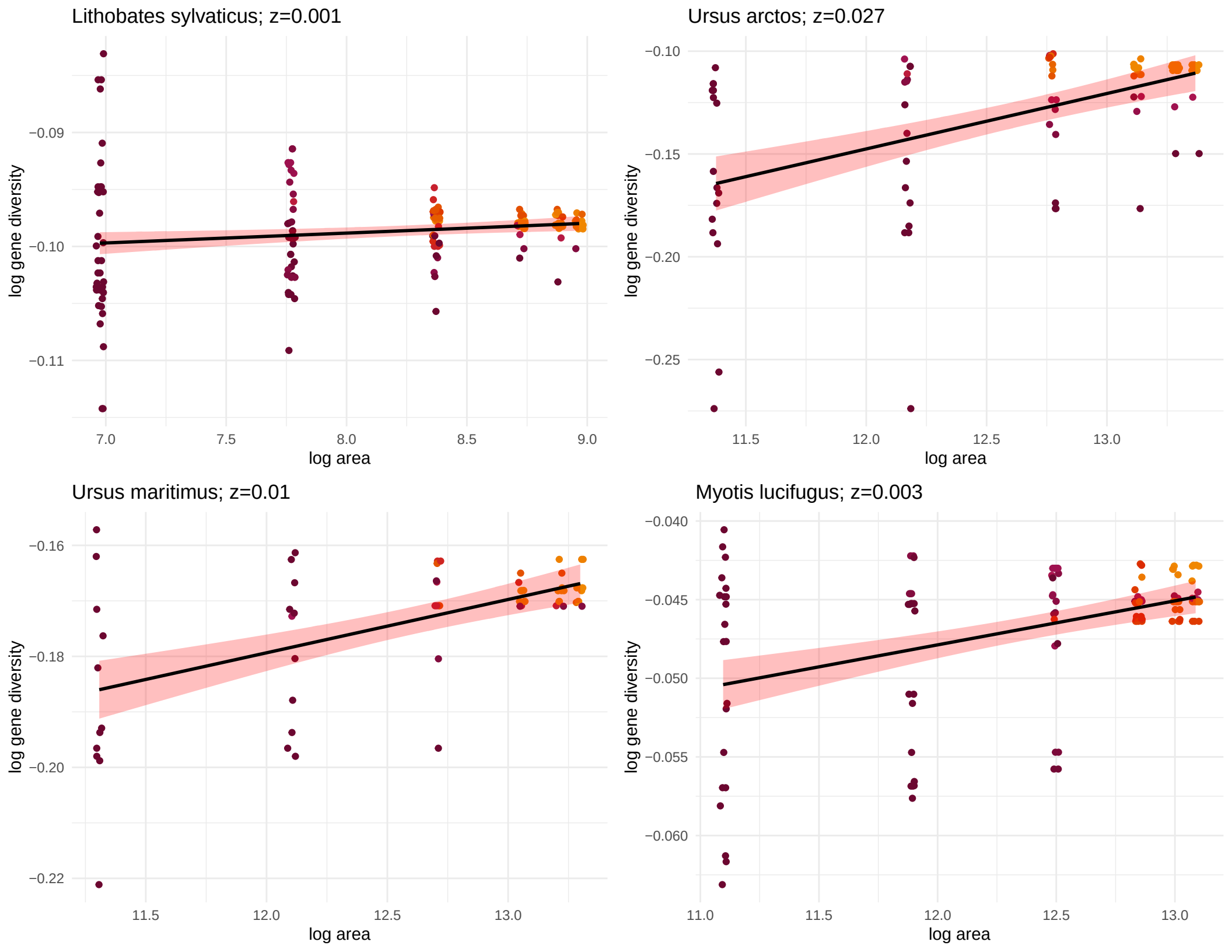
Lithobates sylvaticus; z=0.001
Ursus arctos; z=0.027
Ursus maritimus; z=0.01
Myotis lucifugus; z=0.003
log gene diversity
log area
−0.09
−0.10
−0.11
−0.10
−0.15
−0.20
−0.25
−0.16
−0.18
−0.20
−0.22
−0.040
−0.045
−0.050
−0.055
−0.060
7.0
7.5
8.0
8.5
9.0
11.0
11.5
12.0
12.5
13.0

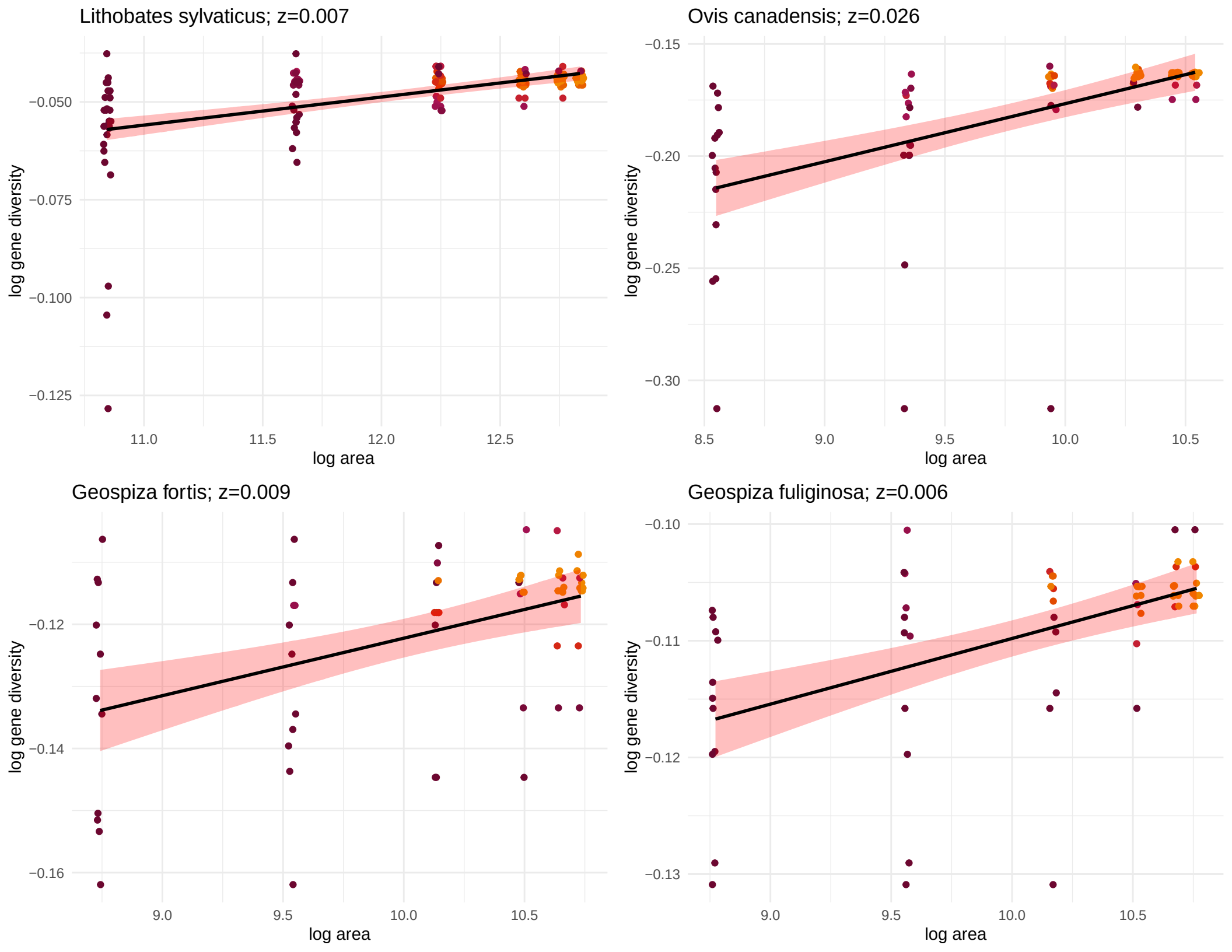
Lithobates sylvaticus; z=0.007
Ovis canadensis; z=0.026
Geospiza fortis; z=0.009
Geospiza fuliginosa; z=0.006
log gene diversity
log area
−0.050
−0.075
−0.100
−0.125
11.0
11.5
12.0
12.5
−0.15
−0.20
−0.25
−0.30
8.5
9.0
9.5
10.0
10.5
−0.12
−0.14
−0.16
−0.10
−0.11
−0.12
−0.13

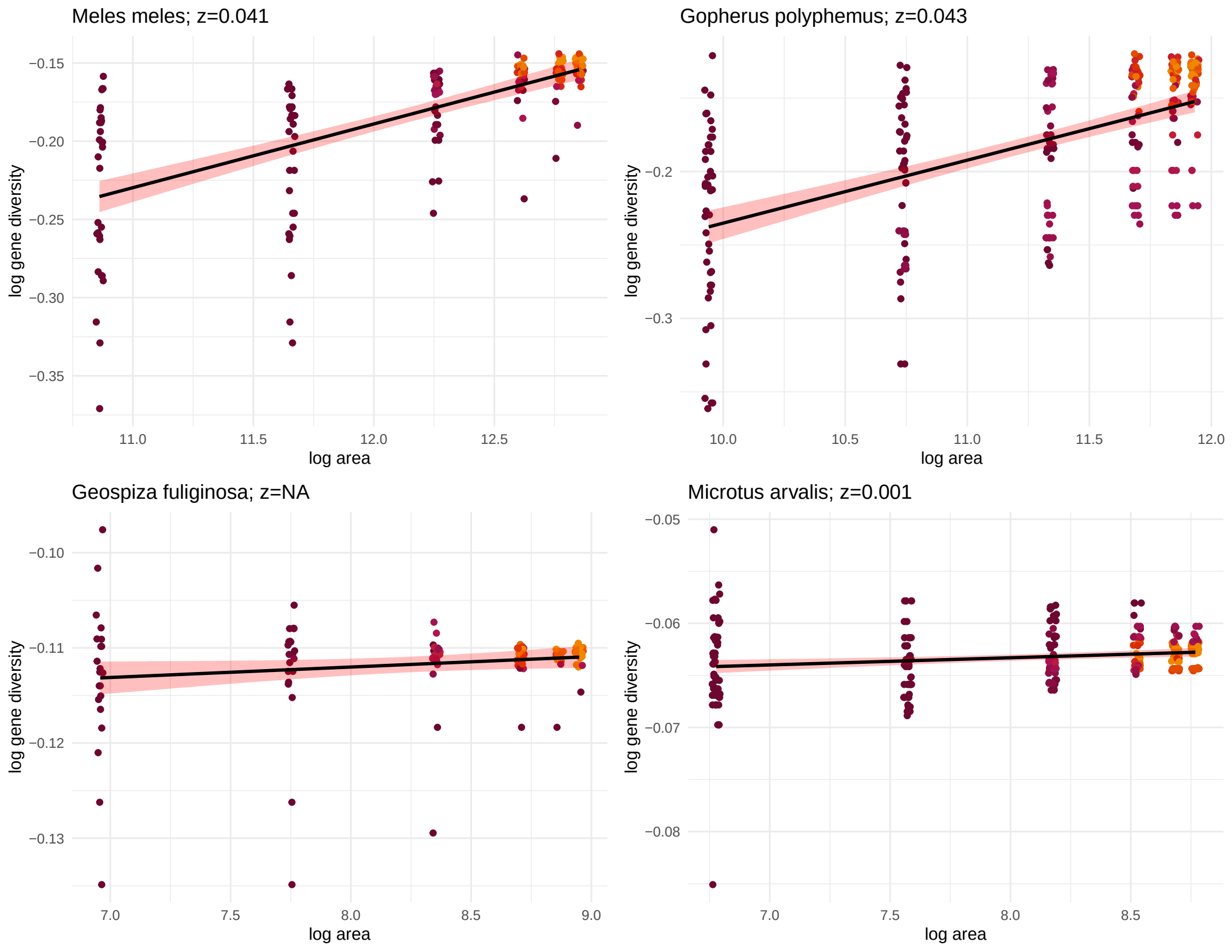
Meles meles; z=0.041
log gene diversity
−0.15
−0.20
−0.25
−0.30
−0.35
11.0
11.5
12.0
12.5
log area
Gopherus polyphemus; z=0.043
log gene diversity
−0.2
−0.3
10.0
10.5
11.0
11.5
12.0
log area
Geospiza fuliginosa; z=NA
log gene diversity
−0.10
−0.11
−0.12
−0.13
7.0
7.5
8.0
8.5
9.0
log area
Microtus arvalis; z=0.001
log gene diversity
−0.05
−0.06
−0.07
−0.08
7.0
7.5
8.0
8.5
log area

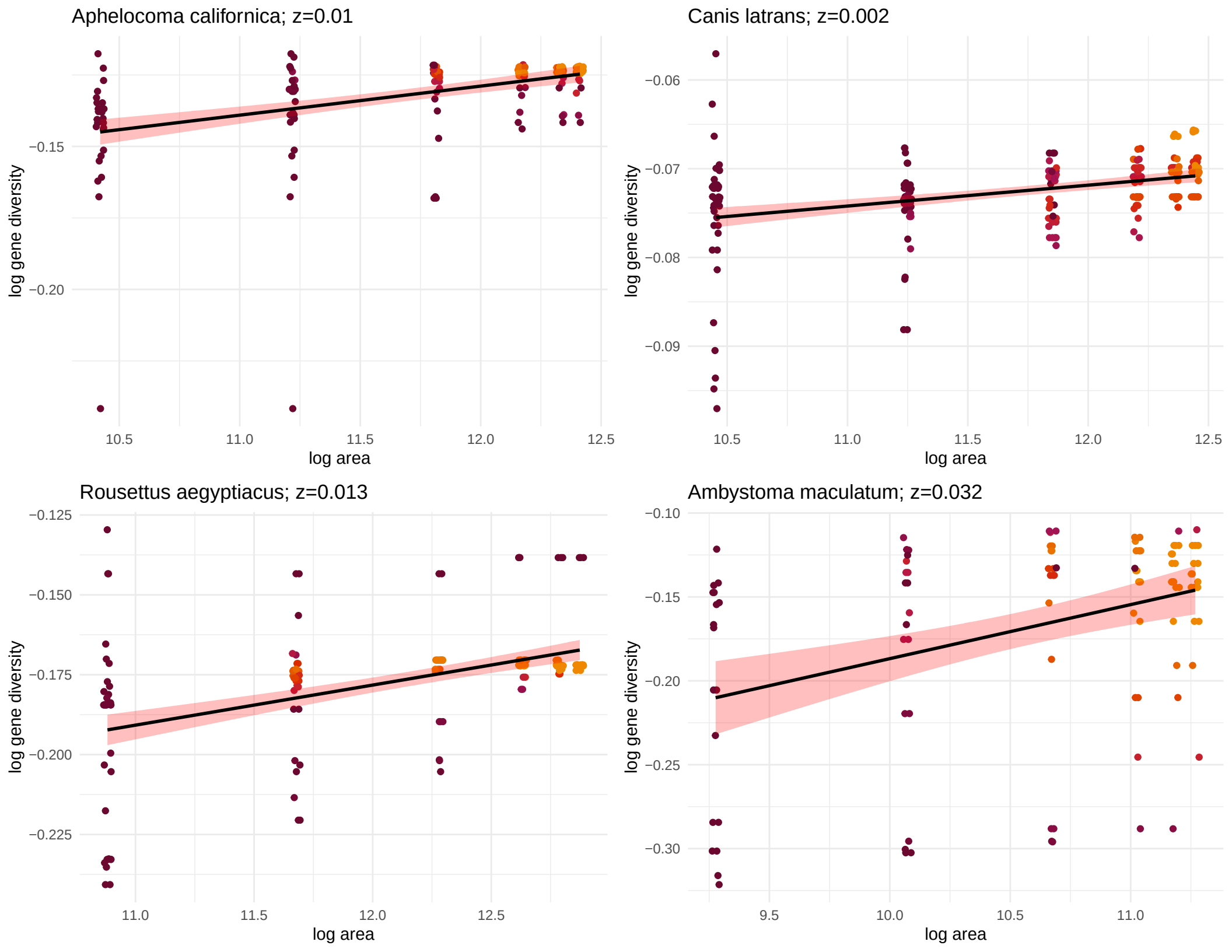
Aphelocoma californica; z=0.01
log gene diversity
−0.15
−0.20
10.5
11.0
11.5
12.0
12.5
log area
Canis latrans; z=0.002
log gene diversity
−0.06
−0.07
−0.08
−0.09
10.5
11.0
11.5
12.0
12.5
log area
Rousettus aegyptiacus; z=0.013
log gene diversity
−0.125
−0.150
−0.175
−0.200
−0.225
11.0
11.5
12.0
12.5
log area
Ambystoma maculatum; z=0.032
log gene diversity
−0.10
−0.15
−0.20
−0.25
−0.30
9.5
10.0
10.5
11.0
log area

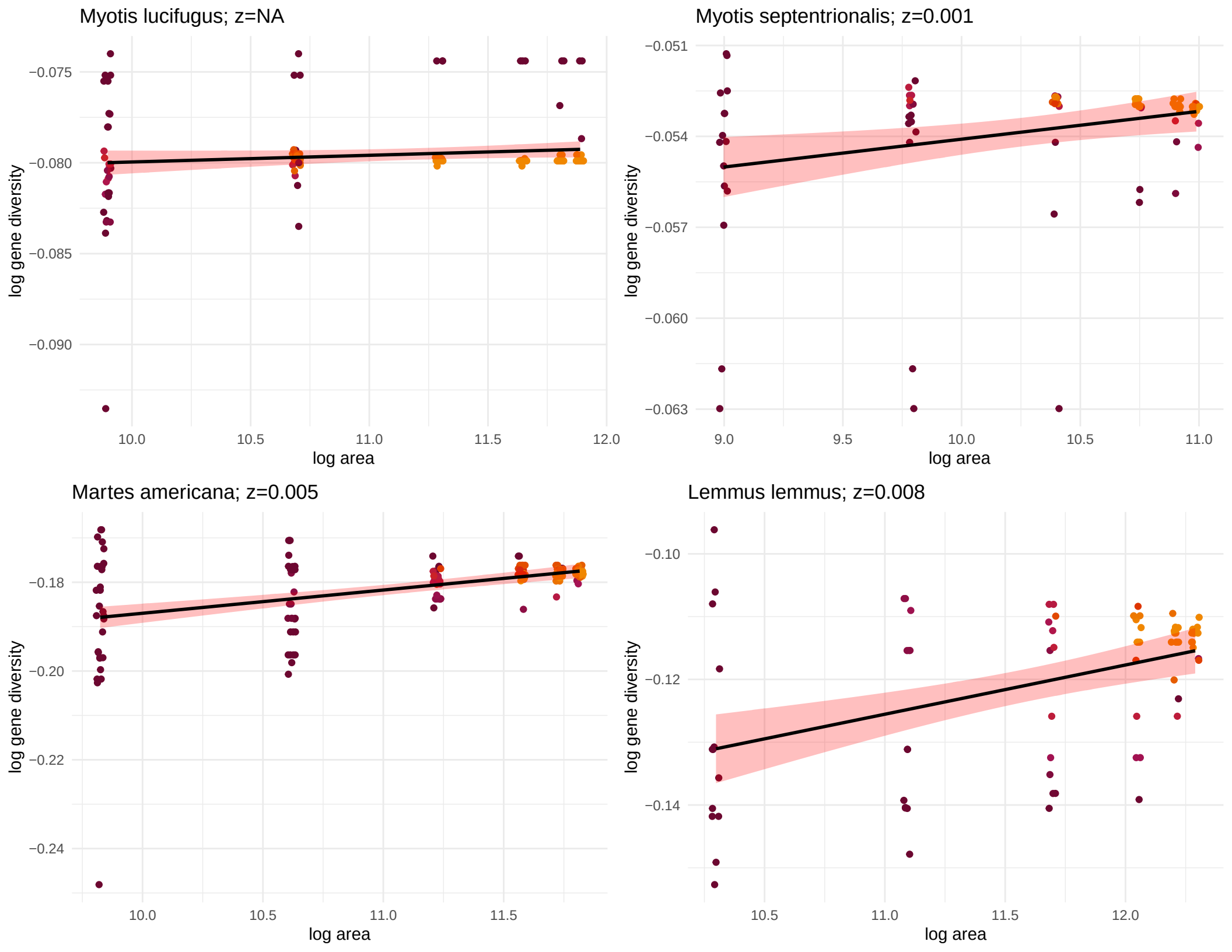
Myotis lucifugus; z=NA
log gene diversity
−0.075
−0.080
−0.085
−0.090
10.0
10.5
11.0
11.5
12.0
log area
Myotis septentrionalis; z=0.001
log gene diversity
−0.051
−0.054
−0.057
−0.060
−0.063
9.0
9.5
10.0
10.5
11.0
log area
Martes americana; z=0.005
log gene diversity
−0.18
−0.20
−0.22
−0.24
10.0
10.5
11.0
11.5
log area
Lemmus lemmus; z=0.008
log gene diversity
−0.10
−0.12
−0.14
10.5
11.0
11.5
12.0
log area

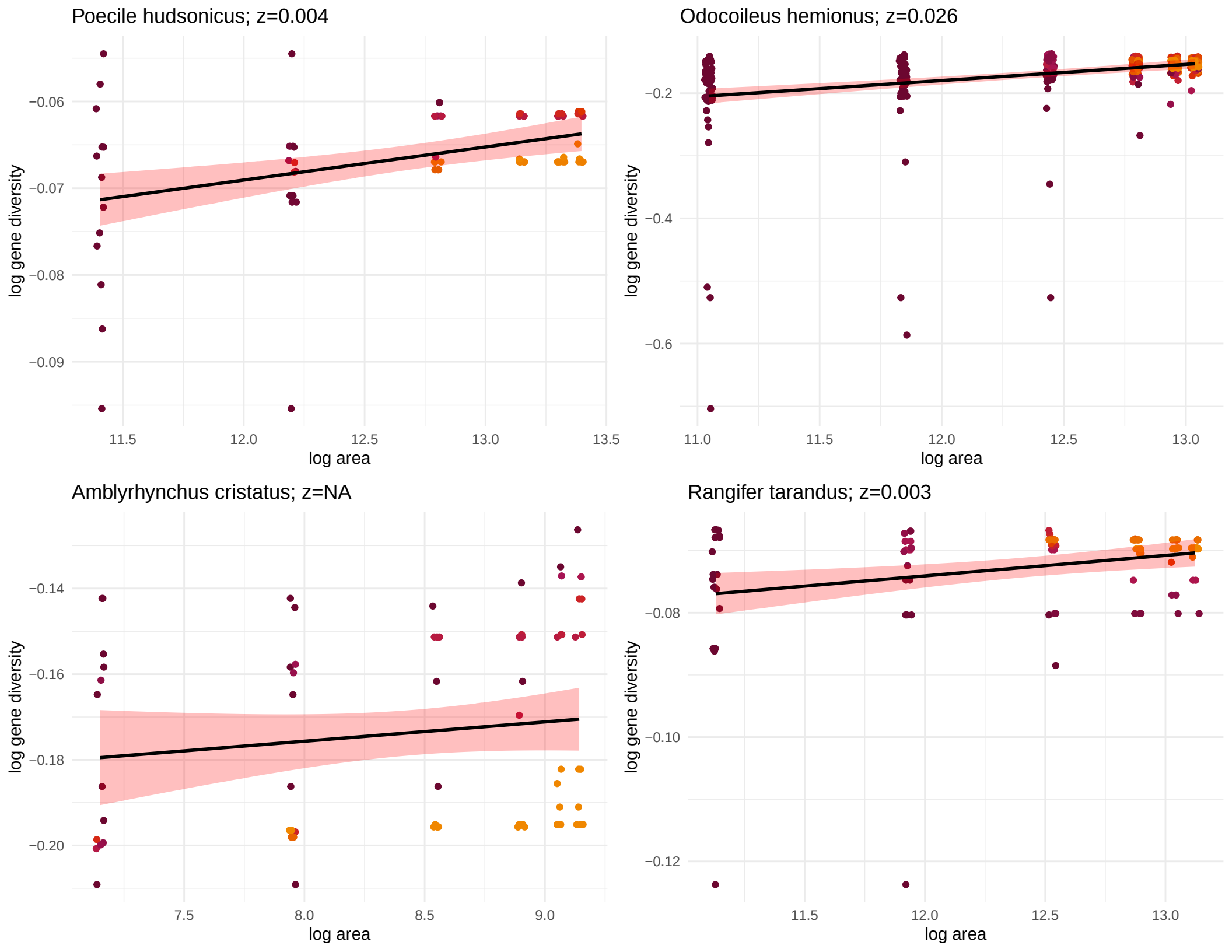
Poecile hudsonicus; z=0.004
Odocoileus hemionus; z=0.026
Amblyrhynchus cristatus; z=NA
Rangifer tarandus; z=0.003
log gene diversity
log area
−0.06
−0.07
−0.08
−0.09
−0.2
−0.4
−0.6
−0.14
−0.16
−0.18
−0.20
−0.10
−0.12
11.5
12.0
12.5
13.0
13.5
11.0
7.5
8.0
8.5
9.0

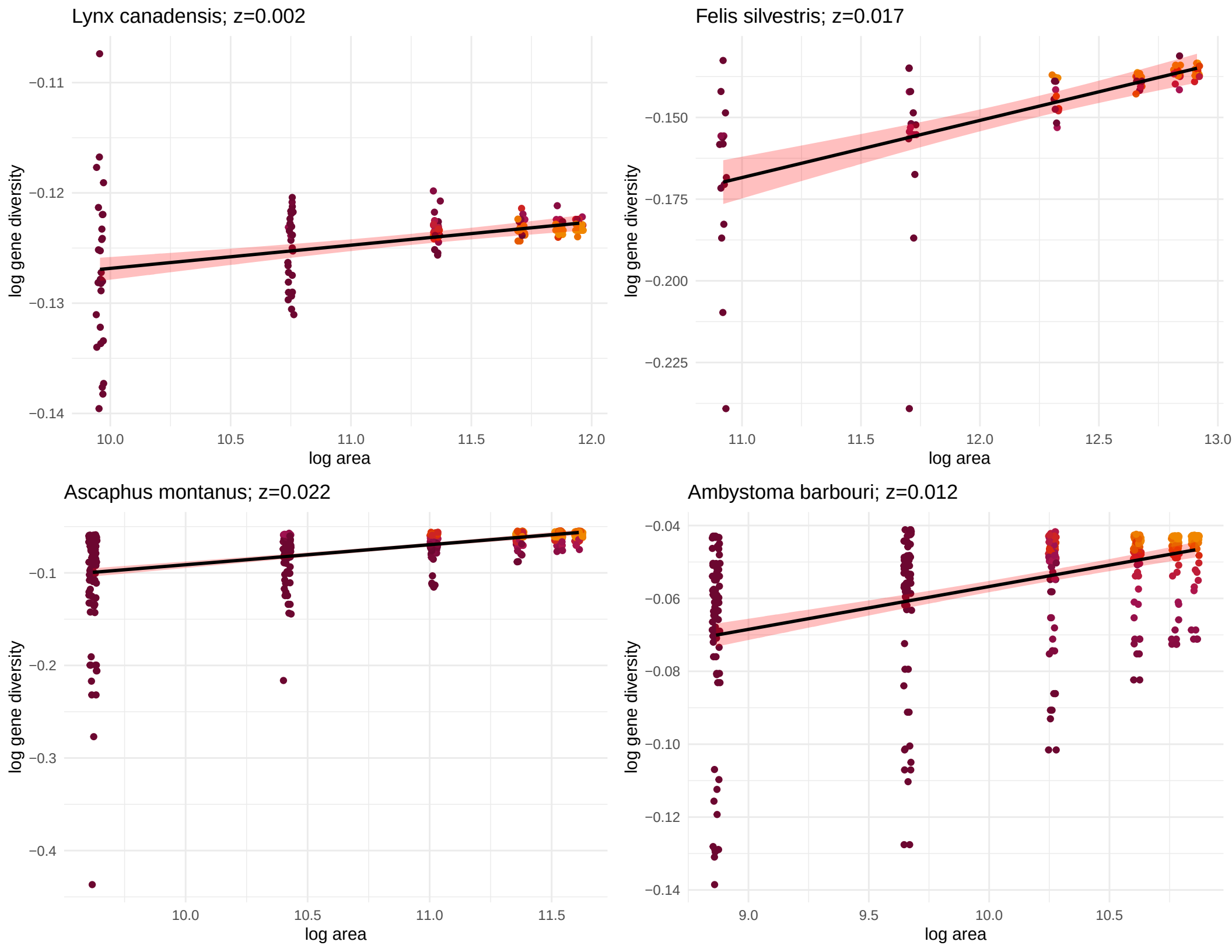
Lynx canadensis; z=0.002
log gene diversity
log area
−0.11
−0.12
−0.13
−0.14
10.0
10.5
11.0
11.5
12.0
Felis silvestris; z=0.017
log gene diversity
log area
−0.150
−0.175
−0.200
−0.225
11.0
11.5
12.0
12.5
13.0
Ascaphus montanus; z=0.022
log gene diversity
log area
−0.1
−0.2
−0.3
−0.4
10.0
10.5
11.0
11.5
Ambystoma barbouri; z=0.012
log gene diversity
log area
−0.04
−0.06
−0.08
−0.10
−0.12
−0.14
9.0
9.5
10.0
10.5

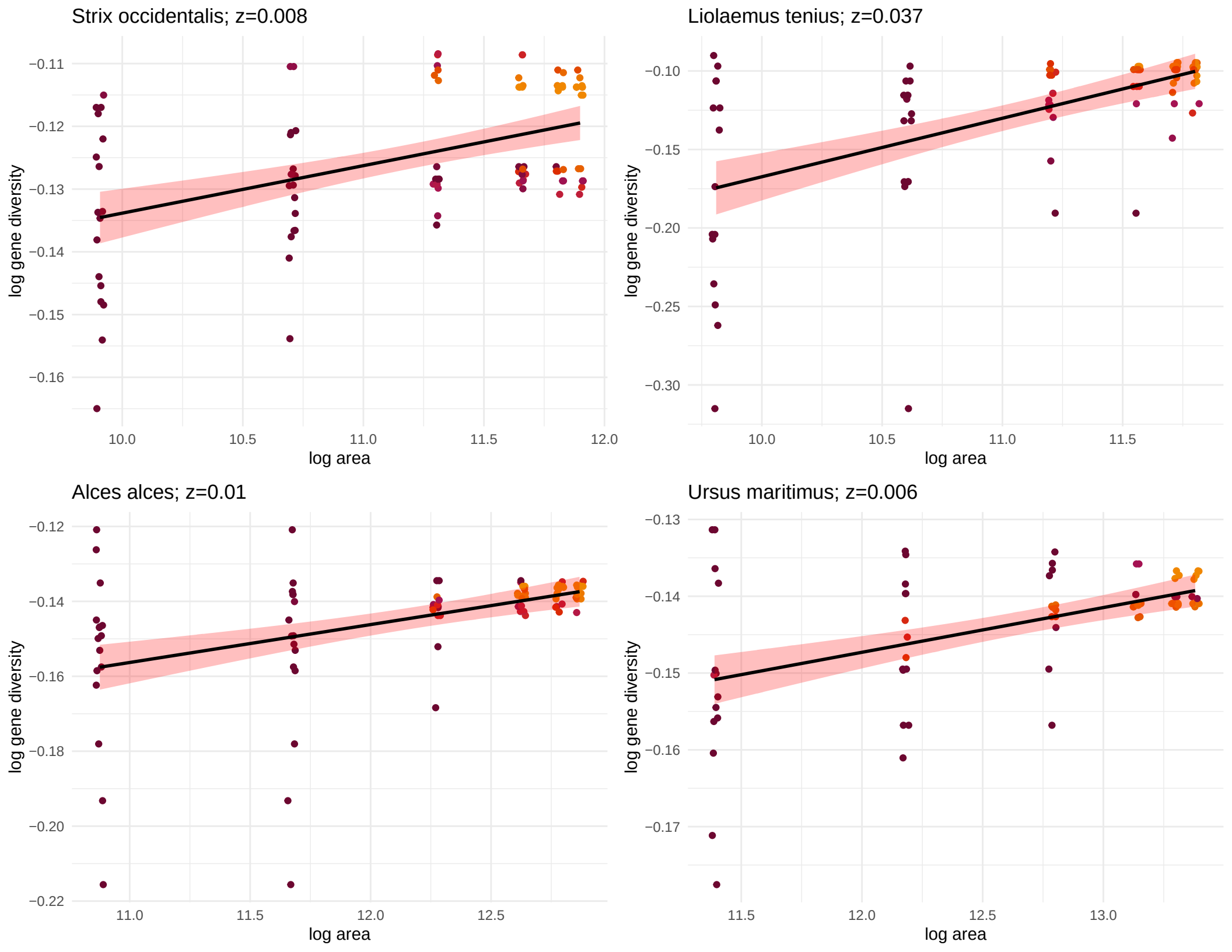
Strix occidentalis; z=0.008
log gene diversity
log area
−0.11
−0.12
−0.13
−0.14
−0.15
−0.16
10.0
10.5
11.0
11.5
12.0
Liolaemus tenius; z=0.037
log gene diversity
log area
−0.10
−0.15
−0.20
−0.25
−0.30
10.0
10.5
11.0
11.5
Alces alces; z=0.01
log gene diversity
log area
−0.12
−0.14
−0.16
−0.18
−0.20
−0.22
11.0
11.5
12.0
12.5
Ursus maritimus; z=0.006
log gene diversity
log area
−0.13
−0.14
−0.15
−0.16
−0.17
11.5
12.0
12.5
13.0

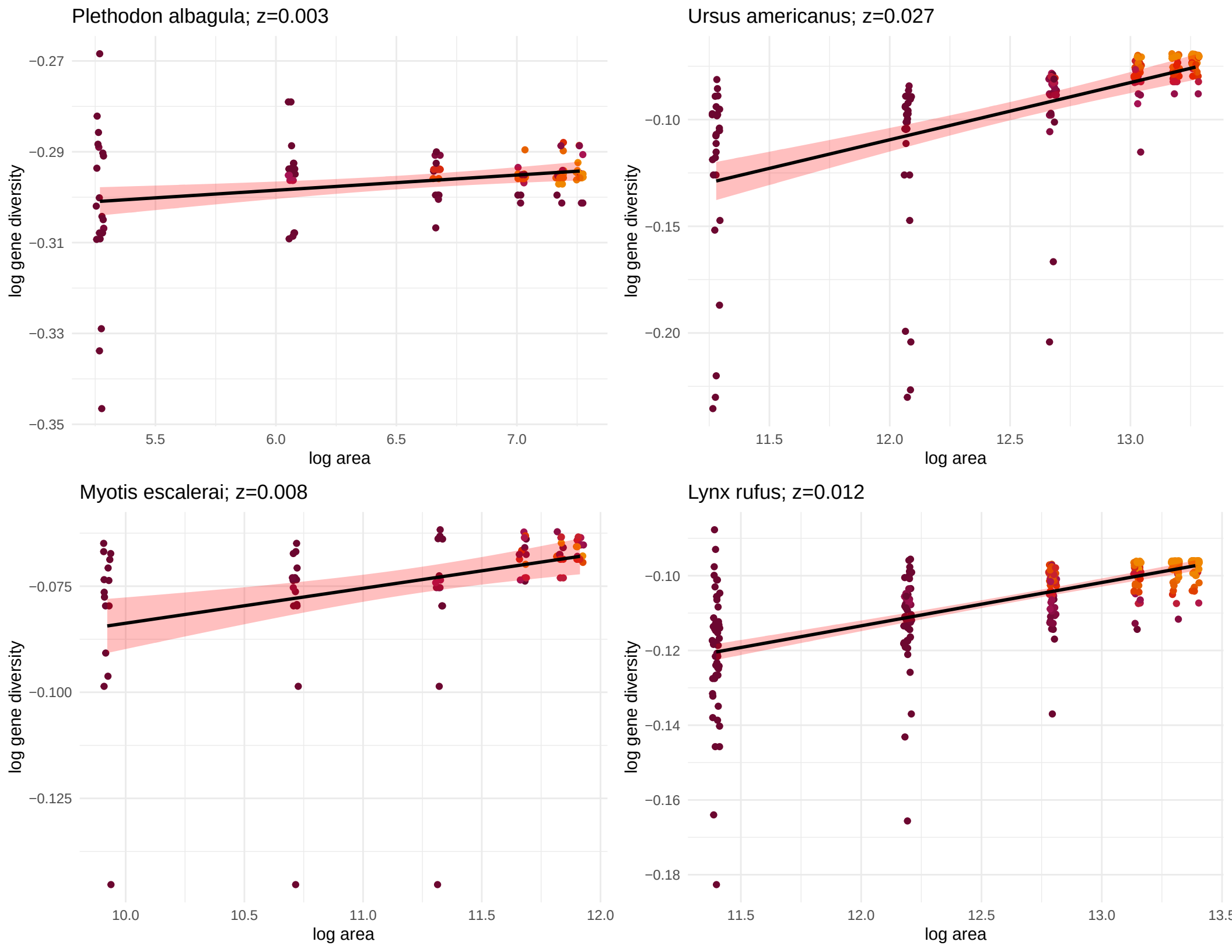
Plethodon albagula; z=0.003
log gene diversity
−0.27
−0.29
−0.31
−0.33
−0.35
5.5
6.0
6.5
7.0
log area
Ursus americanus; z=0.027
log gene diversity
−0.10
−0.15
−0.20
11.5
12.0
12.5
13.0
log area
Myotis escalerai; z=0.008
log gene diversity
−0.075
−0.100
−0.125
10.0
10.5
11.0
11.5
12.0
log area
Lynx rufus; z=0.012
log gene diversity
−0.10
−0.12
−0.14
−0.16
−0.18
11.5
12.0
12.5
13.0
13.5
log area

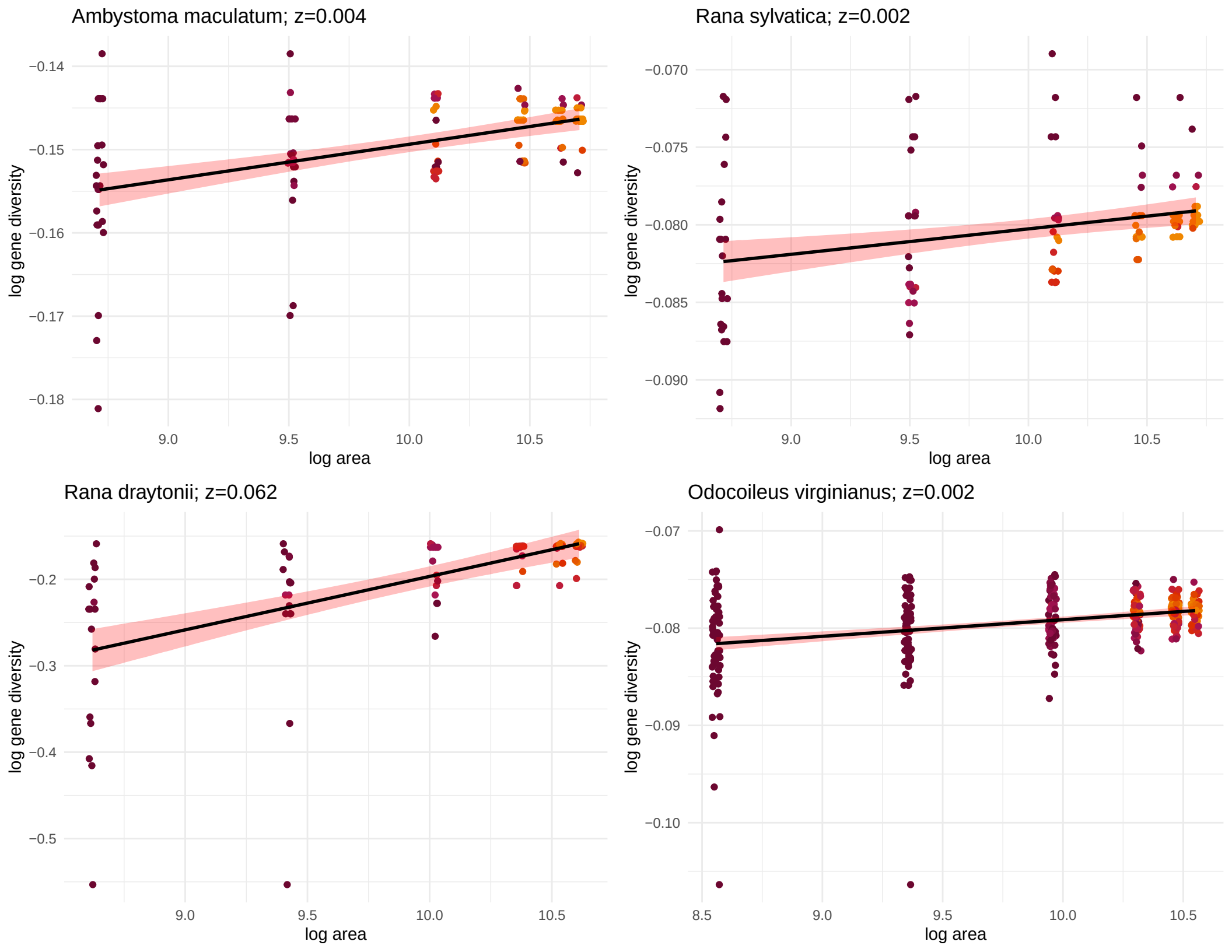
Ambystoma maculatum; z=0.004
Rana sylvatica; z=0.002
Rana draytonii; z=0.062
Odocoileus virginianus; z=0.002
log gene diversity
log area
−0.14
−0.15
−0.16
−0.17
−0.18
−0.070
−0.075
−0.080
−0.085
−0.090
−0.2
−0.3
−0.4
−0.5
−0.07
−0.08
−0.09
−0.10
8.5
9.0
9.5
10.0
10.5

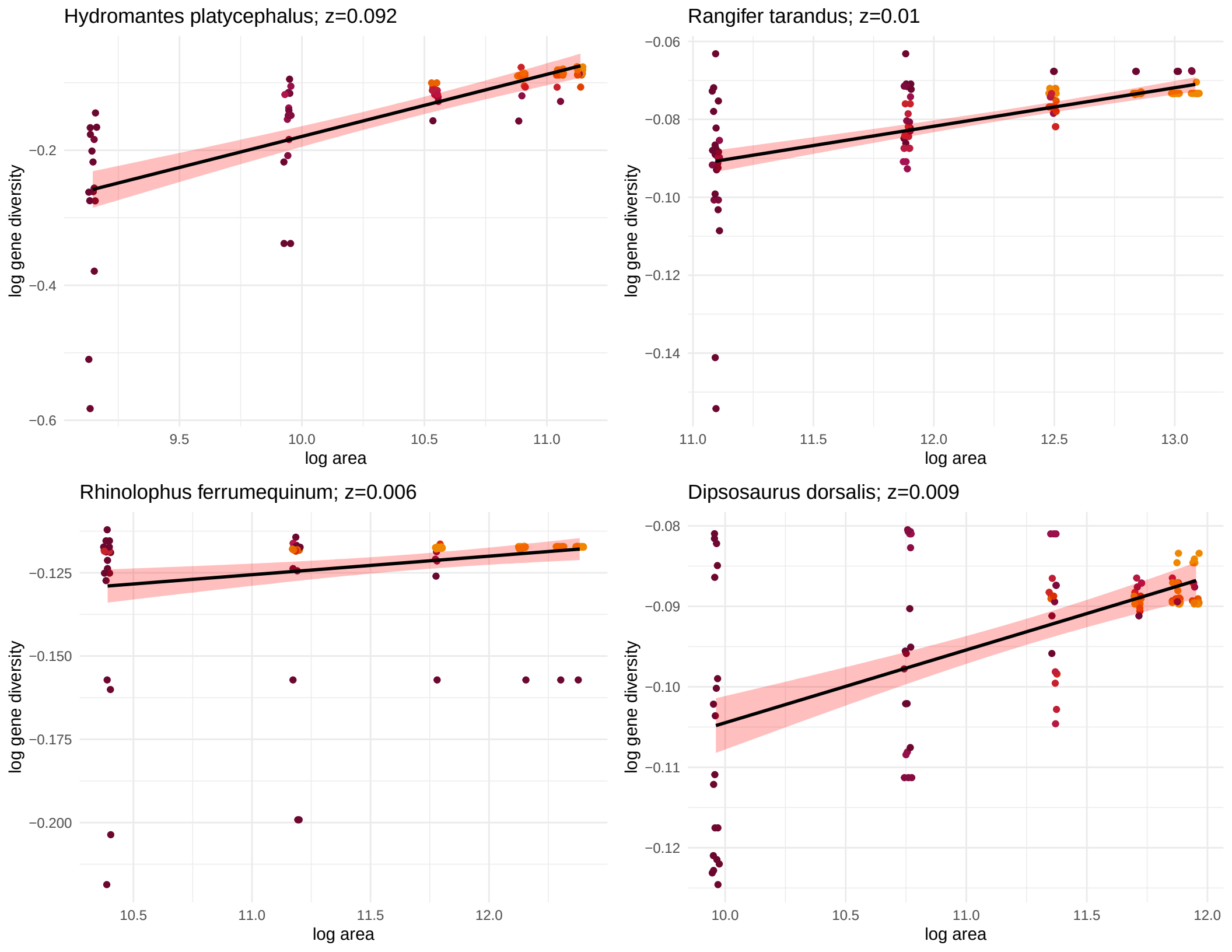
Hydromantes platycephalus; z=0.092
log gene diversity
log area
−0.2
−0.4
−0.6
9.5
10.0
10.5
11.0
Rangifer tarandus; z=0.01
log gene diversity
log area
−0.06
−0.08
−0.10
−0.12
−0.14
11.0
11.5
12.0
12.5
13.0
Rhinolophus ferrumequinum; z=0.006
log gene diversity
log area
−0.125
−0.150
−0.175
−0.200
10.5
11.0
11.5
12.0
Dipsosaurus dorsalis; z=0.009
log gene diversity
log area
−0.08
−0.09
−0.10
−0.11
−0.12
10.0
10.5
11.0
11.5
12.0

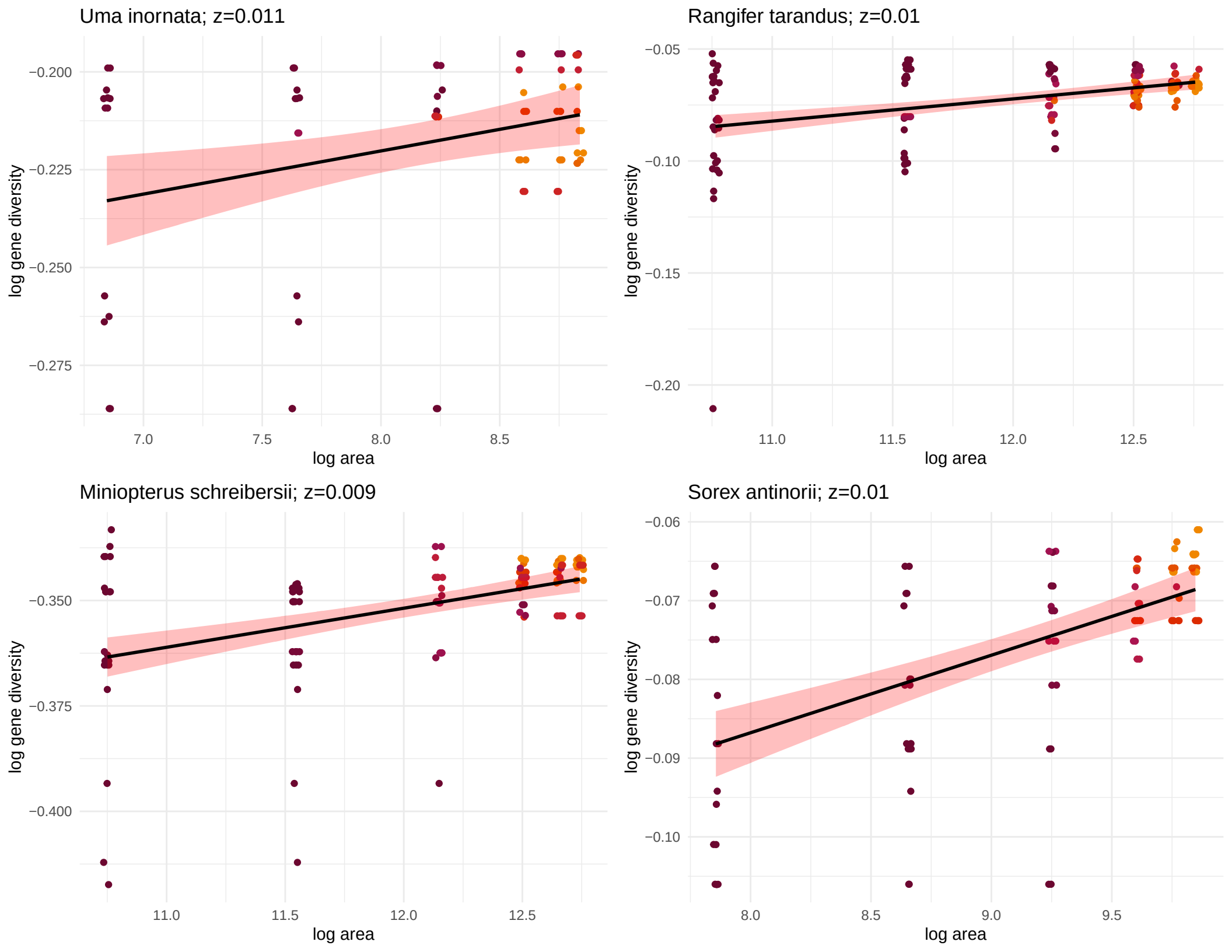
Uma inornata; z=0.011
log gene diversity
−0.200
−0.225
−0.250
−0.275
7.0
7.5
8.0
8.5
log area
Rangifer tarandus; z=0.01
log gene diversity
−0.05
−0.10
−0.15
−0.20
11.0
11.5
12.0
12.5
log area
Miniopterus schreibersii; z=0.009
log gene diversity
−0.350
−0.375
−0.400
11.0
11.5
12.0
12.5
log area
Sorex antinorii; z=0.01
log gene diversity
−0.06
−0.07
−0.08
−0.09
−0.10
8.0
8.5
9.0
9.5
log area

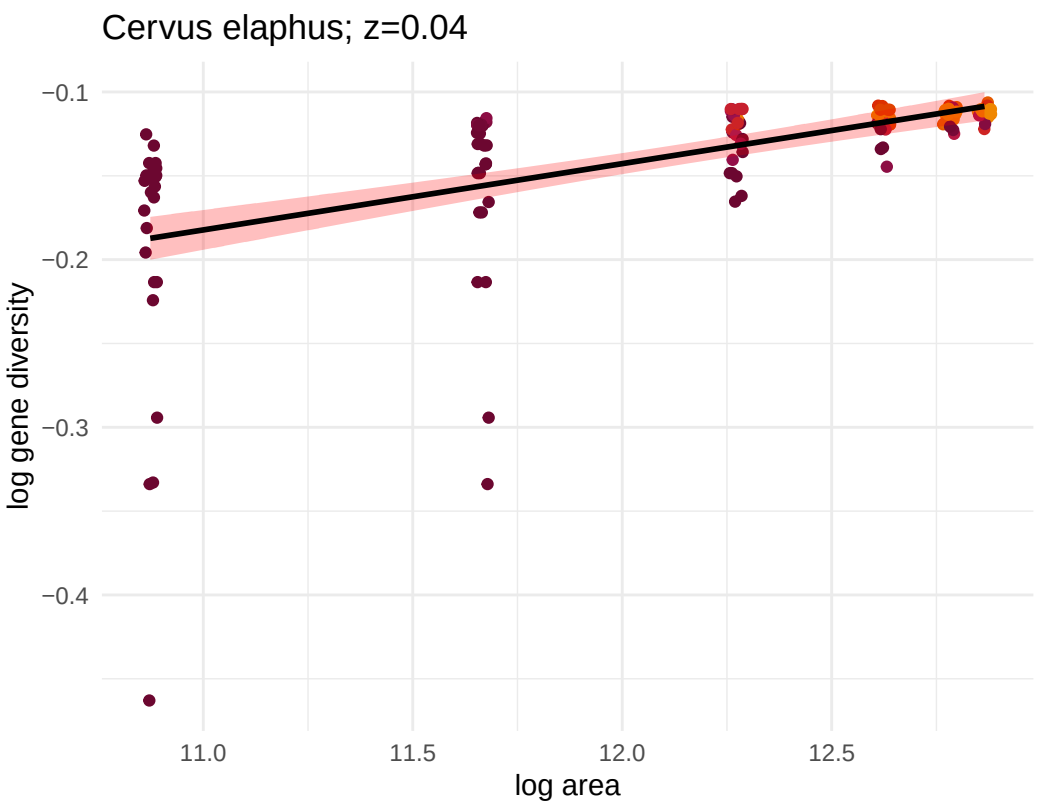
Cervus elaphus; z=0.04
log gene diversity
−0.1
−0.2
−0.3
−0.4
11.0
11.5
12.0
12.5
log area

Figure S3. Comparison of F_{ST} values from the data analyzed here versus mean F_{ST} estimates per species within the mammal MacroPopGen dataset. The red dashed line indicates a perfect correlation.

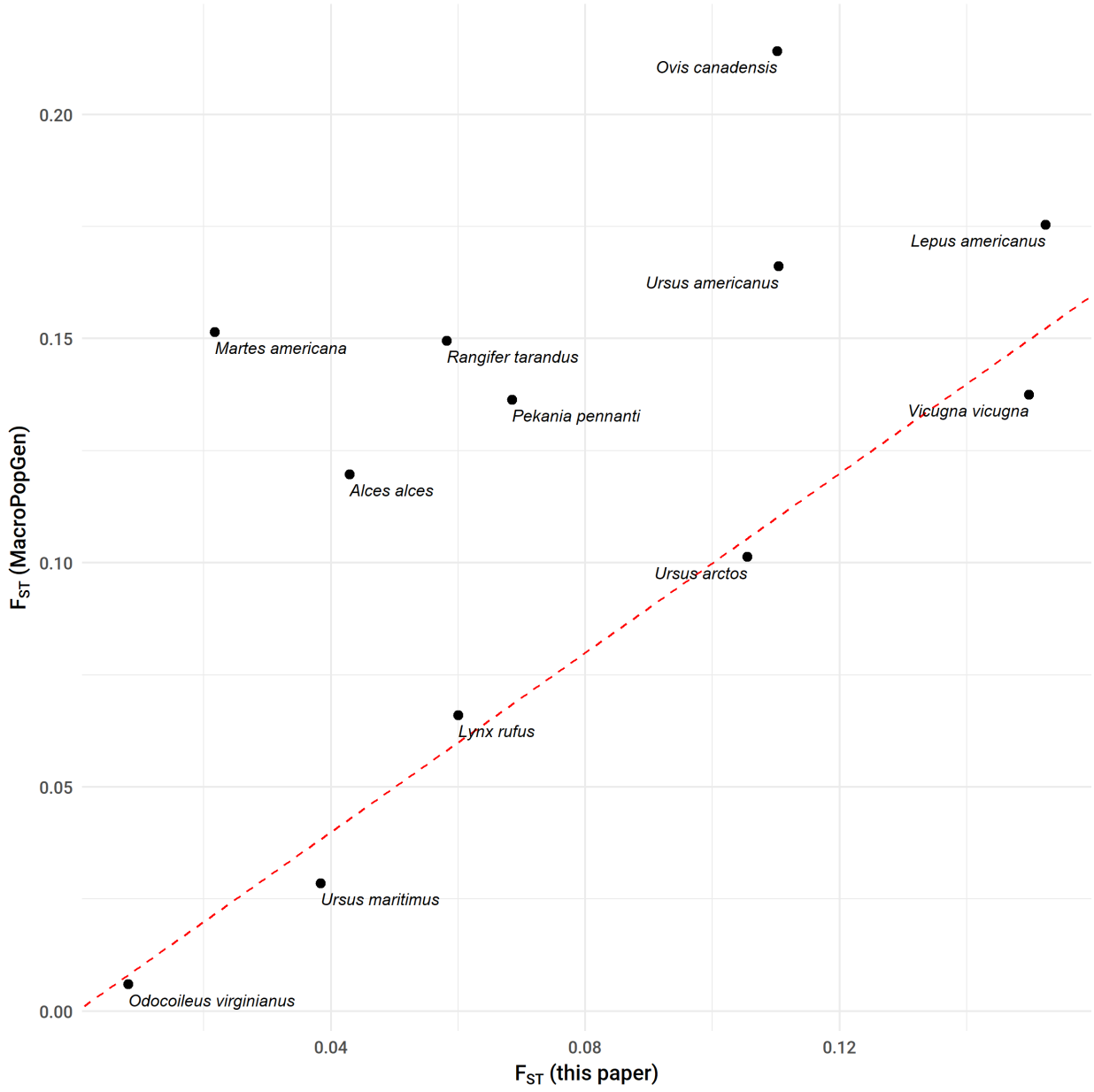

Figure S4. Observed MacroPopGen F_{ST} versus F_{ST} values predicted based on a model derived from the data analyzed here. Plots show predictions for individual datasets in the MacroPopGen database (left, points colored according to species; CV = 1.04) and predictions of the species mean F_{ST} averaged across datasets (right; CV = 0.98). The red dashed line indicates a perfect correlation.